

**MODELING MILLING OF THIN-WALLED PARTS
CONSIDERING DYNAMIC STRUCTURE-PROCESS
INTERACTIONS**

by
SALTUK YILDIZ

Submitted to the Graduate School of Engineering and Natural Sciences
in partial fulfillment of
the requirements for the degree of
Master of Science

Sabancı University
July 2022

Saltuk Yıldız 2022 ©

All Rights Reserved

I would like to dedicate this thesis to my *Family*

ABSTRACT

MODELING MILLING OF THIN-WALLED PARTS CONSIDERING DYNAMIC STRUCTURE-PROCESS INTERACTIONS

SALTUK YILDIZ

MANUFACTURING ENGINEERING MASTER'S THESIS, JULY, 2022

Thesis Supervisor: Assoc. Prof. LÜTFİ TANER TUNÇ

Thesis Co-supervisor: Prof. ERHAN BUDAK

Keywords: Thin-walled Structures, Process Damping, Chatter Stability, Milling Process, Special Cutting Tools

Thin-walled parts are frequently used in industry and many engineering applications. These parts are commonly found especially in the field of aerospace, as they provide a high strength-to-weight ratio due to their inherent geometry. Some examples of thin-walled structures are turbine and compressor blades used in aero-engines, and frame structures used in aircraft. In addition to these, pin-finned structures are commonly utilized in the energy industry as heat exchangers. Machining of these parts is challenging due to their low dynamic rigidity. Therefore, stability analysis by modeling in-process workpiece dynamics is required to predict process stability condition. In this study, finish milling process stability of thin-walled geometries was investigated in detail. In modeling the workpiece dynamics, the effect of the material removal and cutter location at each cutting step on the workpiece dynamics and process stability was considered. In addition, the effect of variable pitch tools and crest-cut tools on thin-wall milling stability was investigated and compared with a standard end mill. In this thesis, the thin-walled workpiece was modeled as a 3D cantilever beam using the finite element method (FEM) and the increase in stiffness from free-end to fixed-end was considered in stability analysis. Moreover, the dominant bending and torsional modes of the workpiece were

taken into account. In machining processes, the dynamic interaction between the cutting edge and the vibration wave left on the surface generates process damping effect, which occurs from process itself in addition to structural damping. Process damping provides deeper stability limits at low cutting speeds. In the stability analysis, process damping was investigated for the flexible part finish milling by selecting optimal parameters such as cutting edge geometry, semi-finish stock thickness and maximum allowable vibration amplitude according to the situation results. Furthermore, the effects of stability, marginal stability, and chatter conditions on the surface finish of the parts were investigated.

ÖZET

İNCE CİDARLI PARÇALARIN FREZELENMESİ İŞLEMİNİN DİNAMİK YAPI- SÜREÇ ETKİLEŞİMLERİNİN HESABA KATILARAK MODELLENMESİ

SALTUK YILDIZ

ÜRETİM MÜHENDİSLİĞİ YÜKSEK LİSANS TEZİ, TEMMUZ, 2022

Tez Danışmanı: Doç. Dr. LÜTFİ TANER TUNÇ

Tez Eş Danışmanı: Prof. Dr. ERHAN BUDAK

Anahtar Kelimeler: İnce Cidarlı Yapılar, Süreç Sönümlenme, Tırlama Kararlılığı, Frezeleme İşlemi, Özel Geometrilik Freze Takımları

İnce cidarlı parçalar endüstride ve birçok mühendislik uygulamasında sıklıkla kullanılmaktadır. Bu parçalar, geometrileri nedeniyle yüksek bir mukavemet-ağırlık oranı sağladıkları için özellikle havacılık alanında yaygın olarak kullanılır. İnce cidarlı yapıların bazı örnekleri, uçak motorlarında kullanılan türbin ve kompresör kanatçıkları ve uçaklarda kullanılan iskelet yapılarıdır. Bunlara ek olarak, pim kanatlı yapılar enerji endüstrisinde ısı değiştiricisi olarak yaygın kullanılmaktadır. Bu parçaların işlenmesi, düşük dinamik rijitlikleri nedeniyle zordur. Bu nedenle, süreç kararlılık durumunu tahmin etmek için süreç içi iş parçası dinamiklerini modelleyerek kararlılık analizi gereklidir. Bu çalışmada ince cidarlı geometrilerin finiş frezeleme süreç kararlılığı detaylı olarak incelenmiştir. İş parçası dinamiğinin modellenmesinde, her kesme adımında talaş kaldırma ve kesici takım konumunun, iş parçası dinamikleri ve süreç kararlılığı üzerindeki etkisi göz önünde bulundurulmuştur. Ek olarak, değişken hatveli takımların ve dalgalı talaş yüzeyli takımların ince cidarlı parça frezeleme kararlılığı üzerindeki etkisi araştırılmış ve standart bir parmak freze ile karşılaştırılmıştır. Bu tezde, ince cidarlı iş parçası, sonlu elemanlar yöntemi (SEY) kullanılarak 3B ankastre giriş olarak modellenmiş ve kararlılık analizinde serbest uçtan sabit uca doğru rijitlikteki artış dikkate alınmıştır. Ayrıca, iş parçasının baskın eğilme ve burulma modları dikkate alınmıştır.

Talaşlı imalat süreçlerinde, kesme kenarı ile yüzeyde kalan titreşim dalgası arasındaki dinamik etkileşim, yapısal sönümlenmeye ek olarak sürecin kendisinden de oluşan süreç sönümlenme etkisi yaratır. Süreç sönümlenmesi, düşük kesme hızlarında daha derin kararlılık limitleri sağlar. Kararlılık analizinde, durum sonuçlarına göre kesici kenar geometrisi, yarı finiş stok kalınlığı ve izin verilen maksimum titreşim genliği gibi optimal parametreler seçilerek esnek parçanın finiş frezelemesi için süreç sönümlenmesi araştırılmıştır. Ayrıca, kararlılık, marjinal kararlılık ve tırlama koşullarının etkisi araştırılmış ve parçaların yüzey kalitesi üzerindeki etkileri değerlendirilmiştir.

ACKNOWLEDGEMENTS

Firstly, I am grateful to my supervisors, Prof. Erhan Budak and Assoc. Prof. Taner Tunc, for their guidance, motivation, mentorship, support and sharing their experience and knowledge throughout my junior level research career. I obtained non-negligible experience from Prof. Budak. Although he is mostly busy, he always shared his time with me for my all questions on chatter stability and structural vibration with strong patience. The mentorship of Prof. Tunc is also non-negligible. He shared his detailed machining knowledge and experience with me in each step of my thesis. I appreciate that Assoc. Prof. Tunc accepted me as a master student and always support me for my future career plans. I would like to thank to jury members; Prof. Burc Misirlioglu, Prof. Yusuf Menciloglu and Assoc. Prof. Umut Karaguzel for their time and significant suggestions on my thesis.

It was a great pride to be a member of the research crew in Manufacturing Research Laboratory (MRL). In my first experience in modal testing in machine tool applications, Kaveh and Faraz shared their times to show me the correct measurement methodology, which needs to have an expertise. Furthermore, we published 2 papers under the supervision of Prof. Budak. I also thank to my dear friend Amin, who helped and supported me on every problem that I faced with them in my master term. The discussions on philosophy and economy with Arash broaden my vision and affected my perspective on life. I would like to thank to Esra, Bora, Burcu, Zahra, Orkun, Beril, Sinem, Saif and Mahzad for their friendship and support. I would like to thank to Ozan Can Ozaner since he suggested me to apply master in Sabancı University. I believe that he will be one of the experts in machining field after his PhD.

I cannot achieve my studies without the help of technicians; Ertugrul Sadikoglu and Suleyman Tutkun. The discussions on thin-wall machining with Emir, who is the most skilled CAM programmer of Maxima Company improved my experimental perspective. The inspirational atmosphere of Sabancı University makes me more motivated during research.

It is time to thank to loves, my family, Fatma Yıldız, Mustafa Yıldız, Sezer Yıldız, for their self-sacrifice, generosity and support throughout my life.

Finally, I would like to express my special thanks to my lovely girlfriend, Ayşenur

Ateş, who always supports and stands with me. She is the best mechanical engineer & researcher in microfluidics and thermodynamics fields that I ever seen.

Table of Contents

1. INTRODUCTION	1
1.1. Machining of Thin-walled Parts and Regenerative Chatter Problem	1
1.2. Low-speed Milling with The Effect of Process Damping	3
1.3. Stabilizing Effect of Special End Mills.....	5
1.4. Objectives.....	6
1.5. Layout of Thesis.....	7
2. LITERATURE SURVEY	9
2.1. Stability Analysis in Milling of Thin-walled Parts	9
2.2. Application of Special End Mills in Chatter Suppression	12
2.3. Process Damping in Stability Analysis.....	13
3. HIGH-SPEED DYNAMICS OF MILLING	18
3.1. Introduction.....	18
3.2. Milling Stability Solution Considering Varying-Dynamics of IPW.....	18
3.3. Modeling of Varying IPW Dynamics	25
3.3.1. Experimental Validation	35
3.4. Application of Special End Mills in Milling of Thin-walled Parts.....	39
3.4.1. Introduction.....	39
3.4.2. Milling Stability Solution Using Discretized-Time Method	40
3.4.3. Stability Analysis Considering Varying-Dynamics of IPW	45
3.4.4. Stability Performance of Crest-Cut & Variable Pitch Tools	50
3.5. Summary	52
4. CHATTER-FREE FLANK MILLING OF THIN-WALLED PARTS	54
4.1. Introduction.....	54
4.2. Process Damping Model	55
4.2.1. Influence of The Cutting Edge Geometry and Modal Frequency	59
4.2.2. Selection of Stock Thickness	61
4.3. Stability Analysis Considering Varying-Dynamics of IPW at Low Cutting Speeds	69

4.4. Experimental Verification.....	75
4.5. Conclusions.....	81
5. SUMMARY OF THESIS.....	83
5.1. Important Outcomes.....	83
5.2. Futureworks	84

List of Tables

Table 1. Modal parameters of the cutting toll.....	24
Table 2. Material Database for Al-7075 [4]	24
Table 3. Workpiece geometries and natural frequencies	28
Table 4. Machining strategies	34
Table 5. Experiment parameters	35
Table 6. Geometrical parameters of end mills.....	50
Table 7. The number of passes and chatter-free area percentages.....	51
Table 8. Modal Parameters of the Milling Tool	63
Table 9. Change of natural frequency and normalized mode shape with stock thickness	65
Table 10. Simulation Cases for Verification with Tests.....	76
Table 11. Surface finish results with stability condition	81

List of Figures

Figure 1.1. Examples of products with thin-walled features	1
Figure 1.2. Surface finish with and without chatter.....	2
Figure 1.3. Milling strategies in impeller machining (a) flank (b) point milling [3].....	3
Figure 1.4. Cutter-workpiece interaction	3
Figure 1.5. Stability limit with process damping.....	4
Figure 1.6. Representative figures of (a) variable pitch and (b) crest-cut end mills [4]...	5
Figure 2.1. Block diagram of 1D regenerative chatter	9
Figure 2.2. Representative stability lobe diagram	10
Figure 3.1. Flexible tool-rigid workpiece system with dynamic chip thickness	19
Figure 3.2. Flexible tool-workpiece system.....	19
Figure 3.3. Procedure of FEA	25
Figure 3.4. a) Single element and b) multi-axial element models	26
Figure 3.5. FEM and multi-axial element stability solution algorithm.	27
Figure 3.6. Simulation result of multi-axial element model for thin-walled Ti6Al4V part presented by [20].	27
Figure 3.7. Real FRFs of Al-7075 plates with different geometries.....	28
Figure 3.8. Multi-axial element stability solution for thin-walled parts with different geometries (a) Plate #1 (b) Plate #2 (c) Plate #4.	29
Figure 3.9. Multi-mode stability analysis (a) Plate #1 (b) Plate #2.....	30
Figure 3.10. Effect of discrete axial element size simulated for Plate #2.....	30
Figure 3.11. Effect of radial depth of cut.....	31
Figure 3.12. Varying-FRF of multi-axial elements of Plate #4.....	32
Figure 3.13. FRF verification of Al-7075 thin-walled workpiece using modal testing at the plate middle-tip point.....	32
Figure 3.14. Stability lobe diagram of the tool-workpiece system.....	33
Figure 3.15. Stability limits of each pass (a) multi-axial element (b) single element models.....	35
Figure 3.16. Stability analysis result comparison for single & multi-element models with cutting tests.....	36
Figure 3.17. Surface finish measurements for (a) test 3 (b) test4 and (c) test 6	36
Figure 3.18. Sound spectrum at different chatter test points a) Test 3 b) Test 4 c) Test 5	

d) Test 6	37
Figure 3.19. Multi-mode and multi-axial element stability solution with local stable point for plate #2.....	38
Figure 3.20. Sound measurement and finished surface of the thin-walled part for local stable condition.....	38
Figure 3.21. Surface finish results for (a) Strategy 2 (b) Strategy 4.....	39
Figure 3.22. Delayed term approximation [22]	42
Figure 3.23. Flowchart of proposed approach with material removal stages of IPW	46
Figure 3.24. Varying-dynamics of IPW in point milling a) 1 st natural frequency b) 2 nd natural frequency c) FRF peak of 1 st mode d) 2 nd mode.....	47
Figure 3.25. Validation of IPW dynamics at different levels.	48
Figure 3.26. Local pitch variation for three different tool types.....	48
Figure 3.27. Varying stability limits on plate considering varying-dynamics of IPW ...	50
Figure 3.28. Surface finish quality maps for proposed STG and verifications.	52
Figure 4.1. Vibration mechanism of the metal cutting system at low and high cutting speeds.....	55
Figure 4.2. Process damping in milling for flexible tool-workpiece system.....	56
Figure 4.3. Effect of cutting edge geometry (a) hone radius (b) clearance angle (c) modal frequency on process stability at low cutting speeds.	60
Figure 4.4. Measurement of cutting edge radius.	61
Figure 4.5. Dominant (a) bending (b) twisting (torsional) modes of thin-walled workpiece with boundary conditions.....	62
Figure 4.6. (a) Workpiece and (b) measured tool FRFs	63
Figure 4.7. Process damping (a)force and (b)constant variation with vibration amplitude [3].....	64
Figure 4.8. Variation in (a)natural frequencies and (b)FRFs with the change of stock thickness.....	66
Figure 4.9. Optimal stock thickness selection as the system vibrates with 15 μ m amplitude (a)1 st mode (b)2 nd mode.	67
Figure 4.10. Low-speed stability limit comparison of 7 μ m and 35 μ m hone radii in flank milling of thin-walled part at 5 μ m vibration amplitude considering multi-mode.....	67
Figure 4.11. Optimal stock thickness selection as the system vibrates with 5 μ m amplitude (a)1 st mode (b)2 nd mode.	68

Figure 4.12. Stability limit including tool dynamics for 5 μ m vibration amplitude and 3.9mm stock thickness	69
Figure 4.13. Flowchart of the FE macro code	70
Figure 4.14. Material removal stages in flank milling of thin-walled part.	71
Figure 4.15. Varying a) FRF and stability limits at different cutting stages b) 1 st Mode c) 2 nd Mode for 20 μ m vibration amplitude and 0.8mm stock thickness.....	72
Figure 4.16. Varying-IPW dynamics FRFs for different finished part thickness (a) 2.9mm (b) 2.8mm (c) 2.7mm (d) 2.4mm (e) 2.2mm (f) 2.1mm.....	73
Figure 4.17. Varying stability limits at different cutting stages (a)1 st Mode (b)2 nd Mode for 25 μ m vibration amplitude and 0.9 mm radial depth of cut.	74
Figure 4.18. Experiment setup for workpiece dynamics verification.....	75
Figure 4.19. IPW dynamics simulation verification	76
Figure 4.20. Experiment points (a) Case 1 (b) Case 2 (c) Case 3 (d) Case 4 (e) Case 5 (f) Case 6.....	77
Figure 4.21. Sound and surface measurements of Case 1, a=40 mm (a) n=365 rpm (b) n=800 rpm.....	78
Figure 4.22. Sound and surface measurements of Case 3, n=800 rpm (a) a=5 mm (b) a=10 mm.	79
Figure 4.23. Sound and surface measurements of Case 6, a=40 mm (a) n=300 rpm (b) n=500 rpm.....	80

1. INTRODUCTION

1.1. Machining of Thin-walled Parts and Regenerative Chatter Problem

Products with thin-walled feature such as aero-engine blisks, impellers, frames, ribs, stiffeners and pin-finned heat sinks are commonly used in the aeronautics & aerospace, biomedical, and energy industries. These components provide superior mechanical performance due to their low weight-to-strength ratio, and some of them are generally manufactured from titanium, nickel, steel, aluminium and their alloys such as Inconel, stainless steel and Ti6Al4V, which have low machinability. Some examples of thin-walled parts are depicted in Figure 1.1.



Figure 1.1. Examples of products with thin-walled features

Although, thin-walled parts have tremendous mechanical properties as a product, machining of thin-walled parts is challenging due to high flexibility, strict tolerances, low structural damping and time-varying dynamics of thin-wall machining system.

In thin-wall machining, self-excited vibration is governed by workpiece dynamics that may result in deteriorated finished surface and lead to sudden tool wear and failure. Surface images of an example thin-walled part finished with and without chatter are demonstrated in Figure 1.2. As low cutting depths and feed rates are used in finishing operations, higher amount of production time is sacrificed in that stage. This leads to high production costs and that can be prevented by a detailed prediction model, which may

make possible to increase productivity without chatter. In conventional stability analysis, only dynamics of the initial workpiece geometry is considered, whereas in-process modeling of finish milling of thin-walled parts is needed to evaluate locational effects of chatter and finish process without chatter to obtain better surface quality with possible higher cutting depths that also reduces polishing time.



Figure 1.2. Surface finish with and without chatter

Due to foregoing reasons, chatter prediction and avoidance in machining of thin-walled parts is one of the most significant research studies in machining community [1]. Thin-walled components are generally produced by subtracting a large amount of mass from initial stock to achieve requirement of the product, thus any error and/or failure at the finishing stage may results high financial damage for the manufacturing companies [2]. In general, thin-walled parts are modeled as a plate-like structure to simplify analysis for developing more accurate prediction of stability condition in thin-wall machining processes.

On the other hand, structural dynamics of the workpiece is the main concern in modeling dynamics of finish milling operation since the most flexible element of the system is the workpiece, which has time-varying nature as material subtracted at each cutting stage. Therefore, workpiece dynamics should be modeled to evaluate dynamics of the in-process for more accurate stability predictions.

There are different milling strategies that the most common methods are flank milling and point milling as illustrated in Figure 1.3.

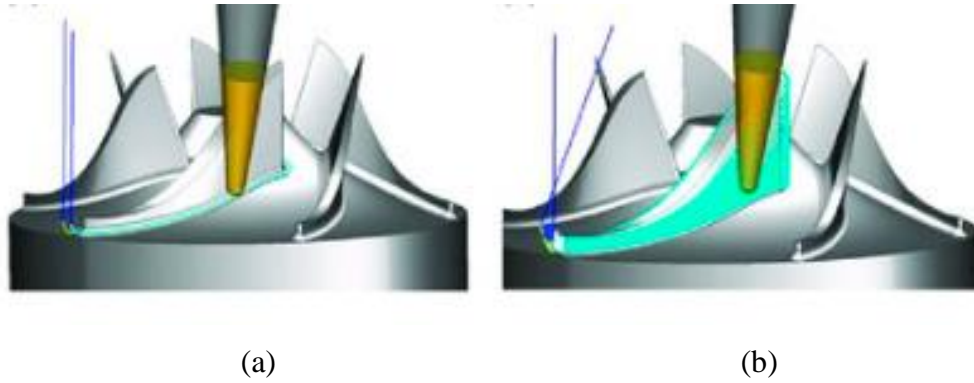


Figure 1.3. Milling strategies in impeller machining (a) flank (b) point milling [3]

Flank milling is the milling with using the periphery of the tool with large depth of cut in each pass. In point milling strategy, the tool tip and workpiece have a point contact and is generally used in milling of the parts with high curvatures, where flank milling cannot be applied due to geometric limitations.

For generalizing the milling of thin-walled parts, investigation can be separated to subsections, which are low-speed and high-speed milling.

1.2. Low-speed Milling with The Effect of Process Damping

Since the materials with low-machinability are widely used as thin-walled structure in industry, stability analysis of thin-wall finish milling requires further modelling at low cutting speeds due to non-linear process damping effect. This effect which provides vibration attenuation due to dynamic contact between cutting edge of the tool and the vibration waves left on the workpiece surface (see Figure 1.4) arises from the process itself in addition to the structural damping and extended chatter-free regions.

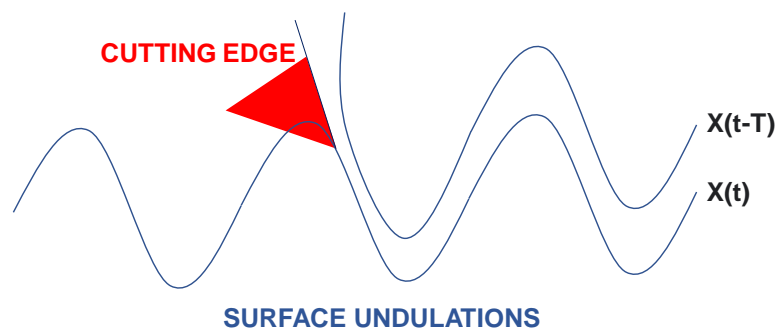


Figure 1.4. Cutter-workpiece interaction

Process damping may enable flank milling (i.e., finish the part with a very few passes) in finishing of thin-walled parts as illustrated in Figure 1.3 (a), and thus it reduces production time and tool wear drastically. Although, the workpiece has high flexibility, which increases chatter tendency, this additional damping provides higher stable depths to cut workpiece with one or few passes using the full length of cutting flute. In conventional chatter stability models, which do not consider non-linear process damping effect, self-excited vibration attenuation at low cutting speeds cannot be predicted accurately, since the stability limit is close to absolute limit as the stability pockets are narrow in comparison to higher speeds. However, higher stable depths can be achieved using the tool with proper cutting edge, optimal stock geometry to benefit process damping. The absolute stability limit variation is illustrated in Figure 1.5 with process damping effect.

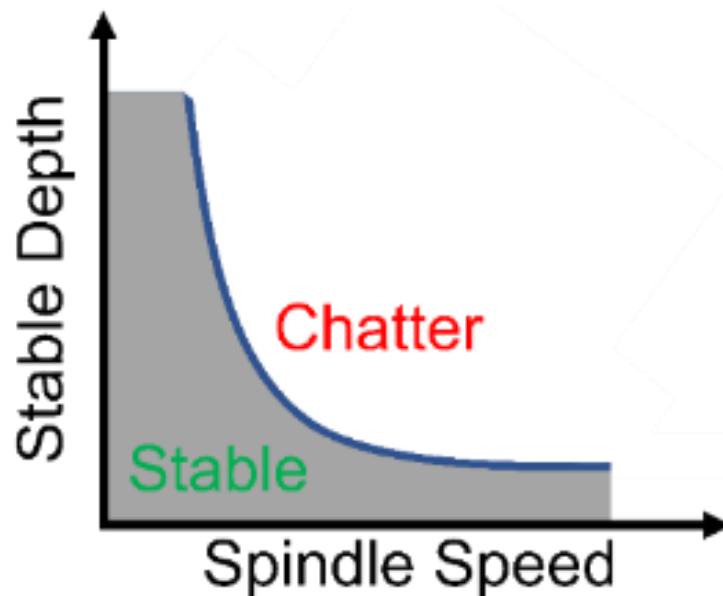


Figure 1.5. Stability limit with process damping.

Previous research has focused on the identification and modeling of process damping in machining using different mathematical and experimental methods. However, as the workpiece becomes more flexible, cutting with higher depth of cuts also becomes more challenging, and a detailed analysis is needed to evaluate milling with process damping. In addition, forced vibration may increase during cutting with process damping effect that may leave errors on the finished surface. In addition to process damping effect, system can be stabilized at low-cutting speeds by selecting semi-finish stock thickness. As material removed at each cutting step, IPW dynamics varies and should be considered for accurate stability prediction

1.3. Stabilizing Effect of Special End Mills

In addition to the process damping, increased stability limits can be obtained using an end mill with special geometry such as variable pitch and crest-cut geometries for desired spindle speed range. Optimal design of variable pitch tools provides enhanced stability at desired speed and frequency, which should be predicted to find optimal pitch variation. These tools generate multiple delays between successive cuts of teeth, which suppresses chatter. However, variable pitch tools provide a high stable cutting depth within a narrow spindle speed range. On the other hand, crest-cut tools have wavy form along the rake face, and both pitch and helix angles vary along the tool axis, leading continuous variation in phase angle (or delay), and thus improved stability within large spindle speed range. Variable pitch and crest-cut end mills are illustrated in Figure 1.6.

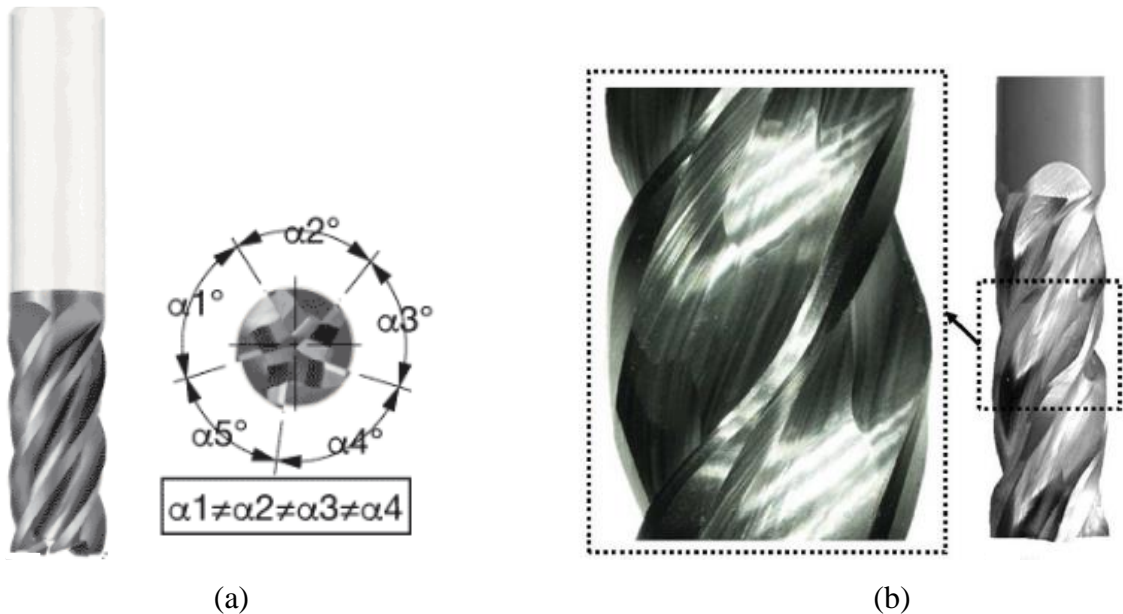


Figure 1.6. Representative figures of (a) variable pitch and (b) crest-cut end mills [4]

Investigation of the special end mill performance on finish milling stability of thin-walled parts is needed to increase productivity.

They can be selected optimally for milling of a specific thin-walled part geometry. If the workpiece has good machinability such as being made of aluminium, copper and zinc etc., it is possible to use high cutting speeds, where the stable regions become wider. Therefore, effectiveness of special end mills is in low-speed milling. Moreover, cutter location has a significant effect on milling stability limits since the dynamic response of

workpiece varies with respect to cutter location. Therefore, the stability analysis should be generalized for the overall milling process of the thin-walled workpiece to perform a stable cut from the start of the process to the end. By modeling the overall process, production time, as well as polishing times after finishing can be reduced since the finishing process can be achieved under completely stable conditions with a high material removal rate.

1.4. Objectives

This thesis aims to investigate stability conditions in milling of thin-walled parts considering varying-dynamics of IPW at low and high cutting speeds. In this respect, different approaches have been proposed as given below:

The case, where the thin-walled workpiece is the most flexible element of milling system needs a detailed stability analysis. In this respect, stability analysis should be performed combining with workpiece dynamics simulations, since the workpiece dynamics has time-varying nature as material removed and cutter location (CL) changes. In some cases, only one the dominant modes of the workpiece may be excited that leads to local stable condition. In this condition, the milling system is only stable or unstable at different CLs. Therefore, multi-modes of the workpiece are taken into account in stability analysis.

In this thesis, stiffness values of axial discrete elements of the workpiece are included stability analysis for improved productivity considering varying-dynamics of the workpiece. This approach is verified with milling experiments as the first time in literature. On the other hand, use of special tools such as variable pitch and crest-cut milling may increase stable depths at desired cutting speeds, but they may lose their effectiveness due to varying modal frequencies due to mass removal. The performance of special end mills is investigated in finish milling of thin-walled parts.

In another investigation of this thesis, process damping effect, which is generally observed at low cutting speeds and occurs due to dynamic penetration between tool flank and surface undulations left on the workpiece. This effect provides higher chatter-free depths and may enable to finish thin-walled part with one or a few passes. In this part, the aim of the study is to achieve deeper stable limits by selecting optimal semi-finish stock thickness and proper cutting edge geometry for increased stabilizing effect of process damping. It is also known that marginal stability during process damping has influence

on surface finish quality that is also evaluated experimentally. In addition, as the workpiece becomes more flexible during material removal, process damping may not be sufficient due to reduction in modal frequency and stiffness. For this purpose, the in-process workpiece is modeled using finite element analysis (FEA) and the multi-mode stability of thin-walled part is considered to evaluate local stable conditions.

1.5. Layout of Thesis

This thesis is organized as follows:

In Chapter 2, a detailed literature survey on stability in milling of thin-walled parts, application of special end mills in chatter suppression, and non-linear process damping effect at low cutting speeds is provided. Then, high-speed milling stability of thin-walled parts is investigated considering varying-dynamics of the workpiece from free-end to fixed-end using discrete axial elements in Chapter 3. This model is firstly proposed by Budak and Altintas [5], and they only consider first bending mode of plate-like structure in stability analysis. Thus, this thesis presents previously developed model considering multi-modes of the structure and varying-dynamics of IPW, and this model is verified through experiments as the first time in literature. In this regard, different cutting strategies are proposed to improve productivity with the benefit of multi-axial element stability model. Moreover, performance of special end mills in thin-wall milling using a novel method in modeling IPW dynamics considering change in CL and material removal is presented. Milling of thin-walled parts can be achieved with higher material removal rates (MRR) without chatter at low-cutting speeds. In Chapter 4, process damping is investigated in low-speed milling of thin-walled part made of titanium-alloy. In this part, optimal selection of semi-finish stock thickness is carried out for increased stability limit. Moreover, varying-dynamics of IPW is considered in analyses. It is known that cutting edge geometry and modal frequency have significant effects on process damping and chatter stability. In this respect, effects of cutting edge geometry and modes of thin-walled part on process damping, and thus chatter stability are demonstrated through simulations. In addition, marginal stable vibration marks left on the surface are identified with surface measurements, and they are also used for verification of simulation results. In low-speed chatter stability analysis, an analytical method developed in [6] is used in simulations. Finally, different cases are simulated and verified through surface and sound

measurements. In Chapter 5, the important outcomes and major contributions of the thesis are summarized. In addition, potential further investigations are discussed.

2. LITERATURE SURVEY

2.1. Stability Analysis in Milling of Thin-walled Parts

Chatter problem in metal cutting operations is observed and reported by Taylor [7] as the first time in literature. Self-excited vibrations is one of the most common limitations in metal cutting applications [1,8], thus determination of stable process parameters (i.e. depth of cut and speed) is significant in machining. Regeneration mechanism, which is mainly due to the delay between two subsequent cuts on the same surface was proposed as the main source of unstable condition in metal cutting systems in literature first in [9,10]. The closed-loop block diagram and regeneration mechanism in orthogonal cutting system are illustrated in Figure 2.1.

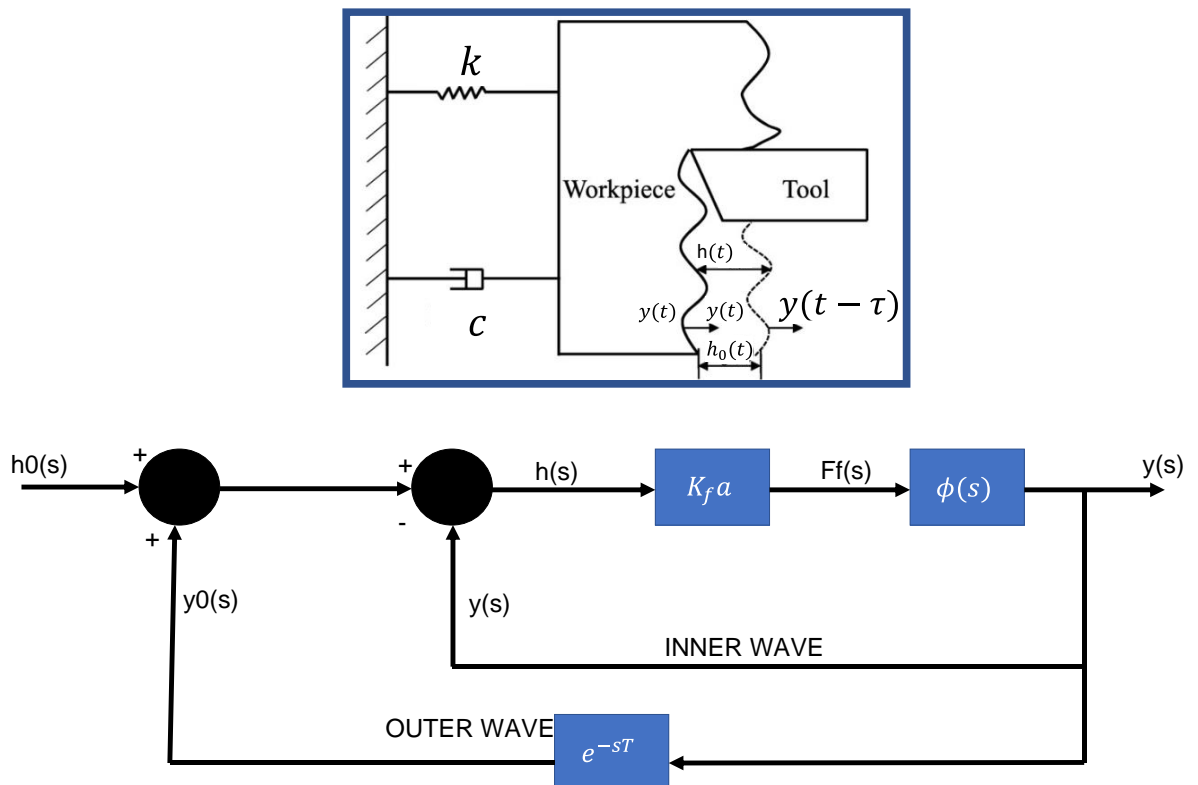


Figure 2.1. Block diagram of 1D regenerative chatter

Stability lobe diagram, which demonstrates stable and unstable cutting depths (see Figure 2.2) with corresponding spindle speeds. The stability lobe diagram was solved analytically for orthogonal cutting system, where the regeneration arises in only one (feed) direction [11–13].

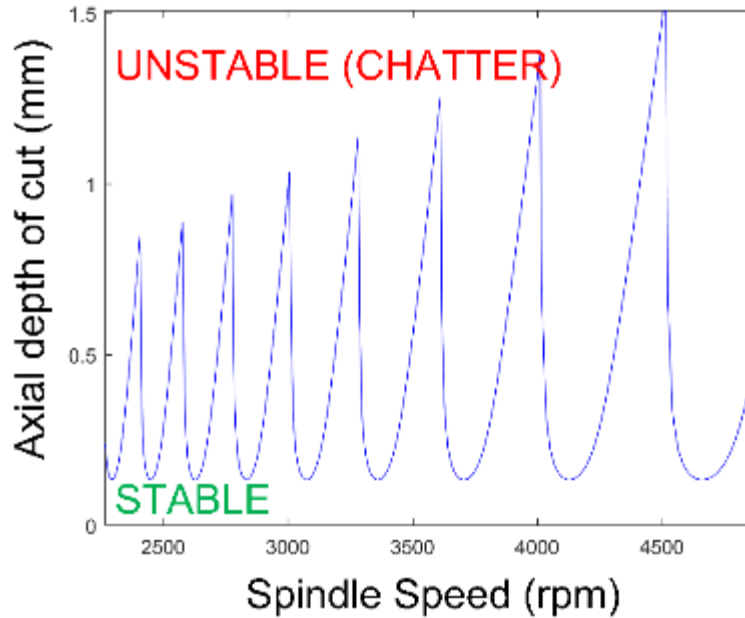


Figure 2.2. Representative stability lobe diagram

Stability analysis of milling is more challenging in comparison to orthogonal cutting and turning, since the dynamic cutting forces and directional coefficients, which relates dynamic chip thickness and cutting forces are time-varying due to interrupted nature of the rotating tool. Prediction of stable and unstable conditions is needed in machining applications, since trial-and-error approach causes costly experimental efforts. In this respect, Tlustý et al. [14,15] solved a milling stability in time-domain, which is time consuming. Their solution includes process damping effect and non-linearities in stability analysis. However, directional coefficients have to be included in stability analysis for accurate prediction of milling stability lobes. Sridhar et al. [16] considered periodic dynamic milling force constants in numerical stability analysis. Numerical time domain simulations bring high computation costs. To handle this, Minis and Yanushevsky [17] firstly developed analytical iterative method using the model proposed by [16]. Lee et al. [18] solved milling stability using a numerical method based on Nyquist criterion in frequency domain. Altintas and Budak [19] presented analytical milling stability lobes

by taking the average term of periodic directional cutting force coefficients. Budak and Altintas [5] reformulated analytical stability solution by including cutting tool and flexible workpiece dynamics as multi-degree of freedom (DOF) system. In this study, the formulation of varying dynamics of the flexible workpiece in the axial direction is presented. After, Budak and Altintas [20] presented the analytical milling chatter stability simulations for single and multi-degree of freedom (DOF) milling systems modeling cutting tool as both flexible and rigid in milling of a thin-walled workpiece. Later, Merdol and Altintas [21] developed a frequency domain solution, which firstly presented by Budak and Altintas [5], which is called as multi-frequency solution for improved chatter prediction accuracy especially as low radial immersion is used. Insperger and Stépán [22] derived semi-analytical method by discretizing time to find stability diagrams of the milling operations.

Chatter vibrations caused by the regeneration effect in metal cutting operations result in poor surface quality, rapid tool failure, and machine tool damage. This phenomenon becomes more prominent in machining thin-walled structures made from hard-to-cut materials. The most commonly used method to avoid regenerative chatter is the application of stability diagrams (SLD) based on the frequency response functions (FRF) of the tool and workpiece [17,19]. Generally, long slender tools show more flexible behavior at the cutting point compared to the workpiece. Hence, the workpiece dynamics and its variation during material removal are neglected in most studies [19]. However, in machining of thin-walled structures, workpiece dynamics have a substantial effect on the process stability. Thus, the stability analysis must include the mass removal effect, i.e., IPW dynamics [23]. Altintas et al. [24] developed a dynamic model for rigid tool-flexible workpiece interaction using the finite element method. The proposed model predicts form errors, displacements of the flexible part at the tool-workpiece engagement region and milling forces. The chip thickness variation and varying dynamics of a flexible workpiece are considered in the calculation of the milling forces and final surface topography. The varying dynamics of thin-walled structures are usually obtained using the finite element (FE) method at CL, considering the material removal. Bravo et al. [25] modelled the machined workpiece using FE analysis at each cutting depth along the height, while Thevenot et al. [26] obtained the stability diagrams for various CLs in the feed direction. For more complex part geometry and tool paths, Biermann et al. [27] coupled the FE

model of the workpiece with time-domain simulation to predict stable and unstable regions in the 5-axis milling of turbine blades.

Budak [28] demonstrated flank milling of flexible parts such as turbine blades is challenging to achieve chatter-free high quality surface finish. This study presents improvements in surface finish and high productivity with chatter attenuation by using an optimal variable pitch tool and adaptive control of cutting forces. Alan et al. [29] investigated the effect of mass removal in flexible plate type workpiece on stability solution using structural modification method. Different strategies are proposed, which are step and layer removal with different element thickness values, and their effects on process stability are presented. Structural modification method is also applied for the modeling dynamics of thin-walled blades, which is used in the stability analysis of five-axis milling by Budak et al. [23]. In this method, FRF is updated by adding removed elements along the tool path. In a different method, Tuysuz et al. [30] obtained the IPW dynamics by replacing the removed mass with a fictitious substructure having opposite dynamics of the removed material. Smith et al. [31] presented different designs of sacrificial structure preforms to support flexible part to increase rigidity of the workpiece. Koike et al. [32] used FE method to update static stiffness of IPW for reducing workpiece deflections. Semi-finish stock geometry has crucial influence on stability, since increasing the dynamic stiffness of the workpiece provides improved stability, while increasing the radial depth decreases stability limit. In this respect, an optimal stock geometry of the thin-walled part was proposed by Tunc and Zatarain [33]. They proposed a method to generate cutter axis and semi-finish tool path considering optimal stock shapes, which varies along feed and axial directions of the thin-walled blade for enhanced stability. Moreover, they have obtained up to 50% increased stability limit by selecting optimal stock geometry.

2.2. Application of Special End Mills in Chatter Suppression

Another method for increasing machining stability is the application of special geometry end mills. Many researchers have reported the advantages of special-geometry tools in suppressing chatter. Slavicek [34] demonstrated the effect of irregular tooth pitch on chatter stability. Budak [35] proposed a design method for variable-pitch (VP) milling

tools to maximize stability limits in machining airfoils. Suzuki et al. [36] showed that the irregular pitch tools designed by their proposed method provide robust chatter suppression under speed and frequency variations, which are the main limitations in applying VP tools. As another type of special tool, chatter suppression with variable helix tools is studied in [37–39]. The stability of serrated tools with more complex geometry is modelled and discussed in [40,41] for rigid workpieces and by Bari et al. [42] in flexible structures. On the other hand, crest-cut tools offer better chatter suppression performance due to their continuously varying pitch and helix angle along the tool axis. Dombovari et al. [43] and Sanz et al. [44] obtained stability diagrams for different cases with crest-cut tools using distributed delays by applying the semi-discretization method. Later, Tehranizadeh et al. [4] used precise geometric models for force and stability predictions of crest-cut tools, and verified them experimentally. They proposed a guideline for selecting the wave geometry of crest-cut tools to maximize stability based on the process conditions. It is demonstrated that crest-cut tools offer much wider stable regions compared to standard and tuned variable-pitch tools for a specific cutting speed [4].

2.3. Process Damping in Stability Analysis

In machining stability research, process damping effect is commonly observed at low cutting speeds due to dynamic interaction between flank face and surface waves left on the surface. It is well known that process damping, provides stabilizing effect in various machining applications such as workpiece material with low-machinability and for machine tools with speed limitation. In addition, process damping enables to improve productivity in machining of thin-walled parts such as turbine blades, heat sinks and frames, where the chatter stability is governed by the dynamics of the flexible workpiece. In literature, there are several studies on identification and modeling of process damping in machining applications. Das and Tobias [45] firstly proposed a theoretical model for regeneration mechanism in orthogonal cutting system including wavelength effect, which increases stability limit at low cutting speeds. However, the dynamic interaction between cutting edge and vibration waves left on the machining surface was not considered in the developed model. Sisson and Kegg [46] investigated low-speed machining stability and the cutting edge geometry (edge radius and clearance angle) effect on process damping as the first time in the literature. Some of the studies [47,48] demonstrated identification

methods for process damping constants experimentally, and provided investigation on the influence of tool vibration and tool wear in low-speed machining. Process damping has a non-linear nature; Tlustý and Ismail [15,49] presented non-linearities in machine tool vibration, stability analysis, and process damping phenomena considering cutter vibration frequency and cutting speed. Process damping is mainly due to contact dynamics between tool edge and wave undulation on workpiece surface during cutting. In this regard, Wu [50] proposed a dynamics model, which includes stress distribution and elastic contact mechanics in cutting zone for orthogonal cutting to present process damping due to tool-workpiece penetration. Later, Montgomery et al. [24] developed milling dynamics model for flexible cutter-workpiece system implementing tool and wavy surface interaction. However, detailed modeling of plunging effect as a function of frequency, wavelength was a further investigation of their study. Later, Elbestawi et al. [51] reformulated Wu's theory [50] for improved stability analysis with process damping that incorporates variation in wave left on the surface and flank wear effect for the case, where the first derivative of the vibration amplitude (i.e. slope of the wave) is higher than the clearance angle. Chou et al. [52] investigated the performance of sharp and tool with worn flank face in turning stability. Furthermore, penetration volume was simplified as prismatic geometry and the mathematical model was presented as an analytical model by finding the roots of characteristic equation in Laplace domain. Clancy et al. [53] generalized the turning stability and process damping with the influence of flank wear by presenting three-dimensional dynamic force solution for more complex cutting tool geometries. This model enables to predict stability chart analytically in frequency domain in a more accurate manner in comparison to previous studies. Huang and Wang [54] developed a process damping model involving friction and plunging into planar dynamic force equations. Moreover, they have examined the effects of machining parameters such as feed rate, cutting depth and velocity on process damping. They also identified the dynamic cutting factor, which has influence on dynamic milling forces from vibration signal using an analytical method mechanistically. Altintas et al. [55] demonstrated a dynamic orthogonal cutting model, which presents a dynamic force constant identification method from various dynamic tests by exciting the cutting tool by fast tool servo. Later on, Eynian and Altintas [56] adapted the same model in turning and they investigated effect of insert geometry by modelling dynamic forces in three-dimension. The proposed method is time consuming and cannot be generalized since there is need to

carry out the cutting tests for different modal parameters, cutting edge features to calculate stability with the effect of process damping. Budak and Tunc [57] presented a practical method, which does not require time-consuming machining tests for identification of process damping. In their identification method, average process damping coefficient is found from the difference between the predicted and experimental stability limits. Then, conservation of energy is used to calculate penetration constant, which depends on the elastic properties of cutter and workpiece material pair by using numerical calculation of penetration volume between flank face of the tools and the waves left on the workpiece surface.

Process damping effect has nonlinearities, thus it increases the marginally stable field within a wide range of cutting depth and speed. Ahmadi and Ismail [58] discussed linear and non-linear models in process damping and investigated them experimentally. Bachrathy and Stépán [59] solved the stability under process damping effect using time-discretization method, whereas the developed model is not accurate since the indentation volume effect was not investigated in depth. Their model is not enough to predict low-speed stability accurately, where the vibration wavelength is lower than the worn land. After, Molnar et al. [60] extended this stability analysis with process damping by modeling the system as one degree-of-freedom, and showed this effect for milling with low radial depth of cuts and speeds. Budak and Tunc [61] showed the analytical solution for stability with process damping in frequency domain for milling and turning applications. They have demonstrated the effect of modal frequency and cutting edge geometry, then verified the analytical predictions with time-domain simulations and experiments. Ahmadi and Ismail [62] proposed an analytical solution to determine region between lower and upper stability boundaries, where the system vibrates with a certain amplitude (i.e. limit cycles) in plunge turning operation. Tunc and Budak [6,63] carried out various analyses and tests to demonstrate the influence of process conditions, vibration behavior and cutting edge geometric parameters on stability limits under process damping effect in detail. They showed that the cylindrical flank geometry end mills have superior stability performance in comparison to planar flank geometries. Jin and Altintas [64] developed a process damping model in micro-milling using finite element analysis (FEA), and they identified modal parameters using piezo-actuator system. Tyler and Schmitz [65] proposed an analytical velocity-based stability model under process damping effect, and identified process damping constant from machining

of flexure workpiece clamping system. Ahmadi and Altintas [66] presented a novel approach to predict the process damping constant. Basically, they obtained damping coefficient from measured tool vibration data using output-only modal analysis method, after indentation constant is calculated using process damping coefficient and indentation volume. In a recent study, Wan et al. [67] proposed inverse process damping identification method, which uses operational modal analysis in milling from stable cutting experiments. Wan et al. [68] used mechanistic method to evaluate process damping in milling considering velocity dependency and penetration effect. They linearized the penetration forces with small amplitude assumption.

In addition to the first dominant mode, machining dynamics system may include other vibration modes that should be considered in stability analysis. In this respect, Mohammadi et al. [69,70] demonstrated the effect of multi-mode at different modal frequencies on stability limit under process damping effect analytically and experimentally. Li et al. [71] presented a dynamic milling model, which includes mode-coupling and process damping effect to predict stability limits and dynamic force induced surface location error using first order semi-discretization and second order full-discretization methods. On the other hand, their model simplifies cutting edge penetration using wear land calculation that reduces prediction accuracy. Later, they [72] applied the same model in milling of thin-walled workpiece, whereas they only considered cutter location and first vibration mode, since second mode of presented workpiece geometry is dynamically rigid, and also their model does not include effect of material removal during cutting.

Modeling dynamics of five-axis milling operations is more complicated since the cutter-workpiece surface interaction changes due to the orientation of the tool or part along the tool path. Tuysuz and Altintas [73] developed a model in five-axis impeller machining using asymptotic stability law with process damping. Later, Tang et al. [74] established a process damping coefficient and stability limit prediction method considering cutter-workpiece engagement (CWE) and finite amplitude stability in five-axis milling.

In comparison to the standard end mill, special geometry such as variable pitch and crest cut tools provide higher stability limits. Tehranizadeh et al. [75] investigated the performance of special end mills in milling of thin-walled workpiece considering varying-dynamics of workpiece with material removal and multi-mode. They proposed surface finish quality maps to evaluate local effects of chatter on thin-walled part.

Recently, Feng et al. [76] predicted process damping in thin-wall milling using velocity-dependent mechanism instead of ploughing mechanism considering change in cutter location at low radial immersions. However, they did not consider varying IPW dynamics. Wang et al. [77] demonstrated process damping in thin-wall milling with and without material removal effect considering change in cutter location (CL) and multiple dominant modes of the plate, and they modelled IPW by combining FEA and structural modification methods. In addition, they showed the finished topographies with the vibration waves left on the surface texture as the process is stable and unstable. Feng et al. [78] developed a modeling approach including both velocity-dependency and ploughing effects for process damping. Their model also considers change in penetration due to deflections of cutter-workpiece pairs. Li et al. [79] proposed an end mill with micro-chamfering edge to improve stability limit at low cutting speeds in machining of thin-walled Ti-6Al-4V. They solved stability limit numerically, which is time-consuming.

All these foregoing research studies focus on the identification and modeling approaches of process damping in machining using different mathematical and experimental methods. However, as the workpiece becomes more flexible, cutting with higher depth of cuts becomes more challenging, and a detailed analysis is needed to evaluate stability in milling with process damping. In addition, forced vibration may increase during cutting with process damping effect that may leave errors on the finished surface. Furthermore, effect of stock thickness by relating varying-dynamics of IPW on milling stability under process damping effect has not been investigated in literature.

3. HIGH-SPEED DYNAMICS OF MILLING

3.1. Introduction

In this chapter, high-speed stability of thin-wall milling systems is investigated considering varying-dynamics of the workpiece. The influence of axial elements of the workpiece (i.e., from free-end to fixed-end) included in stability solution. This model demonstrates that higher chatter-free axial depths can be achieved in comparison to conventional single-element model. Multi-axial element model is simulated considering multi-mode of the workpiece and the model is verified with various tests as the first time in literature. Stability performance of special end mills such as variable pitch and crest-cut is also investigated in milling of thin-walled parts made of hard-to-cut material. In this study, thin-walled part dynamics is modeled using FE analysis and a practical approach is proposed to prevent high number of iterations between workpiece dynamics and stability simulations.

3.2. Milling Stability Solution Considering Varying-Dynamics of IPW

Analytical solution of milling stability, which is zeroth order approximation (ZOA) was developed by Altintas and Budak [19]. This solution takes the only DC component (average term) of time-varying periodic directional dynamic force coefficients in their Fourier expansions. Milling dynamics, where the tool is the most flexible component of the cutting system and dynamic chip thickness are illustrated in Figure 3.1.

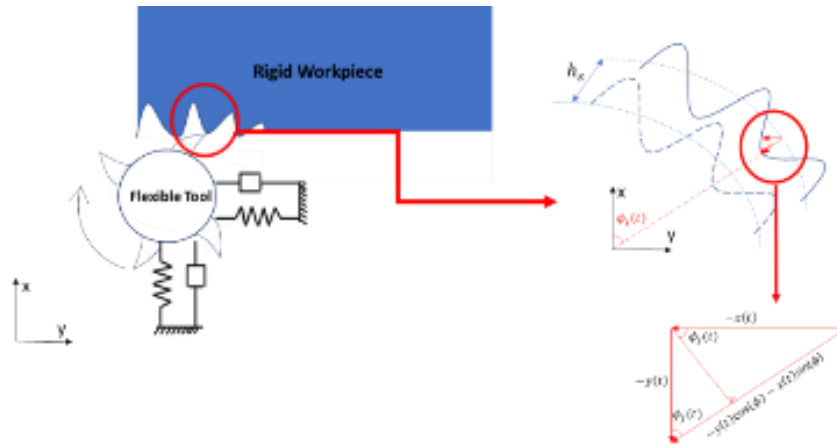


Figure 3.1. Flexible tool-rigid workpiece system with dynamic chip thickness

Later, they extended the analytical stability solution for flexible tool-workpiece system [5].

In this part of the thesis, ZOA is presented for flexible tool-workpiece systems. The dynamic milling system is modelled as multi degree-of-freedom (DOF), where the flexible components of the system are the cutting tool and thin-walled part. As tool goes from free-end to fixed-end of the structure, stability limit increases due to their higher elemental stiffness, where more than one axial elements may in cut. In this regard, varying-dynamics of tool and workpiece from free-end to fixed-end is considered as multi-axial element, which provides improved stability limit and that model is simulated and experimentally verified. The multi DOF flexible tool-workpiece model is illustrated in Figure 3.2.

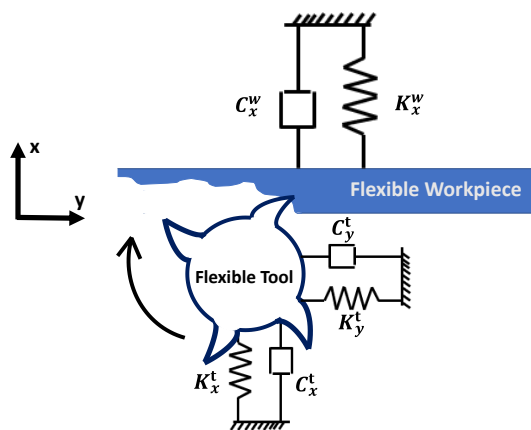


Figure 3.2. Flexible tool-workpiece system

Dynamic displacements of the tool and the thin-walled part system in x - y direction are

expressed as follows:

$$\begin{aligned}\delta_x &= [(x^t(t) - x^t(t - \tau)) - (x^w(t) - x^w(t - \tau))] \\ \delta_y &= [(y^t(t) - y^t(t - \tau)) - (y^w(t) - y^w(t - \tau))]\end{aligned}\quad (3.1)$$

In Eq. (3.1), $x^t(t)$, $x^t(t - \tau)$, $y^t(t)$, $y^t(t - \tau)$ are the dynamic inner and outer vibration wave modulations due to tool vibrations generated by two successive cutting edges of the tool in x - y direction respectively. $x^w(t)$, $x^w(t - \tau)$, $y^w(t)$, $y^w(t - \tau)$ are the dynamic inner and outer vibration wave modulations due to workpiece vibrations generated by two successive cutting edges of the tool in x - y direction respectively.

The total dynamic chip thickness in radial direction can be expressed as:

$$h(\phi_j) = \delta_x \sin(\phi_j) + \delta_y \cos(\phi_j) \quad (3.2)$$

Dynamic milling forces in tangential and radial direction can be written as:

$$\begin{aligned}F_{tj} &= K_{tc} a h(\phi_j) g(\phi_j), \quad F_{rj} = K_r F_{tj} \\ \text{where,} \\ g(\phi_j(t)) &= \begin{cases} 1 & \text{if } \phi_{en} < \phi_j(t) < \phi_{ex} \\ 0 & \text{else} \end{cases}\end{aligned}\quad (3.3)$$

In Eq. (3.3), K_{tc} , a , $g(\phi_j(t))$, ϕ_{en} , ϕ_{ex} are tangential cutting force coefficient, stability limit, unit step function, enter and exit angles, which decides the tool in cut or out of cut respectively. The local dynamic milling forces can be expressed in planar x - y coordinates for the system, where the tool has N number of cutting edges as below:

$$\begin{aligned}F_x &= \sum_{j=0}^{N-1} (-F_{t,j} \cos \phi_j - F_{r,j} \sin \phi_j) \\ F_y &= \sum_{j=0}^{N-1} (F_{t,j} \sin \phi_j - F_{r,j} \cos \phi_j)\end{aligned}\quad (3.4)$$

The dynamic planar milling forces are expressed in matrix form as follows [19]:

$$\begin{Bmatrix} F_x \\ F_y \end{Bmatrix} = \frac{1}{2} aK_{tc} \begin{bmatrix} \alpha_{xx} & \alpha_{xy} \\ \alpha_{yx} & \alpha_{yy} \end{bmatrix} \begin{Bmatrix} \delta x \\ \delta y \end{Bmatrix} \quad (3.5)$$

Time-variant periodic directional dynamic milling force coefficients, which relates dynamic force and vibration. The average terms of coefficients can be written as follows:

$$\begin{aligned} \alpha_{xx}^0 &= \frac{1}{2} [\cos(2\phi) - 2K_r\phi + K_r\sin(2\phi)]_{\phi_{ex}}^{\phi_{en}} \\ \alpha_{xy}^0 &= \frac{1}{2} [-\sin(2\phi) - 2\phi + K_r\cos(2\phi)]_{\phi_{ex}}^{\phi_{en}} \\ \alpha_{yx}^0 &= \frac{1}{2} [-\sin(2\phi) + 2\phi + K_r\cos(2\phi)]_{\phi_{ex}}^{\phi_{en}} \\ \alpha_{yy}^0 &= \frac{1}{2} [-\cos(2\phi) - 2K_r\phi - K_r\sin(2\phi)]_{\phi_{ex}}^{\phi_{en}} \end{aligned} \quad (3.6)$$

Vibrations of the tool and workpiece at chatter frequency are formulated as given below [5]:

$$\begin{aligned} \{\delta^t(j\omega_c)\} &= [\Phi^t(j\omega_c)]\{F\}e^{j\omega_c t} \\ \{\delta_0^t(j\omega_c)\} &= e^{-j\omega_c T}\{\delta^t(j\omega_c)\} \\ \{\delta^w(j\omega_c)\} &= -[\Phi^w(j\omega_c)]\{F\}e^{j\omega_c t} \\ \{\delta_0^w(j\omega_c)\} &= -e^{-j\omega_c T}\{\delta^w(j\omega_c)\} \end{aligned} \quad (3.7)$$

In Eq. (3.7), $[\Phi^t(j\omega_c)]$ and $[\Phi^w(j\omega_c)]$ are frequency response function (FRF) matrices of cutting tool and workpiece respectively. From Eqs. (3.5) and (3.7) following formula is obtained [19]:

$$\{F\}e^{j\omega_c t} = \frac{1}{2} aK_{tc} (1 - e^{j\omega_c T}) [\Phi(j\omega_c)] \{F\}e^{j\omega_c t} \quad (3.8)$$

$\omega_c T$ is the phase difference between two subsequent cuts. Eq. (3.8) has non-trivial solution since:

$$\det \left[[I] - \frac{1}{2} K_{tc} a (1 - e^{j\omega_c T}) [\alpha_0] [\Phi(j\omega_c)] \right] = 0$$

where,

$$[\Phi(j\omega_c)] = \begin{bmatrix} \Phi_{xx}^t & \Phi_{xy} \\ \Phi_{yx} & \Phi_{yy}^t - \left(- \sum_{k=1}^m (\Phi_{yy,k}^w) \right) \end{bmatrix} \quad (3.9)$$

In Eq. (3.9), tool and workpiece FRFs are superposed in flexible y -direction of the workpiece since the workpiece is rigid in x -direction. In addition, k stand for number of workpiece modes. Eigenvalue of the Eq. (3.9) is expressed as:

$$\Lambda = -\frac{N}{4\pi} a K_t (1 - e^{-j\omega_c T}) \quad (3.10)$$

As the dynamic chip thickness varies in planar x - y directions, cross FRFs (Φ_{xy} and Φ_{yx}) becomes zero and the characteristic equation can be obtained as [5]:

$$a_0 \Lambda^2 + a_1 \Lambda + 1 = 0$$

where,

$$a_0 = \Phi_{xx}^t(i\omega_c) (\Phi_{yy}^t(i\omega_c) + \sum_{k=1}^m (\Phi_{yy,k}^w(i\omega_c))) (\alpha_{xx}^0 \alpha_{yy}^0 - \alpha_{xy}^0 \alpha_{yx}^0) \quad (3.11)$$

$$a_1 = \alpha_{xx}^0 \Phi_{xx}^t(i\omega_c) + \alpha_{yy}^0 (\Phi_{yy}^t(i\omega_c) + \sum_{k=1}^m (\Phi_{yy,k}^w(i\omega_c)))$$

After finding the roots of the quadratic equation in (3.11):

$$\Lambda = -\frac{1}{2a_0} \left(a_1 \pm \sqrt{a_1^2 - 4a_0} \right) \quad (3.12)$$

From Eq. (3.10), stability limit can be written substituting $\Lambda = \Lambda_R + j\Lambda_I$ and $e^{-j\omega_c T} = \cos(\omega_c T) - j\sin(\omega_c T)$ as [19]:

$$a_{LIM} = -\frac{2\pi}{NK_t} \left[\frac{\Lambda_R(1 - \cos \omega_c T) + \Lambda_I \sin \omega_c T}{(1 - \cos \omega_c T)} + j \frac{\Lambda_I(1 - \cos \omega_c T) - \Lambda_R \sin \omega_c T}{(1 - \cos \omega_c T)} \right] \quad (3.13)$$

Since stability limit a_{LIM} is a real quantity, imaginary part of the Eq. (3.13) must be vanish and the stability limit can be expressed as given below [19]:

$$a_{LIM} = -\frac{2\pi\Lambda_R}{NK_{tc}} (1 + \kappa^2) \quad (3.14)$$

where;

$$\kappa = \frac{\Lambda_I}{\Lambda_R} = \sin(\omega_c T) / (1 - \cos(\omega_c T)) = \tan(\eta)$$

In Eq. (3.14), η stand for phase shift of the eigenvalue and $\omega_c T$ can be written as:

$$\omega_c T = \cos^{-1} \left(\frac{\kappa^2 - 1}{\kappa^2 + 1} \right) = -\cos^{-1} (2\eta) \quad (3.15)$$

$$\omega_c T = \epsilon + 2k\pi$$

where, (3.16)

$$\epsilon = \pi - 2\eta$$

In Eq. (3.16), ϵ is the phase difference between two successive waves left on the part surface. Finally, spindle speed can be expressed as given below [19]:

$$n = \frac{60\omega_c}{N(\epsilon + 2k\pi)} \quad (3.17)$$

In Eq. (3.17), k stands for number of vibration waves or number of lobes.

In this study, 10 mm diameter carbide end mill is used in cutting tests and the FRF of the tool is measured at first using impact hammer test, and then the modal parameters are extracted and provided in Table 1.

Table 1. Modal parameters of the cutting toll

D-10 mm Carbide End Mill	Natural Freq. (Hz)	Modal Stiffness (N/m)	Damping Ratio (%)
<i>x-direction</i>	3479	8.6×10^6	2,20
<i>y-direction</i>	3500	1.2×10^7	1,52

The end mill has rake and helix angles of 7° and 39° , respectively.

Static cutting force coefficients are calculated using the material database given in Table 2. K_{tc} and K_r are identified as 959 MPa and 0.26 respectively. Cutting force coefficients are identified from experimentally calibrated data provided by [4].

Table 2. Material Database for Al-7075 [4]

$\tau_s = 297.1 + 1.1\alpha$ $\beta_n = 18.8 + 6.7h + 0.0076V_c + 0.26\alpha_n$ $\phi_n = 24.2 + 36.7h + 0.005V_c + 0.3\alpha_n$
--

Static milling force coefficients, which depends on cutting edge geometry and tool-workpiece material are expressed as follows [80]:

$$K_{tc} = \frac{\tau_s}{\sin(\phi_n)} \frac{\cos(\beta_n - \alpha_n) + \tan^2(\beta_n) \sin(\beta_n)}{\sqrt{\cos^2(\phi_n + \beta_n - \alpha_n) + \tan^2(\beta_n) \sin^2(\beta_n)}}$$

$$K_{rc} = \frac{\tau_s}{\sin(\phi_n) \cos(\beta_n)} \frac{\sin(\beta_n - \alpha_n)}{\sqrt{\cos^2(\phi_n + \beta_n - \alpha_n) + \tan^2(\beta_n) \sin^2(\beta_n)}}$$
(3.18)

where,

$$K_r = \frac{K_{rc}}{K_{tc}}$$

In Eq. (3.21), τ_s , ϕ_n , β_n and α_n are shear stress, shear angle, helix angle and rake angle respectively.

3.3. Modeling of Varying IPW Dynamics

For the workpiece dynamics simulations, FE modal analysis is used to extract normalized mode shapes and natural frequencies of dominant structure modes (bending and twisting) of cantilever plate. A fundamental FE analysis approach schematics is demonstrated in Figure 3.3.

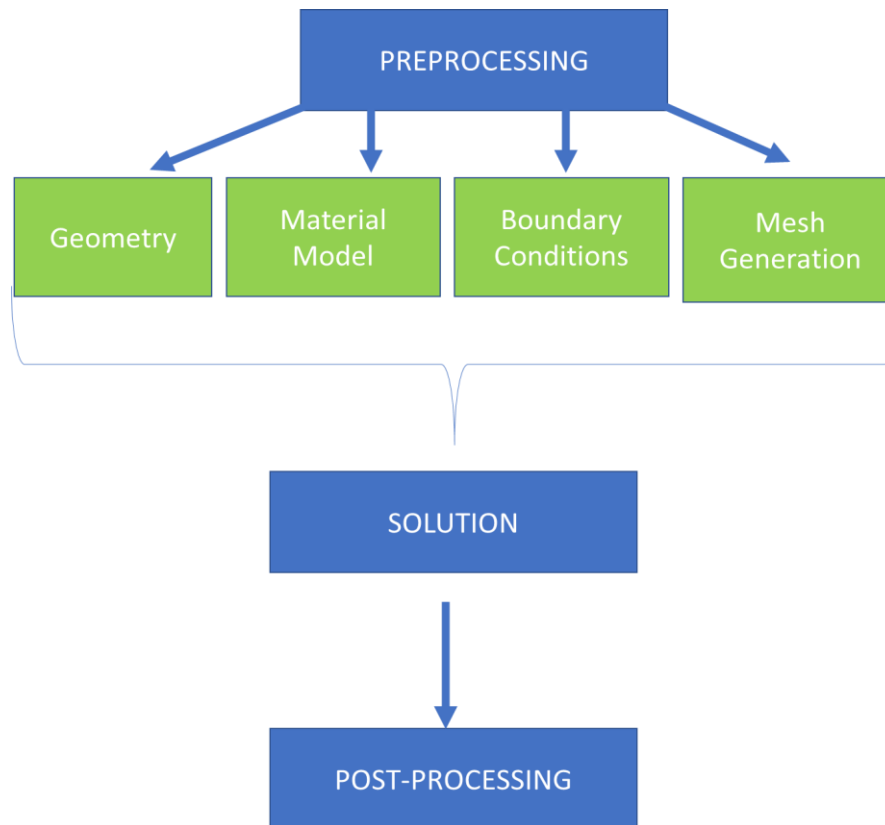


Figure 3.3. Procedure of FEA

Stability analysis for milling of thin-walled parts considering stiffness of multi-axial elements, which are listed through free-end to fixed-end of the cantilever beam is firstly proposed in reference [20].

Stability analysis for milling of thin-walled part simulated with the algorithm, which considers varying-dynamics of thin-walled part in axial direction. First, the thin-walled workpiece is modeled and analyzed using FE algorithm, developed in ANSYS APDL software. After, general approach of modal analysis with FE analysis is carried out for modal parameter extraction such as eigenfrequencies and eigenvectors for dominant bending and twisting modes of thin-walled workpiece.

Harmonic analysis is generally used for numerical FRF calculation, whereas it may be time-consuming. For instance, FRFs should be found at different cutter locations on thin-walled structure for in-process stability evaluation. Therefore, the following analytical FRF calculation formula is used after natural frequencies and normalized mode shapes are extracted from FE analysis:

$$\Phi^w(\omega_j) = \sum_{k=1}^m \frac{\{u_k\}^2}{-\omega_j^2 + \sqrt{-1}\omega_j 2\zeta_k \omega_{n,k} + \omega_{n,k}^2} \quad (3.19)$$

In conventional stability analysis, only the most flexible elements of the tool-workpiece (i.e., tool and plate tip points) are considered in stability analysis. However, in this part, the workpiece is divided into i number of discrete axial element at tool-workpiece contact with the size of δ_z . Previously explained stability analysis is used to find elemental stability limits. As tool goes from free-end to fixed-end of the plate more than one discrete axial elements may in cut, and they increase stability due to their higher stiffness. The schematics of single and multi-element models are given in Figure 3.4.

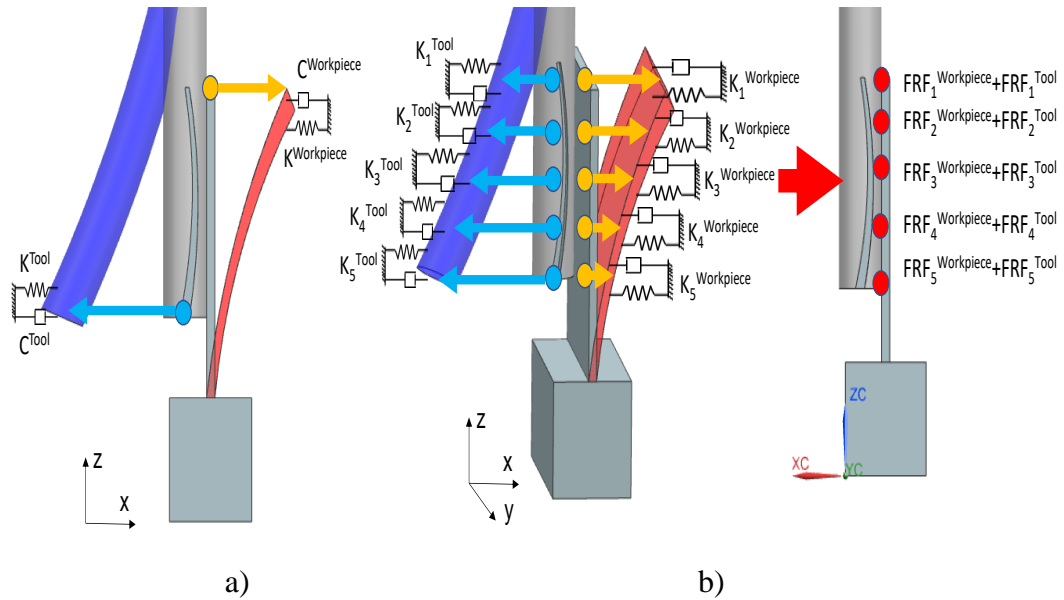


Figure 3.4. a) Single element and b) multi-axial element models

The flowchart of the algorithm is provided in Figure 3.5.

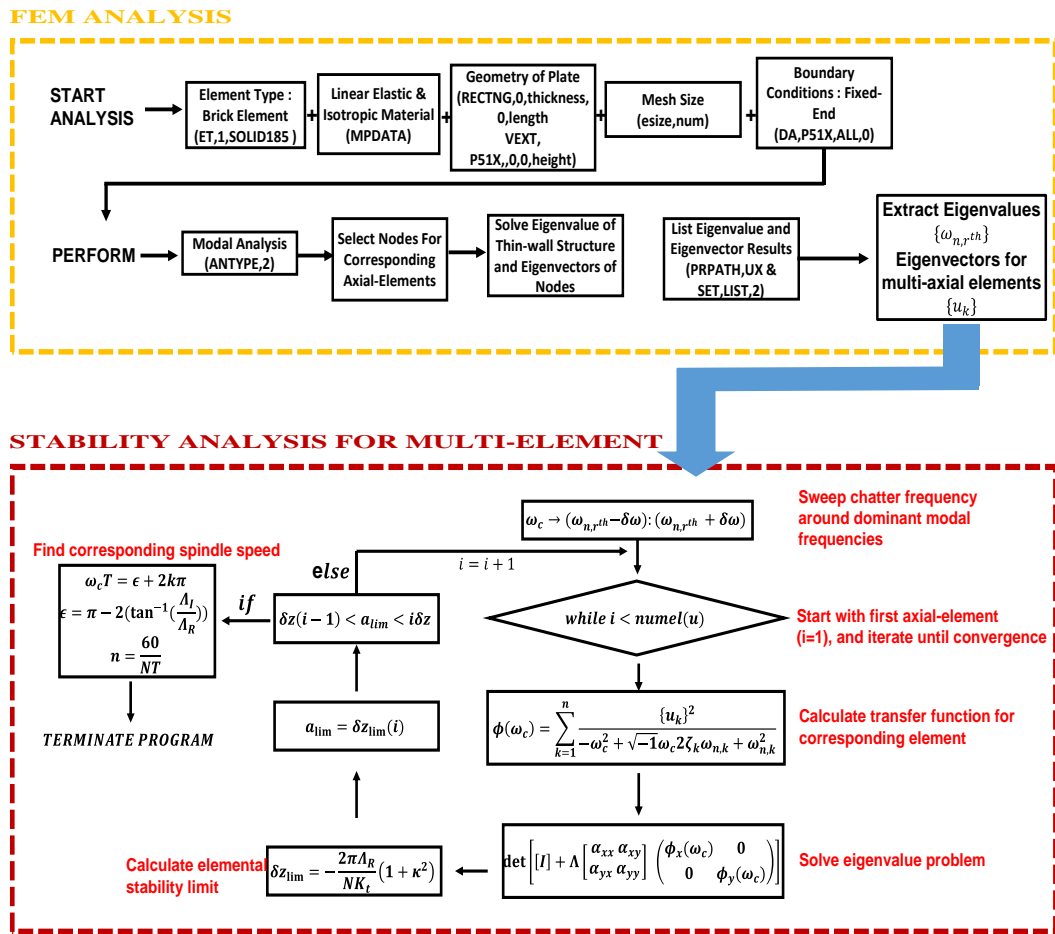


Figure 3.5. FEM and multi-axial element stability solution algorithm.

First of all, the proposed model in Ref. [5] is simulated for the case, where the Ti6Al4V is used as thin-walled workpiece given in Figure 3.6.

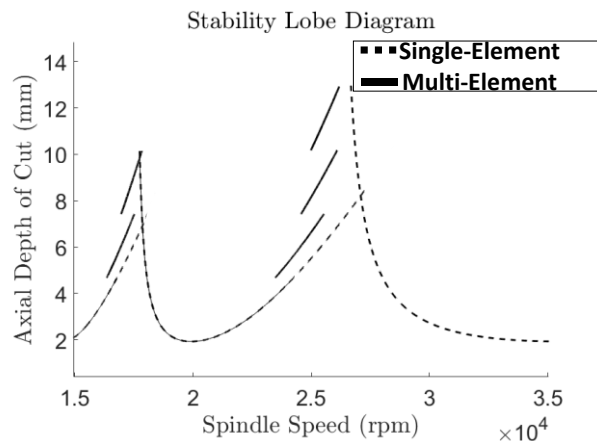


Figure 3.6. Simulation result of multi-axial element model for thin-walled Ti6Al4V part presented by [20].

Since the Ti6Al4V has low machinability, slow cutting speeds are preferred in practical applications, and it is hard to use benefit of multi-axial elements at low spindle speeds (without process damping effect). However, using high cutting speeds provides high axial depths, that leads to higher axial contact between tool and workpiece. In this part of the thesis, Al-7075 is used as workpiece material to demonstrate the effect of multi-axial elements on stability at high cutting speeds. The model is simulated for different plate structures given in

Table 3.

Table 3. Workpiece geometries and natural frequencies

	Thin-walled Workpiece Geometry (mm)			Natural Frequency (Hz)	
	Thickness	Height	Length	First Nat. Freq.	Second Nat. Freq.
Plate #1	3.5	30	60	3218	4779
Plate #2	3.5	40	60	1819	3232
Plate #3	3.5	50	60	1163	2416
Plate #4	3.5	60	60	803	1916

FRFs of each plate is simulated using FE and Eq. (3.19) and the FRF results are depicted in Figure 3.7 for 1st bending and 2nd twisting modes of the plates.

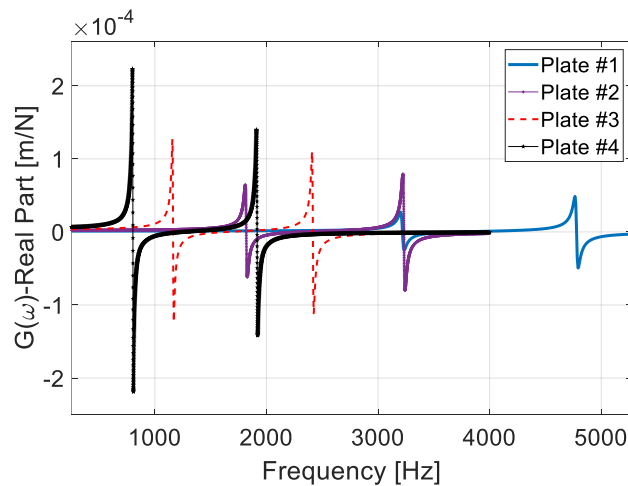


Figure 3.7. Real FRFs of Al-7075 plates with different geometries.

As seen from Figure 3.7, from Plate #1 to Plate #4, dynamic rigidity of the workpiece and

natural frequency reduces (i.e., higher FRF amplitude and low natural frequency). The main reason is to demonstrate effectiveness of the multi-axial element model by relating dynamic rigidity of the plate-like structure. Single mode stability analysis is performed for Plate #1, #2 and #4 and the results are provided in Figure 3.8.

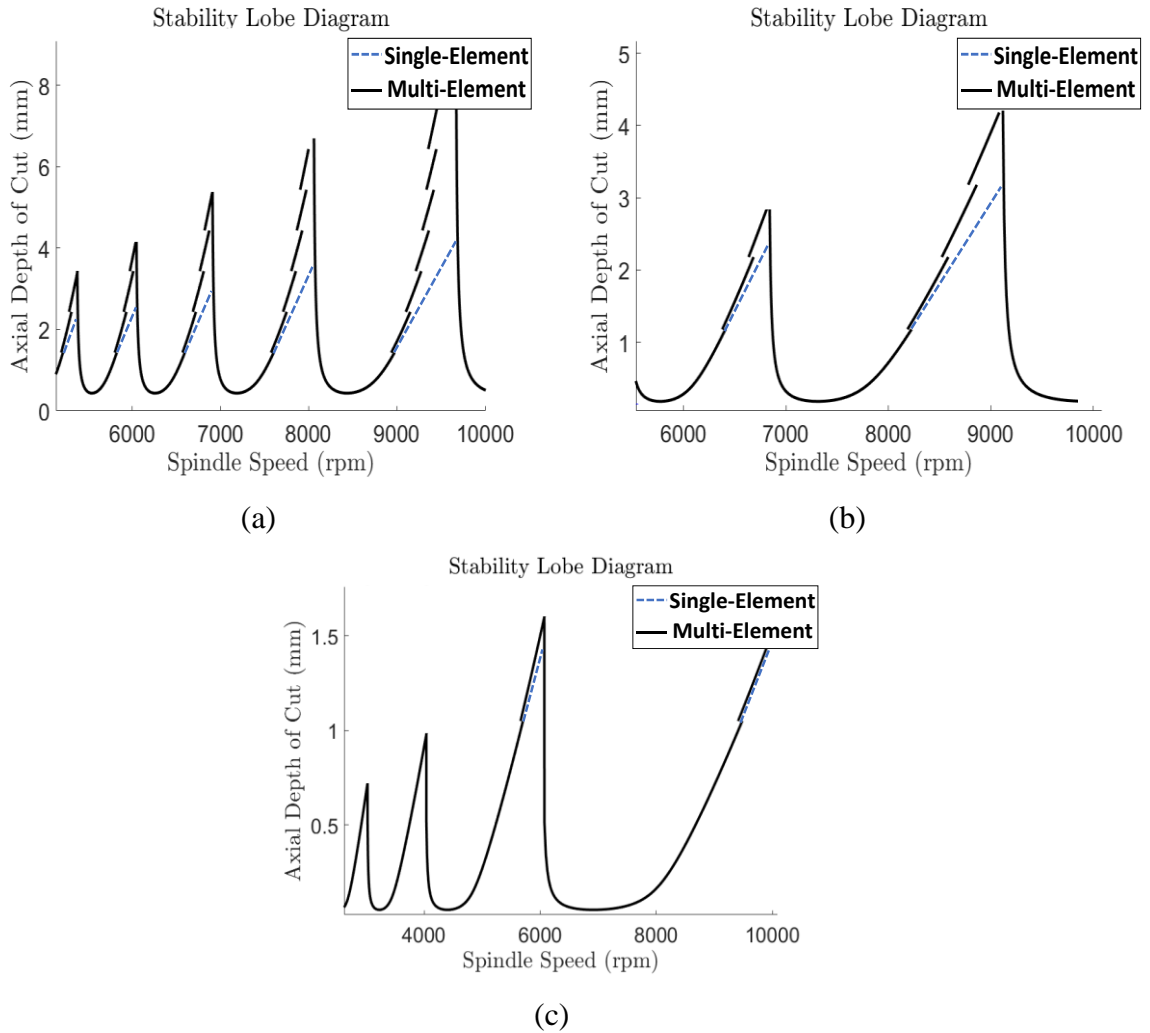


Figure 3.8. Multi-axial element stability solution for thin-walled parts with different geometries (a) Plate #1 (b) Plate #2 (c) Plate #4.

Figure 3.8 demonstrates that as the plate becomes more flexible, multi-element model lose its effectiveness, since tool reaches low number of discrete elements in the first pass, where the most flexible elements of the workpiece are in cut.

In each plate given in

Table 3, second twisting mode is more flexible than the first bending mode, thus the multi-mode stability analysis is needed for better stability prediction. In this respect, multi-mode

stability analysis is carried out for Plate #1 and Plate #2 considering multi-axial elemental response of each mode. Multi-mode stability results are given in Figure 3.9.

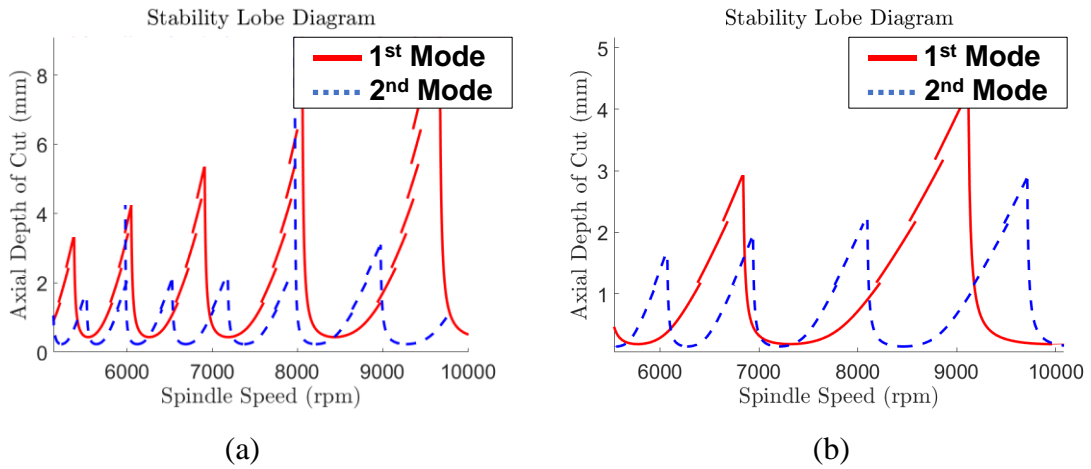


Figure 3.9. Multi-mode stability analysis (a) Plate #1 (b) Plate #2.

As seen from Figure 3.9, stability limit obtained from 2nd mode’s FRF provides lower stable limit in comparison to stability limit of 1st mode due to higher FRF amplitude. As stability limits of Plate #1 and Plate #2 are compared, more multi-axial elements contribute the stability analysis since Plate #1 has higher dynamic rigidity than Plate #2. In addition to multi-mode analysis, discrete axial element size δ_z selection is significant since it has influence on prediction accuracy. Thus, stability simulation of Plate #2 is carried out for different discrete axial element size and given in Figure 3.10.

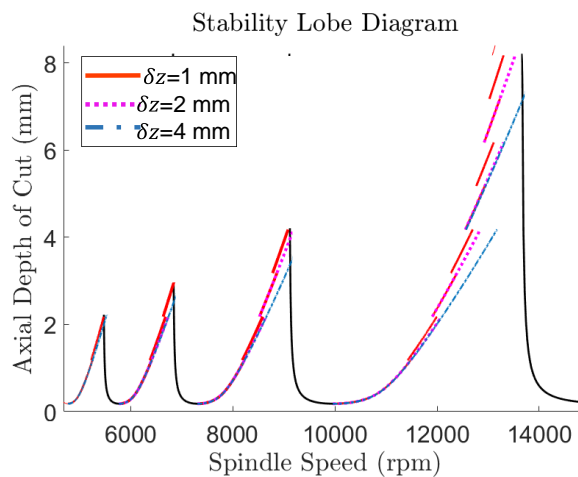


Figure 3.10. Effect of discrete axial element size simulated for Plate #2

Figure 3.10 shows that using low discrete element size δ_z enables to see higher depths can be achieved with multi-element model. In addition, the model is robust in finish milling operations with low radial immersions. Effect of radial depth of cut is depicted in Figure 3.11.

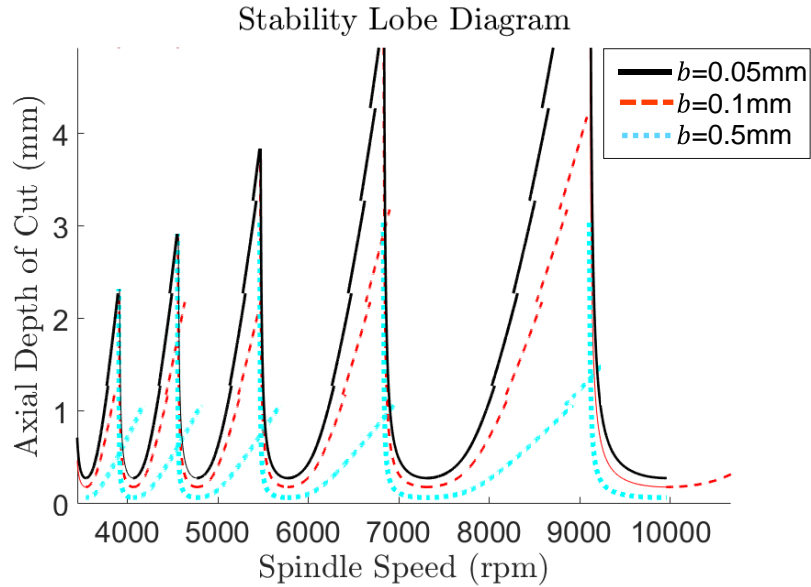


Figure 3.11. Effect of radial depth of cut.

The main reason is that as high radial depths are used, stability tool cannot reach high number of discrete elements in the first pass, where the most flexible elements of the workpiece are in cut.

High speed stability analysis is performed with the effect of multi-axial element in milling of an aluminium-alloy (Al7075) thin-walled workpiece with the dimensions of 50x60x3.5mm. Normalized mode shape of the workpiece for the first bending mode is found for each discrete axial element as follows:

$$u_y = [11.56, 11.21, 9.74, 10.87, 10.53, 10.18, 9.84, 9.49, 9.15, 8.81\dots]$$

FRFs of first 10 discrete axial elements from free-end to fixed-end for the first bending mode is simulated and provided in Figure 3.12.

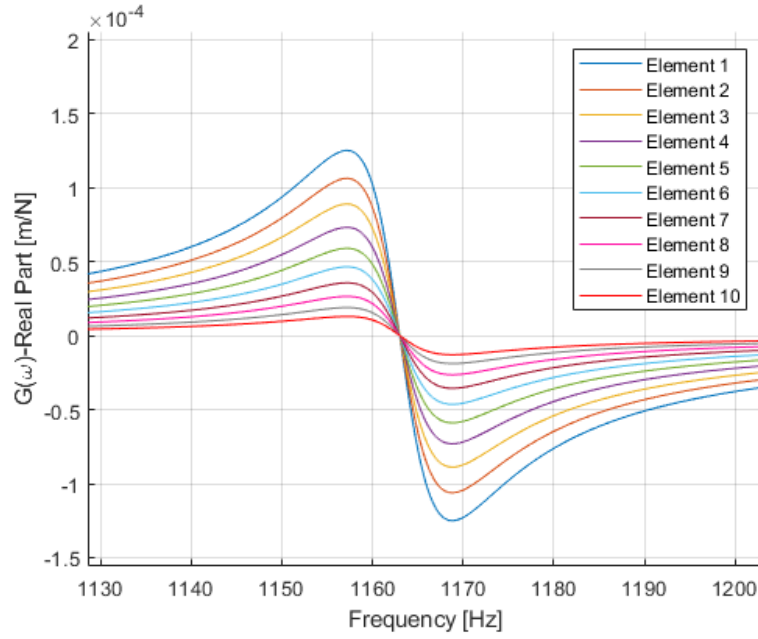


Figure 3.12. Varying-FRF of multi-axial elements of Plate #4.

FRF of the Plate #4 verified using impact hammer test and verification result is demonstrated in Figure 3.13.

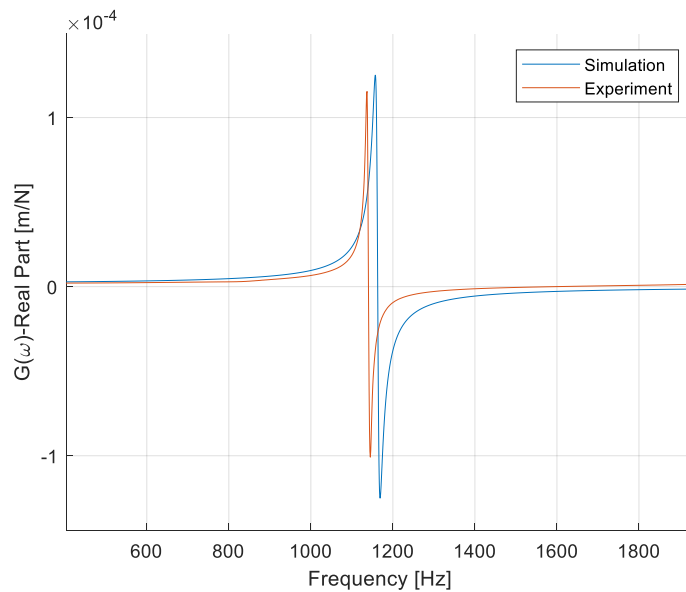


Figure 3.13. FRF verification of Al-7075 thin-walled workpiece using modal testing at the plate middle-tip point.

Stability is solved using presented approach for the milling system, where the Plate #4 is considered as workpiece and the stability lobe diagram is given in Figure 3.14.

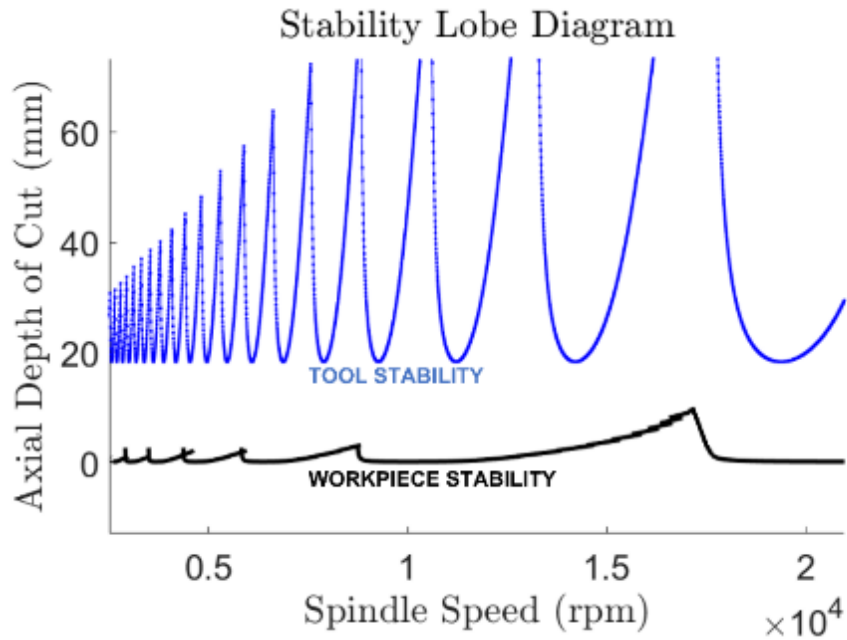


Figure 3.14. Stability lobe diagram of the tool-workpiece system.

As obtained in Figure 3.14, although multi-elements of the workpiece are considered in the analysis for improved stability limit, absolute stability limit, which comes from tool tip dynamics is higher since the tool has much more dynamic rigidity than workpiece in this case. Therefore, multi-elements of the cutting tool from tool tip to holder do not participate stability analysis since they have higher stiffness values.

Different machining strategies are developed for milling of Plate #4 given in Table 4. In these chatter-free machining strategies, only change in CL is considered in feed and axial directions. Effect of material removal is not considered in stability analysis. The main reason is that first natural frequency of semi-finished part (Plate #4) is found as 1163 Hz, after finish milling operation, the thickness of the workpiece reduced to 3.4 mm (i.e., 0.1 mm radial depth) and the first natural frequency of the final part is calculated as 1130 Hz, thus there is 3% change in natural frequency after material removal. This small change in natural frequency does not lead to shift in stability lobes. In addition, there is no significant variation in local normalized mode vector of first mode as CL changes in feed direction. However, local normalized mode vector of second mode drastically changes as CL is updated in feed direction. The dynamic response of plate tip edges is the highest in comparison to the plate middle tip point as twisting mode is considered.

In this part of the thesis, different machining strategies are proposed to demonstrate using

multi-element model, higher stable cuts can be achieved, and thus productivity increases without chatter. In the first and second strategies, chatter-free axial depths are selected to suppress only first bending mode of the plate. The main idea is that self-excitation of one of the modes can be disclaimed for improved productivity. This approach may reduce polishing time after finish milling operation. On the other hand, in the 3rd and 4th strategies, bending and twisting modes are suppressed to stabilize all process. In strategies 1st and 3rd, use of constant chatter-free axial depths are proposed. In these strategies, stable axial depths are selected considering the most flexible case in the simulations at first, then they are used for all finishing process as constant chatter-free axial depths. On the other hand, varying chatter-free axial depths are used in the strategies 2nd and 4th. In these strategies, change of CL in axial direction and its effect on stability is taken into account. In addition, change of CL in feed direction and multi-modal response are considered in each strategy.

Table 4. Machining strategies

	Chatter-Free Number of Passes		Improvement in Productivity
	Single-Element Model	Multi-Element Model	
Strategy 1	10	5	100%
Strategy 2	4	3	33%
Strategy 3	17	13	31%
Strategy 4	6	5	20%

In each strategy, spindle speed is used as 17200 rpm since that speed provides to cut in stability pocket. In strategy 1, multi-element model provides 100% improvement in productivity in comparison to conventional single-element model. Strategy 2 enables to suppress only bending mode, whereas varying axial depths are used to finish workpiece and using the multi-element model leads to 33% increased productivity. Strategy 3 enables to finish workpiece using constant chatter-free axial depths, which suppresses both dominant modes of the workpiece. In strategy 4, varying chatter-free axial depths are simulated for both single and multi-element models and these stability limits are illustrated in Figure 3.15.

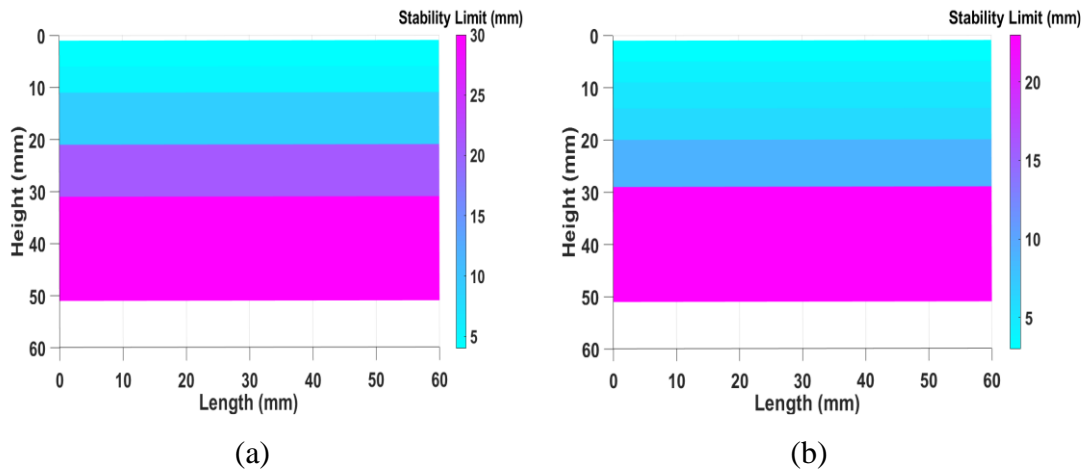


Figure 3.15. Stability limits of each pass (a) multi-axial element (b) single element models.

As a result using multi-element model compared to single-element model and varying chatter-free axial depths compared to constant chatter-free axial depths, productivity can be increased up to 100% and 183% respectively.

3.3.1. Experimental Validation

In this section, multi-element model presented for milling stability of thin-walled structures is experimentally validated by performing cutting tests. These machining tests are performed using DMU 75 Monoblock 5-axis Milling Center. Sound data is acquired using a microphone and data is processed using LabView and MATLAB software.

In each test, 0.05 mm/(rev-tooth) feed rate and 0.1 mm radial depth of cut are used. Experimental conditions are provided in Table 5.

Table 5. Experiment parameters

Test No	Cutting Speed (m/min)	Depth of Cut (mm)
1	534	8
2	440	6
3	534	6
4	440	4
5	534	4
6	534	3

Simulated stability lobe diagram for both single and multi-axial element model with chatter test locations given in Table 5 are shown in Figure 3.16.

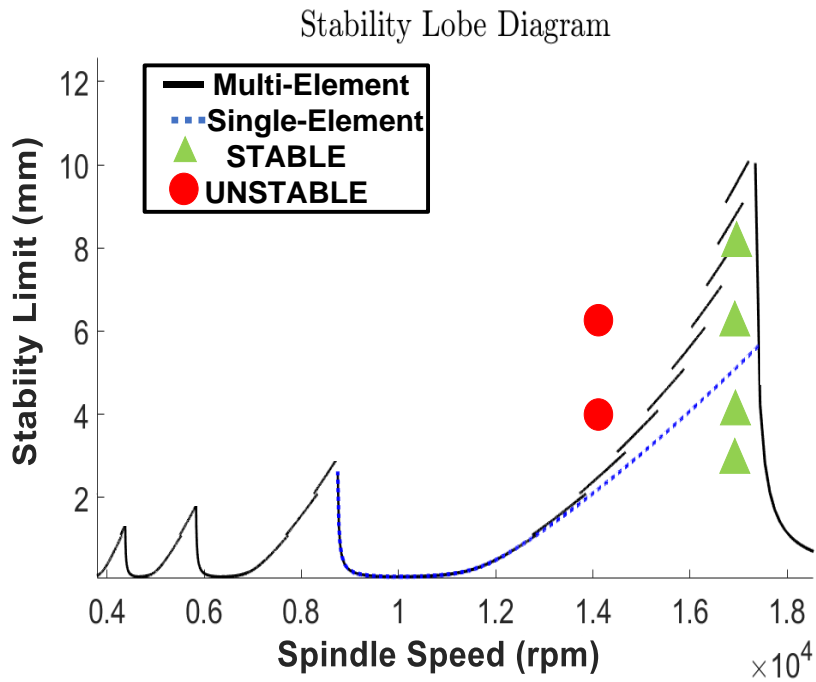


Figure 3.16. Stability analysis result comparison for single & multi-element models with cutting tests.

Multi-element model is verified as the first time in literature. It is observed that even 100% stable cut can be achieved using this model. Finished surface textures for tests 3, 4 and 6 are demonstrated in Figure 3.17.

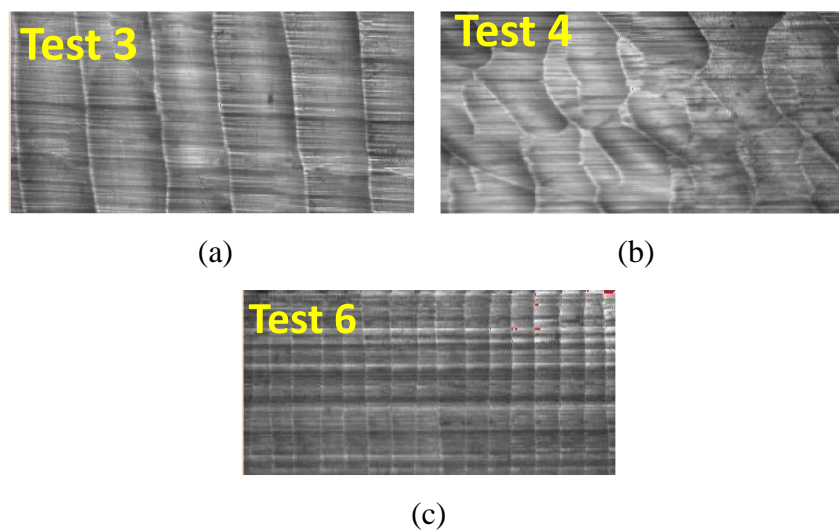


Figure 3.17. Surface finish measurements for (a) test 3 (b) test4 and (c) test 6

In addition to the finished surfaces, captured sound spectrum converted in frequency domain using FFT analysis to demonstrate stability condition of tests and the results for tests 3, 4, 5 and 6 are given in Figure 3.18.

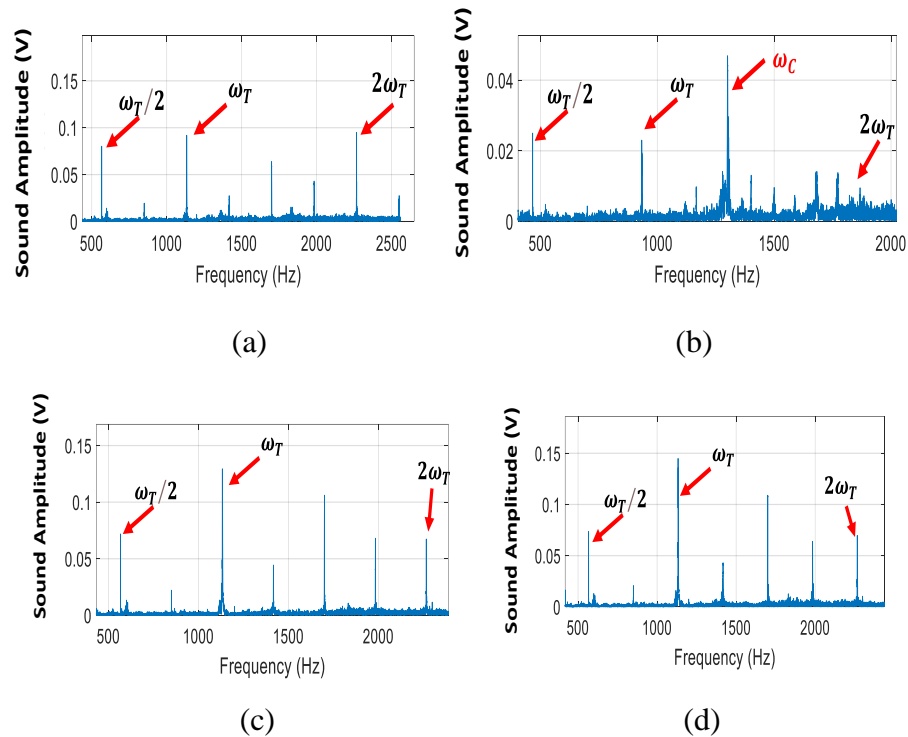


Figure 3.18. Sound spectrum at different chatter test points a) Test 3 b) Test 4 c) Test 5 d) Test 6

In tests 3, 5 and 6; tooth passing frequency is measured as 1133 Hz, and its harmonics are found as 566 Hz and 2266 Hz respectively as seen from Figure 3.18. On the other hand, process becomes unstable as predicted in Test 4, where the tooth passing frequency is 933 Hz and its harmonics are 466 Hz, 1866 Hz respectively, and the chatter frequency is obtained as 1300 Hz.

As depicted in Figure 3.19, cutting test is performed at 2.5 mm depth of cut and 8600 rpm to demonstrate that while the first mode of the thin-walled workpiece is suppressed, system behaves local stable due to excitation of second mode as given in Figure 3.20.

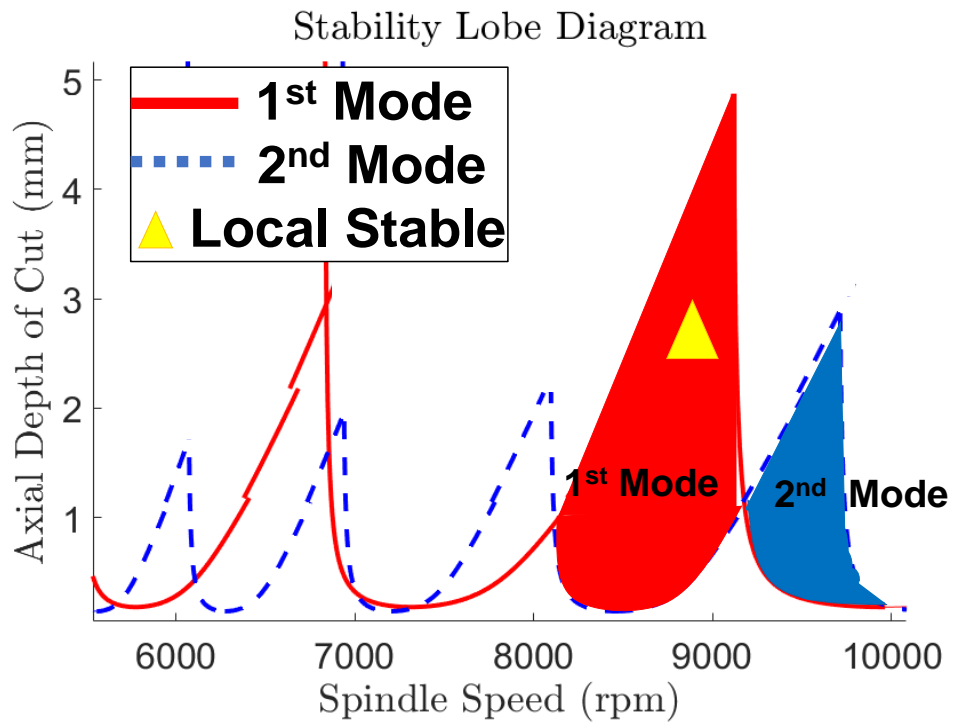


Figure 3.19. Multi-mode and multi-axial element stability solution with local stable point for plate #2.

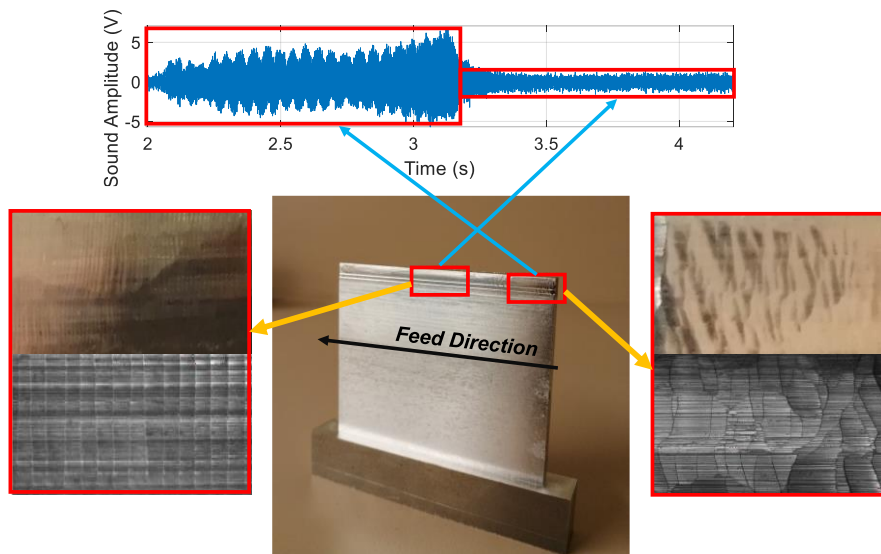


Figure 3.20. Sound measurement and finished surface of the thin-walled part for local stable condition.

In previous section, different machining strategies are discussed and the strategies 2 and 4 are simulated. In this section, these two machining strategies are experimentally verified.

Finished surface of the plates, which are obtained using an optical microscope are demonstrated in Figure 3.21 after machining with strategies 2 and 4. In each test, feed rate and spindle speeds are taken as 0.05 mm/(rev-tooth) and 17200 rpm respectively.

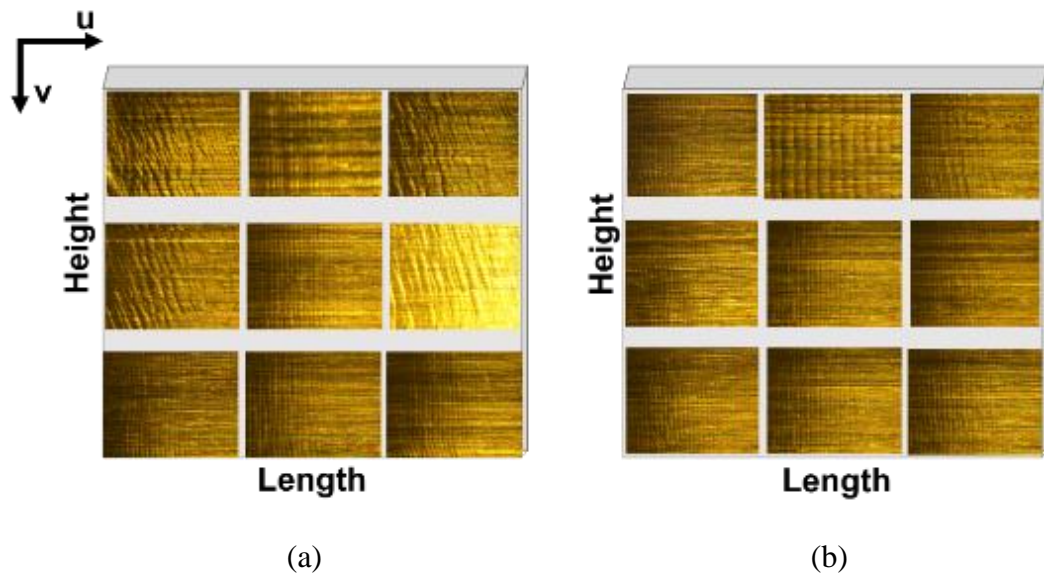


Figure 3.21. Surface finish results for (a) Strategy 2 (b) Strategy 4

Although, using strategy 2 provides 67% higher productivity in comparison to strategy 4, second mode cannot be suppressed that leads to local stability as seen from Figure 3.21 (a). In this strategy, chatter marks are observed at the tip and middle edges of the workpiece, where the twisting mode is dominant. On the contrary, machining with strategy 4 suppresses both two modes of the finished workpiece as seen from Figure 3.21 (b). In this strategy, better surface finish, which may reduce polishing time is observed.

3.4. Application of Special End Mills in Milling of Thin-walled Parts

3.4.1. Introduction

Machining thin-walled structures introduces challenges in terms of process stability due to the varying in-process workpiece dynamics. This study compares the effectiveness and performance of standard, variable-pitch, and crest-cut tools on chatter suppression in milling thin-walled parts. The novel stability maps are generated based on varying stability limits caused by in-process workpiece dynamics. Using the obtained stability maps, the performance of different cutting strategies is compared considering

productivity and surface finish quality. The experimentally verified results demonstrate the superiority of crest-cut tools as a robust solution for overcoming chatter in thin-wall machining.

Variable pitch tools can be used at low cutting speeds [81] to suppress chatter vibrations. However, due to the existence of multiple dominant modes and varying IPW dynamics, their use in milling thin-walled parts does not always provide a satisfactory solution for chatter suppression. Crest-cut tools, on the other hand, provide chatter suppression capability over a wider frequency and speed range [4], and can be highly effective for suppression of chatter in milling of thin-walled parts. This superior capability of crest-cut tools is due to their special geometry, which has to be designed considering important modes and IPW dynamics of thin-walled structures. Therefore, crest-cut end mills are proposed as a solution for improved stability of the process in milling thin-walled structures.

In this study, a novel method is used in stability analysis and varying IPW dynamics of thin-walled parts, which considers both change in CL and natural frequency due to element removal to reduce calculation cost. For the first time in the literature, a stability map of the whole plate is generated for different tool geometries based on the IPW dynamics [75]. According to the obtained stability map of each tool, different cutting strategies are explored, surface finish quality maps are derived, and compared in terms of cycle time and chatter-free surface area. The proposed simulations are validated through experiments. Both simulations and experiments confirm the superiority of crest-cut tools over variable-pitch and standard end mills, and the results show that these tools can be utilized as a robust solution against changes in IPW dynamics of thin-walled parts. All stability analysis is performed using semi-analytical time discretization method presented in [22] due to its high prediction accuracy especially for end mills with special geometries.

3.4.2. Milling Stability Solution Using Discretized-Time Method

In this part, semi-analytical time discretization method is described since this method is used in stability analysis for multiple-delay systems in following section.

First, as the 1-DOF milling system is considered, the equation of motion in x -direction can be formulated as follows in the dynamic milling system.

$$\frac{d^2x}{dt^2} + 2\zeta\omega_n \frac{dx}{dt} + \omega_n^2 x(t) = -\frac{a\alpha(t)}{m}(x(t) - x(t - \tau))$$

where,

$$m = \frac{K}{\omega_n^2}$$

The dynamic milling force Eq. (3.20) is non-autonomous (i.e. time-variant) delay differential equation (DDE). Due to regeneration mechanism, the time delay ($t-\tau$) arises between inner and outer waves left on the cutting surface. In Eq (3.20) ω_n, ζ, m are the modal parameters and they stand for natural frequency, damping ratio and modal mass respectively. Moreover, $a, \alpha(t)$ and x stand for axial depth of cut, directional milling force coefficient and dynamic displacement respectively. In Eq. (3.20) K is the modal stiffness. In addition, cutting forces changes due to rotation of the cutting tool since the term, which is the directional milling force coefficient $\alpha(t)$ is included into the equation of motion.

The formulation of directional milling force coefficient is given as below:

$$\alpha(t) = \sum_{j=1}^N g(\phi_j(t)) (\sin(\phi_j(t)) (K_{tc} \cos(\phi_j(t)) + K_{rc} \sin(\phi_j(t))))$$

where,

$$\phi_j(t) = \left(\frac{2\pi\omega}{60}\right)t + j\frac{2\pi}{N}$$

If the milling mode is up, $\phi_{en} = 0$ and $\phi_{ex} = \cos^{-1}(1 - 2w/D)$, on the other hand, for down milling mode $\phi_{ex} = \cos^{-1}(2b/D - 1)$ and $\phi_{en} = 180^\circ$ where $2b/D$ is the radial immersion ratio.

Basically, directional milling force coefficient relates the milling forces to the vibration amplitude as cutting tool rotates. In milling, delayed time is equal to the period of the tooth ($\tau = T$). Insperger and Stépán [82] developed the semi-discretization method which provides semi-analytical solution for stability in 1-DOF and 2-DOF dynamic milling systems.

In this part of the thesis, milling stability of 1D and 2D milling is explained with the semi-discretization method (SDM). In SDM, the delay and time-variant terms are

approximated constant equations, by using this, non-autonomous DDEs are reduced into autonomous ordinary differential equations (ODEs). First, the delay is discretized with integer number of discretization interval k over a tooth period:

$$\Delta t = \frac{T}{k} = \frac{60}{kN\omega}$$

$$t_i = i\Delta t$$

where,

$$i = 0, 1, 2, 3, 4, \dots, k - 1$$
(3.22)

After performing time discretization, time-variant parameters can be written as time-invariant within each discretization interval $[t_i, t_{i+1})$ as follows [82]:

$$\alpha_i = \frac{1}{\Delta t} \int_{t_i}^{t_{i+1}} \alpha(t) dt$$
(3.23)

$$\frac{d^2 x}{dt^2} + 2\zeta\omega_n \frac{dx}{dt} + \left(\omega_n^2 + \frac{a\alpha_i}{m}\right) x(t) = \frac{a\alpha_i}{m} x_{\tau,i} \quad t \in [t_i, t_{i+1})$$
(3.24)

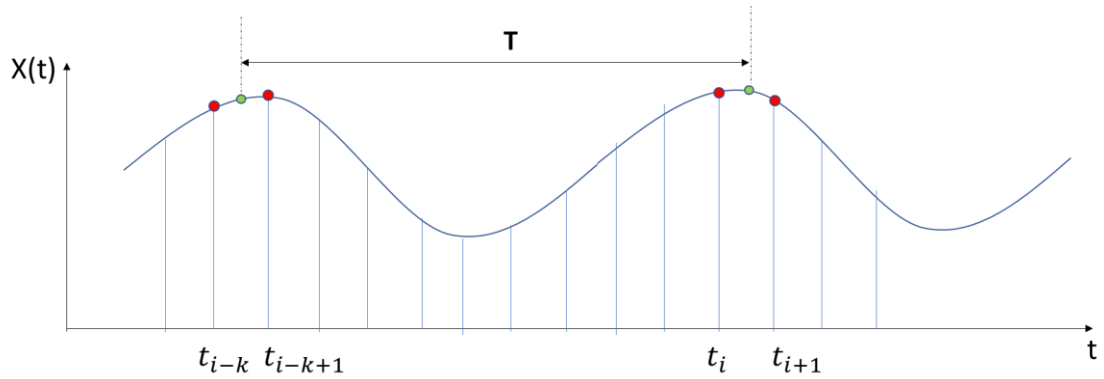


Figure 3.22. Delayed term approximation [22]

The delayed terms can be approximated as a weighted linear combination of discrete values X_{i-k+1} and X_{i-k} :

$$x(t - \tau) = \frac{(x_{i-k} + x_{i-k+1})}{2} = x_{\tau,i}$$
(3.25)

Substituting the Eqs. (3.23) and (3.25) into Eq (3.20), the autonomous ODE is obtained as follows:

$$\dot{X}(t) = L_i X(t) + \frac{B}{2}(X_{i-k+1} + X_{i-k})$$

where,

$$L_i = \begin{pmatrix} 0 & 1 \\ -\left(\omega_n^2 + \frac{a\alpha_i}{m}\right) & -2\zeta\omega_n \end{pmatrix}, B_i = \begin{pmatrix} 0 & 0 \\ \frac{a\alpha_i}{m} & 0 \end{pmatrix}, X(t) = \begin{pmatrix} x(t) \\ \dot{x}(t) \end{pmatrix}$$

By solving the Eq. (3.26) using the initial condition, which is $x(t_i) = x_i$:

$$X(t) = e^{(L_i(t-t_i))}(X_i + L_i^{-1}BX_{\tau,i}) - L_i^{-1}BX_{\tau,i}$$

After, following the same procedure, by equating $t_i = t_{i+1}$ and $x(t_i) = x(t_{i+1})$:

$$X_{i+1} = P_i X_i + \frac{R_i}{2}(X_{i-k+1} + X_{i-k})$$

where,

$$P_i = e^{(L_i \Delta t)}$$

$$R_i = (e^{(L_i \Delta t)} - I)L_i^{-1}B$$

After, discrete map is given as follows:

$$X_i = \{x_i, \dot{x}_i, x_{i-1}, \dots, x_{i-k}\}^T$$

$$X_i = C_i X_i$$

$(k+2)$ -dimensional coefficient matrix [82]:

$$C_i = \begin{bmatrix} P_{i,11} & P_{i,12} & 0 & 0 & \dots & 0 & \frac{1}{2}R_{i,11} & \frac{1}{2}R_{i,11} \\ P_{i,21} & P_{i,22} & 0 & 0 & \dots & 0 & \frac{1}{2}R_{i,21} & \frac{1}{2}R_{i,21} \\ 1 & 0 & 0 & 0 & \dots & 0 & 0 & 0 \\ 0 & 0 & 1 & 0 & \dots & 0 & 0 & 0 \\ \vdots & \vdots & \vdots & \ddots & \ddots & \vdots & \vdots & \vdots \\ 0 & 0 & 0 & 0 & \ddots & 0 & 0 & 0 \\ 0 & 0 & 0 & 0 & \dots & 1 & 0 & 0 \\ 0 & 0 & 0 & 0 & \dots & 0 & 1 & 0 \end{bmatrix}_{(k+2) \times (k+2)}$$

The transition matrix can be found by multiplying coefficient matrices as follows:

$$\Psi = C_{k-1}C_{k-2}C_{k-3} \dots C_1C_0 \quad (3.31)$$

From Floquet theory, if the eigenvalues of the transition matrix $eig[\Psi]$ are placed inside the complex plane circle, the dynamic system is stable, if not the dynamic system is unstable.

In 2-DOF (x - y directions) milling stability solution with SDM, the only difference is dimensions of the matrices. The dynamic system equation becomes as given below:

$$\begin{aligned} \begin{pmatrix} \ddot{x}(t) \\ \ddot{y}(t) \end{pmatrix} + \begin{pmatrix} 2\zeta\omega_n & 0 \\ 0 & 2\zeta\omega_n \end{pmatrix} \begin{pmatrix} \dot{x}(t) \\ \dot{y}(t) \end{pmatrix} + \begin{pmatrix} \omega_n^2 + \frac{a\alpha_{xxi}}{m} & \frac{a\alpha_{xyi}}{m} \\ \frac{a\alpha_{yxi}}{m} & \omega_n^2 + \frac{a\alpha_{yyi}}{m} \end{pmatrix} \begin{pmatrix} x(t) \\ y(t) \end{pmatrix} \\ = \begin{pmatrix} \frac{a\alpha_{xxi}}{m} & \frac{a\alpha_{xyi}}{m} \\ \frac{a\alpha_{yxi}}{m} & \frac{a\alpha_{yyi}}{m} \end{pmatrix} \begin{pmatrix} x_{\tau,i} \\ y_{\tau,i} \end{pmatrix} \end{aligned} \quad (3.32)$$

The directional milling force coefficients have to be defined in 2-DOF systems in x - y plane as follows:

$$\begin{aligned} \alpha_{xx}(t) &= \sum_{j=1}^N g(\phi_j(t)) \sin(\phi_j(t)) (K_{tc} \cos(\phi_j(t)) + K_{rc} \sin(\phi_j(t))) \\ \alpha_{xy}(t) &= \sum_{j=1}^N g(\phi_j(t)) \cos(\phi_j(t)) (K_{tc} \cos(\phi_j(t)) + K_{rc} \sin(\phi_j(t))) \\ \alpha_{yx}(t) &= \sum_{j=1}^N g(\phi_j(t)) \sin(\phi_j(t)) (-K_{tc} \sin(\phi_j(t)) + K_{rc} \cos(\phi_j(t))) \\ \alpha_{yy}(t) &= \sum_{j=1}^N g(\phi_j(t)) \cos(\phi_j(t)) (-K_{tc} \sin(\phi_j(t)) + K_{rc} \cos(\phi_j(t))) \end{aligned} \quad (3.33)$$

($2k+4$)-dimensional coefficient matrix [82]:

$$C_i = \begin{bmatrix} P_{i,11} & P_{i,12} & P_{i,13} & P_{i,14} & 0 & \dots & 0 & \frac{1}{2}R_{i,11} & \frac{1}{2}R_{i,12} & \frac{1}{2}R_{i,11} & \frac{1}{2}R_{i,12} \\ P_{i,21} & P_{i,22} & P_{i,23} & P_{i,24} & 0 & \dots & 0 & \frac{1}{2}R_{i,21} & \frac{1}{2}R_{i,22} & \frac{1}{2}R_{i,21} & \frac{1}{2}R_{i,22} \\ P_{i,31} & P_{i,32} & P_{i,33} & P_{i,34} & 0 & \dots & 0 & \frac{1}{2}R_{i,31} & \frac{1}{2}R_{i,32} & \frac{1}{2}R_{i,31} & \frac{1}{2}R_{i,32} \\ P_{i,41} & P_{i,42} & P_{i,43} & P_{i,44} & 0 & \dots & 0 & \frac{1}{2}R_{i,41} & \frac{1}{2}R_{i,42} & \frac{1}{2}R_{i,41} & \frac{1}{2}R_{i,42} \\ 1 & 0 & 0 & 0 & 0 & \dots & 0 & 0 & 0 & 0 & 0 \\ 0 & 1 & 0 & 0 & 0 & \dots & 0 & 0 & 0 & 0 & 0 \\ 0 & 0 & 0 & 0 & 1 & \dots & 0 & 0 & 0 & 0 & 0 \\ \vdots & \vdots & \vdots & \vdots & \vdots & \ddots & \vdots & \vdots & \vdots & \vdots & \vdots \\ 0 & 0 & 0 & 0 & 0 & \dots & 1 & 0 & 0 & 0 & 0 \\ 0 & 0 & 0 & 0 & 0 & \dots & 0 & 1 & 0 & 0 & 0 \\ 0 & 0 & 0 & 0 & 0 & \dots & 0 & 0 & 1 & 0 & 0 \end{bmatrix}_{(2k+4) \times (2k+4)}$$

The SDM solution is used to find stability limits of special end mills in following section of the thesis.

3.4.3. Stability Analysis Considering Varying-Dynamics of IPW

As structures become more flexible or thinner, the effect of removed material during machining becomes more prominent, leading to significant variation in IPW dynamics and, therefore, stability limits. This section presents the procedure used for modelling material removal in thin-walled structures through FE analysis. In the implemented approach, the dependency of the IPW dynamics prediction procedure on the stability limits, and thus iterations and long simulation time, are eliminated. For this purpose, the unmachined flexible plate is meshed with an element size of 0.6 mm. The elements from the meshed structure are removed, similar to the mass removal during the machining cycle (see Figure 3.23). The in-process FRFs are obtained at five different CLs along the feed direction (U) for each elemental depth along the plate height (V).

Flowchart of proposed approach is given in Figure 3.23. Note that the element height in is exaggerated for better visualization.

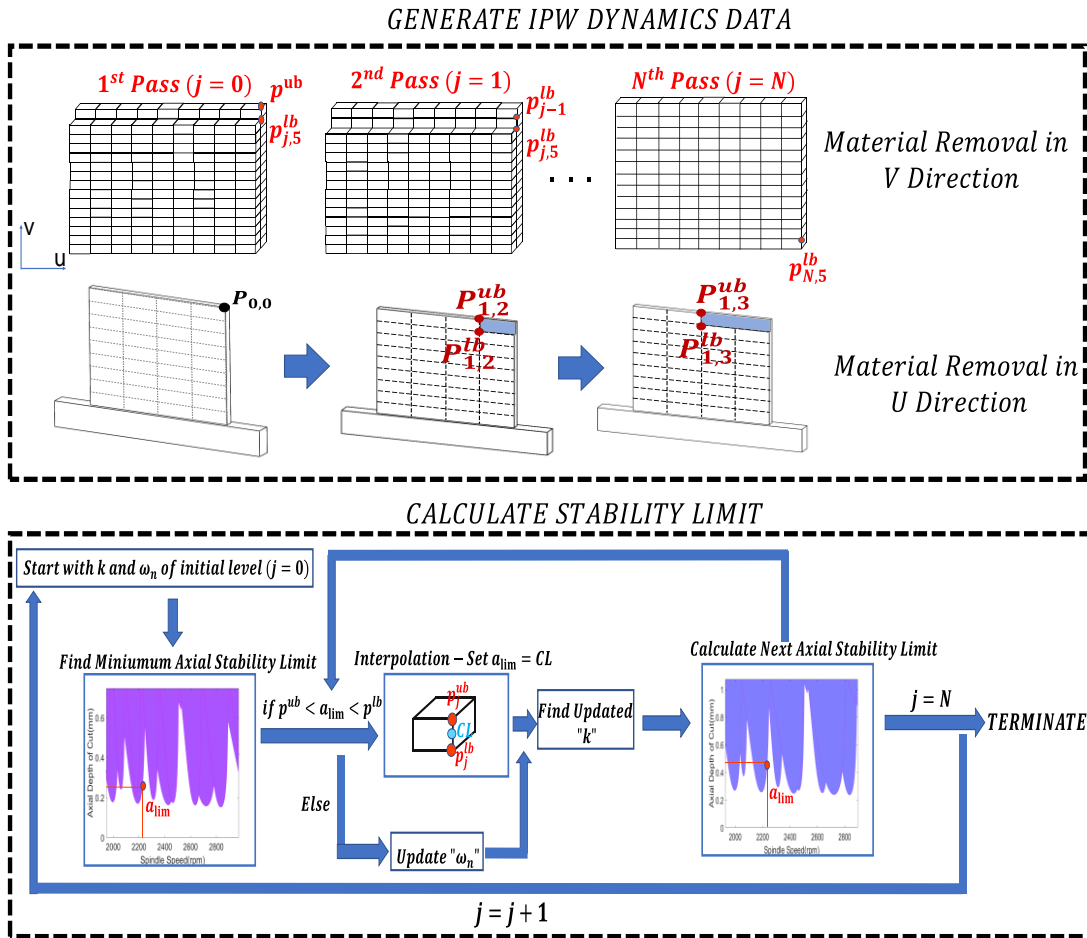


Figure 3.23. Flowchart of proposed approach with material removal stages of IPW

Points $P_{v,u}$ in Figure 3.23, are represented IPW FRF identification points on the plate. The points $P_{0,u}$ are the FRF identification points on the tip of the uncut plate, Level 0 ($j = 0$). The next FRF identification locations are one element lower ($j = 1$), which are identified by removing the elements at that level which are shown as $P_{1,u}$. Since the material is removed at each step, the FRFs of the points with the same coordinates from the previous step are updated. For instance, at point $P_{1,2}$, two FRFs are identified, upper limit and lower limits. The lower limit $P_{1,2}^l$ is the FRF of current state, and the upper limit $P_{1,2}^u$ is the updated FRF of point $P_{0,2}$ which has the same coordinate. The same procedure is repeated for Level 2 by removing the elements in Level 1. Similarly, the FRF of point $P_{1,2}^l$ is updated as $P_{2,2}^l$ to include the effect of material removal (See Figure 3.23). This procedure helps to identify the IPW FRF of any CL located between the upper and lower limits using interpolation. Figure 3.24 shows the natural frequency and peak amplitude of each point on the plate for the first and second modes by updating the FRFs due to the

material removal effect for a Ti6Al4V plate with the dimension of 40×65×3 mm. In the following simulations, the element size is kept equal to a radial depth of cut (0.6 mm) to prevent excessive simulation time in FE analysis.

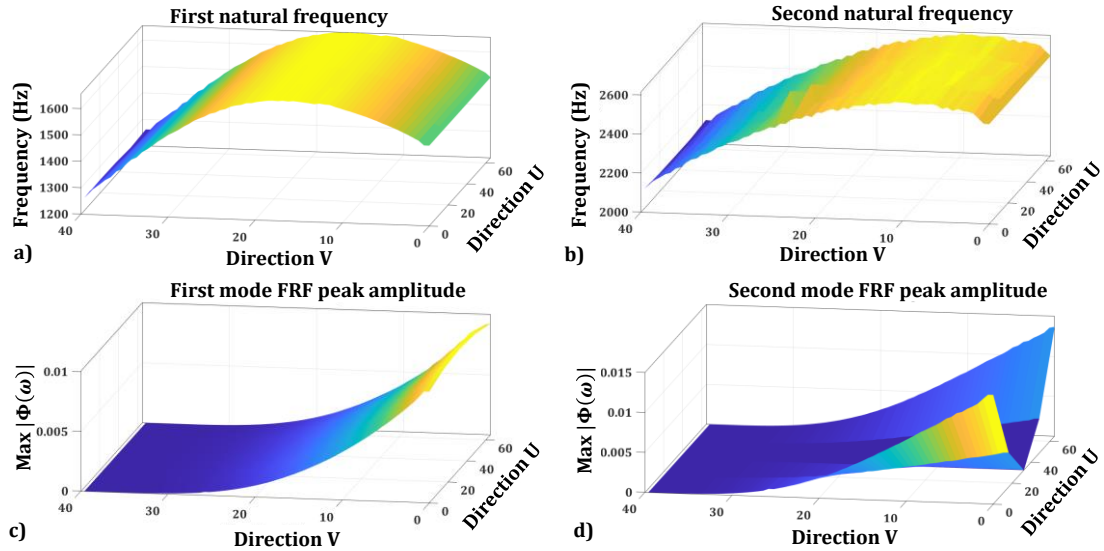


Figure 3.24. Varying-dynamics of IPW in point milling a) 1st natural frequency b) 2nd natural frequency c) FRF peak of 1st mode d) 2nd mode

According to the results shown in Figure 3.24, both the plate's natural frequency and IPW FRFs vary drastically for both modes along the plate length and height directions, which requires multi-mode stability analysis. This scheme helps to identify the FRF of any CL on the plate for evaluation of stability limit considering the material removal effect. Note that, the damping ratios employed in simulations are identified from hammer tests at different plate locations considering the IPW dynamics scheme. In Figure 3.25, experimental and FE results at two points and levels on the plate are presented. In Figure 3.25 (a), measurements and predictions at two points (corner and middle) along the feed direction at the tip of the uncut plate are illustrated. Figure 3.25 (b) shows the results for the same corresponding points in the feed direction at level 54 (27mm in plate depth from free end) after the material is removed up to this level. The maximum difference between predicted and simulated natural frequencies is less than 4%.

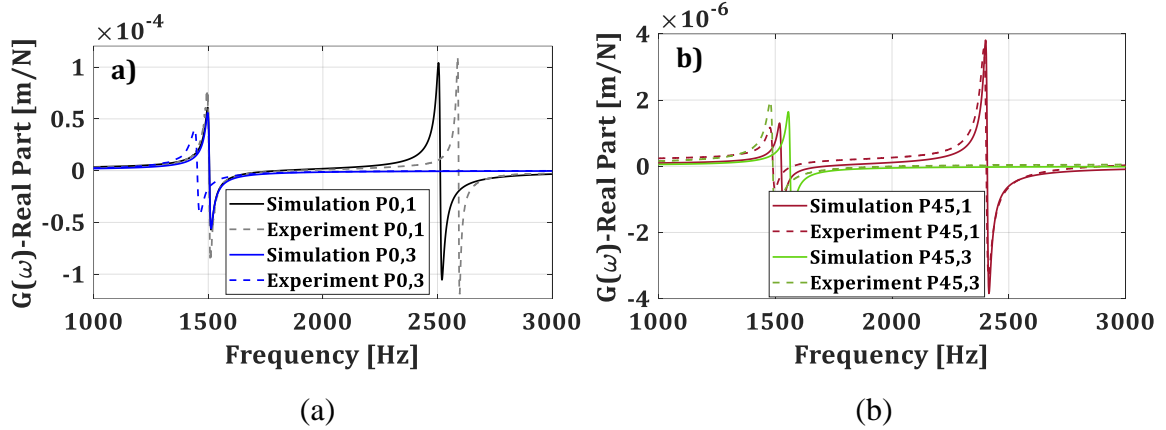


Figure 3.25. Validation of IPW dynamics at different levels.

Unlike standard end mills, special end mills have varying pitch or helix angles, or both, which can introduce higher stability limits than standard end mills. Crest-cut tools with waves on their rake face have harmonically varying helix and local pitch angles along their axis. This wavy edge shape increases the number of delays generated in the cutting process, disrupting the regeneration effect and increasing stability limits. The geometrical model and edge shape definitions are discussed in detail by Tehranizadeh et al.[4]. Based on the proposed model in [4], the local pitch angle variation of crest-cut tools along the tool axis is illustrated in Figure 3.26 (a) and compared to variable-pitch and standard tools. The unfolded view of the cutting edges and their pitch variations is shown in Figure 3.26 (b).

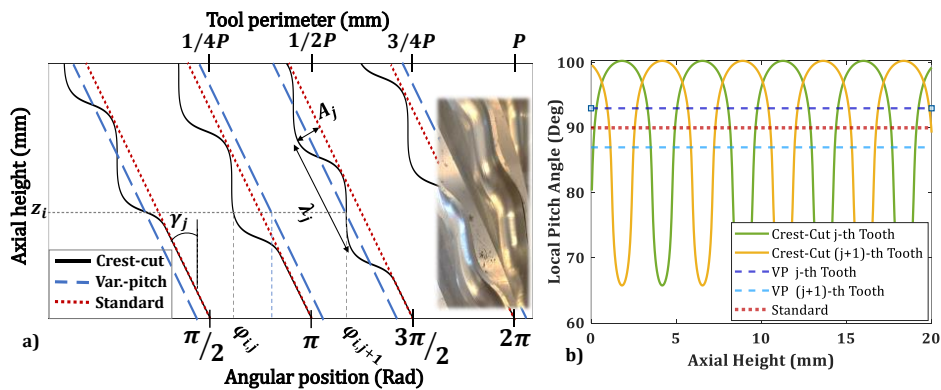


Figure 3.26. Local pitch variation for three different tool types.

The variable-pitch and crest-cut tools offer a significant possibility to attain high stability limits by tuning their geometry to a certain spindle speed [4,35,37]. In this study, the geometry of the tools is optimized considering the desired spindle speed of 2123 rpm

(corresponds to 80m/min for 12mm tool diameter (D_t)). Two different variable-pitch tools with alternating pitch variations are designed to suppress chatter for each mode of the plate with the method presented in [35].

$$\begin{aligned} \Delta P &= \pi \frac{\Omega}{\omega_c} && \text{for even } N_t \\ \Delta P &= \pi \frac{\Omega}{\omega_c} \frac{N_t \pm 1}{N_t} && \text{for odd } N_t \end{aligned} \quad (3.35)$$

where Ω is spindle speed (rps), ω_c is chatter frequency, and N_t is the number of teeth. In order to consider the changes in chatter frequency due to the presence of pitch variation, an iterative method presented by Comak et al. [37] is used to find optimum pitch angles. According to the natural frequencies of the part and the desired spindle speed (2123 rpm), VP1 and VP2 tools are selected to suppress chatter. These tools are designed considering the average value of the first and second modal frequencies of the plate in its most flexible zone (0-20 mm in the V direction), 1590 Hz, and 2550 Hz, respectively. The presence of multi modes with varying frequencies due to IPW dynamics causes different chatter frequencies at different cutting points on the part. As variable pitch end mills are designed for a target chatter frequency and spindle speed, they lose their effectiveness in machining of thin-walled parts.

On the other hand, crest-cut end mills can suppress chatter in wider frequencies and speed ranges due to the wavy edges resulting in continuous pitch variations in the cutting zone. In order to determine the optimum crest-cut wave shape for a target spindle speed, the procedure presented in [4] is applied. However, as crest-cut tools introduce multiple delays, their effectiveness is not limited to the specified frequency as they can perform effectively in wider ranges. Optimally selected special end mill geometries are given in Table 6. Crest-cut tool has 1mm edge wave amplitude (A) and 6mm edge wavelength (λ) that shows superior stability at 2123 rpm.

Table 6. Geometrical parameters of end mills.

Type	D_t	N_t	γ	Pitch	A	λ
STD	12 mm	4	38°	[90°-90°-90°-90°]	-	-
CC				[90°-90°-90°-90°]	1mm	6mm
VP1				[88°-92°-88°-92°]	-	-
VP2				[88.75°-91.25°-88.75°-91.25]	-	-

3.4.4. Stability Performance of Crest-Cut & Variable Pitch Tools

Using SDM, each point's stability limit along the tool path is obtained according to the varying IPW dynamics. The resulting stability limits which are varying in both feed (U) and plate depth (V) are illustrated for different tool types in Figure 3.27. Note that stability limits corresponding to 80 m/min are calculated for each tool.

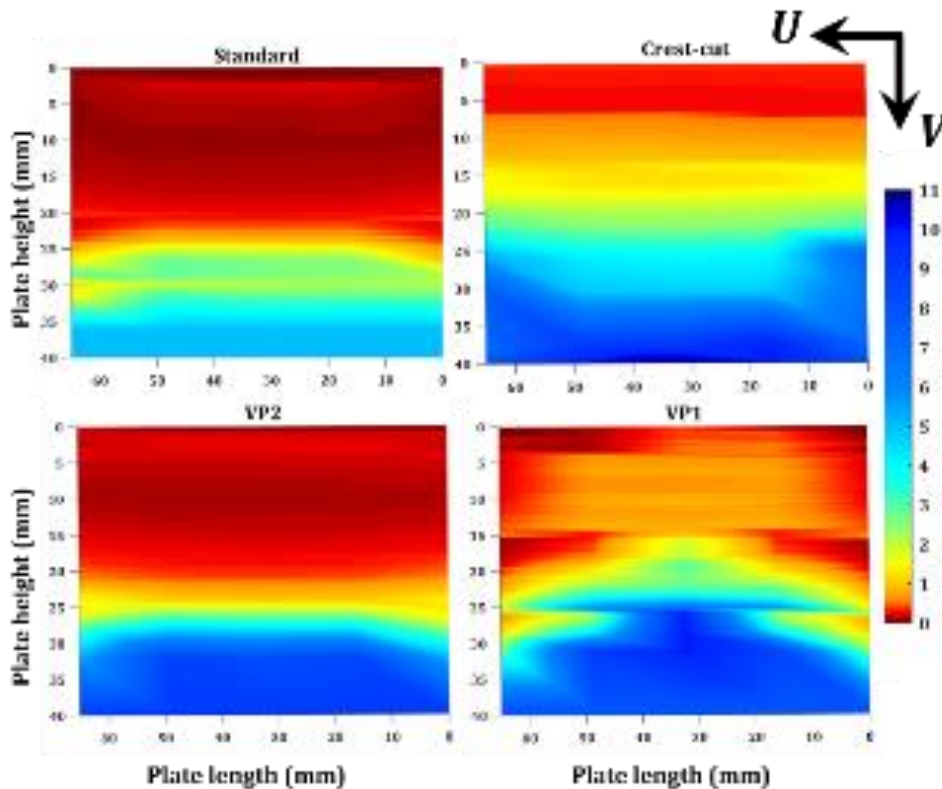


Figure 3.27. Varying stability limits on plate considering varying-dynamics of IPW

According to Figure 3.27, it is seen that the crest-cut tools represent the best stability

performance, when compared to the other tools since the low-stable-depth region (red) is narrow and the high-stable-depth region (blue) is considerably large. Further, the variation of stability limits in feed direction is negligible since crest-cut tools can suppress chatter in a more comprehensive range of frequencies [4]. Stability limits for the VP1 tool at the middle of the plate are higher compared to the edges as expected since this tool was designed to suppress chatter around the first bending mode of the plate. VP2 was tuned according to the chatter frequencies in the vicinity of the second mode of the plate. However, stability is limited by the first mode of the plate, and thus the changes in the feed direction are not significant. As expected, the worst stability map with considerably low stability limits belongs to the standard tool. Once the stability maps are evaluated (see Figure 3.27), a milling strategy is used. In this strategy, the plate is divided into constant stepdown values, which is a practical cutting strategy and used with all tools. Number of passes (NP) and chatter-free area percentages (CFAP) with milling of each tool is given in Table 7.

Table 7. The number of passes and chatter-free area percentages.

	Standard		Crest-cut		VP1		VP2	
	NP	CFAP	NP	CFAP	NP	CFAP	NP	CFAP
STG	100	47	100	83	100	70	100	52

In order to evaluate the strategy in terms of productivity, the number of passes (NP) is calculated according to the stepdown value. Here, Relative Stability Index (RSI), the ratio of the local stability limit at a point to the stepdown value, is used to represent the chatter condition related to the surface finish quality (SFQ). Then, the SFQ map is obtained based on the local RSI values over the workpiece surface, where darkening in the color represents the transition from a stable to unstable condition. Low values of CFAP mean higher workpiece area with poor surface finish requiring further processing such as polishing.

This issue is considered in STG, where a constant stepdown value of 0.4 mm is used all around the part. The SFQ maps together with the actual machined surfaces for this strategy, are shown in Figure 3.28. According to the maps, the crest-cut tool offers higher CFAP compared to the other tools. As also illustrated in Figure 3.28, there is a good agreement between the SFQ maps and the surface finish obtained in the milling tests.

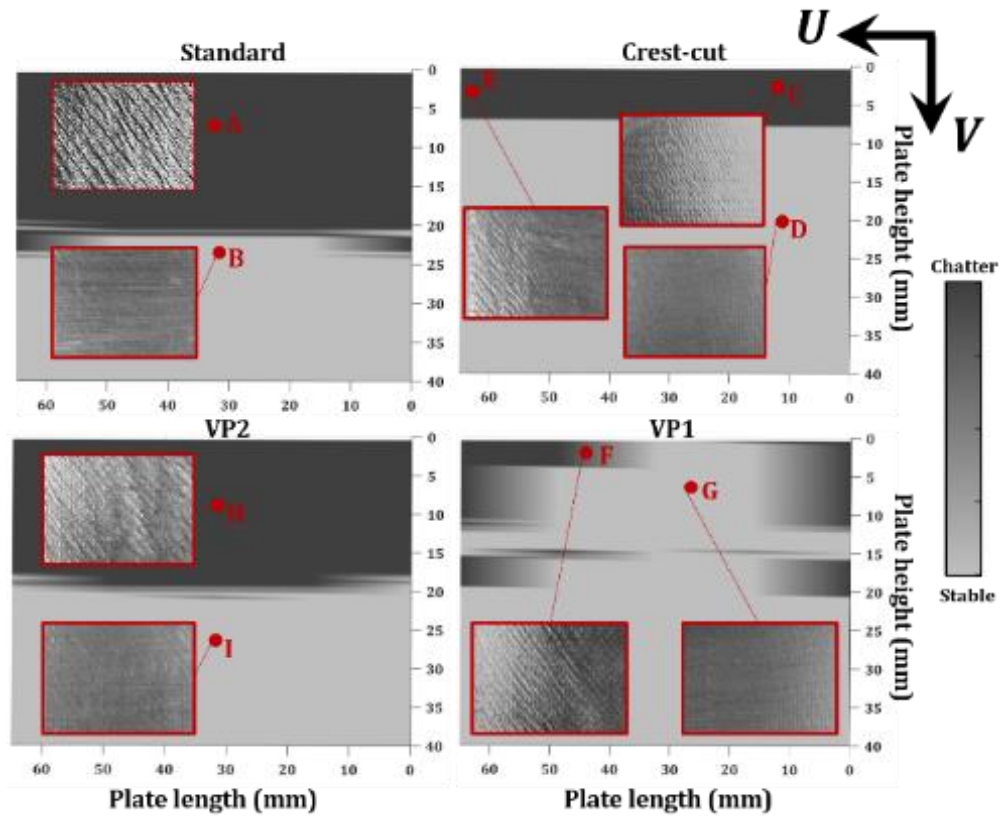


Figure 3.28. Surface finish quality maps for proposed STG and verifications.

The darker areas in the SFQ map represent very poor surface finish, whereas the points in the light-colored areas indicate much better surface finish.

3.5. Summary

In this chapter, stability model including multi-axial element stiffness is solved for multi-mode thin-wall milling system and verified by experiments as the first time in literature. Chatter can be suppressed using higher depths using benefit of multi-axial stiffness stability model. This model is presented for different cases, and the effect of process parameters and plate geometry is discussed in depth. Different cutting strategies are proposed to demonstrate effectiveness of multi-element model.

Stability performance of special end mills such as variable pitch and crest-cut is also investigated in milling of hard-to-cut thin-walled parts and compared with standard end mill. In this thesis, thin-walled part dynamics is modeled using FE analysis and a practical approach is proposed to prevent high number of iterations between workpiece dynamics

and stability simulations. According to the generated stability maps, crest-cut tools show outstanding performance in milling of thin-walled parts when compared to the variable pitch and standard end mills. It can be concluded that selecting the machining strategy considering varying stability limits along CLs has significant consequences on machining time and CFAP, thus productivity and part quality. SFQ maps show that the crest-cut tool has superior performance considering surface quality and productivity. Variable pitch tools may suppress chatter in one of the plate modes, but they lose their effectiveness on different CL points due to frequency variations of multiple modes under mass removal effects. On the other hand, crest-cut tools provide much higher stability limits in a wide frequency range with high robustness against frequency variation.

4. CHATTER-FREE FLANK MILLING OF THIN-WALLED PARTS

4.1. Introduction

Stable cutting with higher depth of cuts is getting more challenging, as the workpiece is thin-walled structure. Thus, a detailed analysis is needed to predict stable depths in milling under the effect of process damping. In addition, forced vibration may increase during cutting with process damping effect that may left error on the finished surface in stable and marginally stable conditions. On the other hand, effect of stock thickness with varying-dynamics of IPW on stability limit under process damping effect is not investigated currently in literature.

In this chapter, an approach is proposed for the machining parameter selection to achieve higher chatter-free cutting depths in milling of thin-walled parts at low cutting speeds with the effect of process damping. In this regard, a detailed stability analysis is performed considering varying dynamics of workpiece and dynamic interactions arising from process itself. In addition, selection of semi-finish stock thickness is carried out to demonstrate finishing process can be stabilized with the effect of process damping with optimal stock left from the semi-finishing stage. The cutting edge geometry (i.e. hone radius and clearance angle) has a significant role to achieve higher stable cutting depths at low cutting speeds and its influence on process damping is investigated through simulations. In this respect, a proper cutting edge geometry is selected and its performance in finishing of thin-walled part is demonstrated.

The workpiece dynamics model is developed in finite element (FE) environment to show the effect of varying-IPW dynamics on stability limits at low cutting speeds. As the system may vibrate a certain amplitude during process damping (i.e., limit cycles), vibration marks arise left on the finished surface with higher amplitude due to forced vibration. These vibrations and its effect on surface finish quality are evaluated experimentally with surface measurements, which are also carried out for experimental verification after various cutting tests.

Process damping, which is affected by process, geometric and modal parameters is one of the most significant tools for increased stability limits occurring at low cutting speeds and comes from process itself. Process damping constants should be identified to find

stability limits at first that is presented in the reference [61] for milling by using inverse stability solution and finding penetration constant using energy balance equations. In this part of the thesis, modeling of process damping provided briefly for identified penetration constant, which depends on tool and workpiece material pair.

4.2. Process Damping Model

Penetration area, which is the function of vibration parameters such as amplitude, wave slope and cutting edge geometry such as hone radius and clearance angle is the main source of process damping effect arising at low cutting speeds (see Figure 4.1). Numerical procedure was developed by Budak and Tunc [57] for the calculation of penetration area by dividing overall penetration area to discrete areas as illustrated in Figure 4.2. The same procedure is followed to calculate penetration area, which is used in finding process damping constants this study.

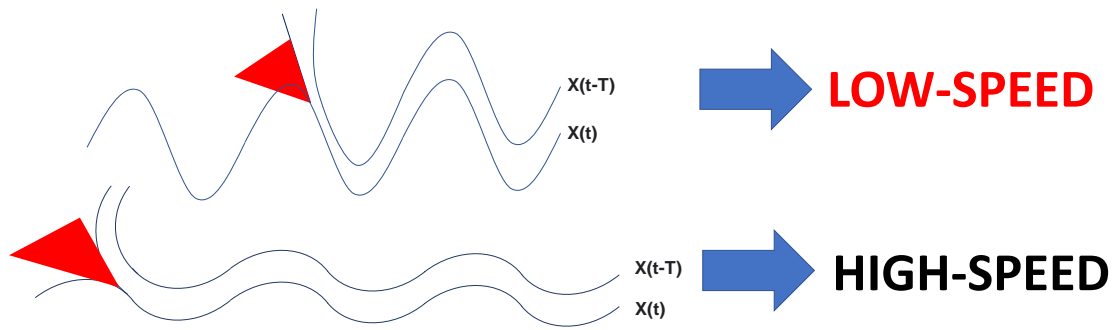


Figure 4.1. Vibration mechanism of the metal cutting system at low and high cutting speeds.

The cutting edge moves along the periodic vibration waves with the amplitude A and frequency ω_c in dynamic chip thickness direction:

$$x = A + A\sin(\omega_c t), \quad \frac{dx}{dt} = A\omega_c \cos(\omega_c t) \quad (4.1)$$

An end mill generates vibration waves left on the finishing surface, while the tool and flexible workpiece vibrate and the cutting edge of the tool penetrates the wave into radial direction as demonstrated in Figure 4.2. Hence, penetration forces occur in tangential and

radial directions on the cutting edge, that absorbs energy, and thus stabilize the process. In this part, process damping effect owing to the damping forces planar directions is demonstrated by including process damping constants, c_x^{pd} and c_y^{pd} into the equation of motion. In reference [61], its more practical and used for identification of process damping using inverse stability approach easily.

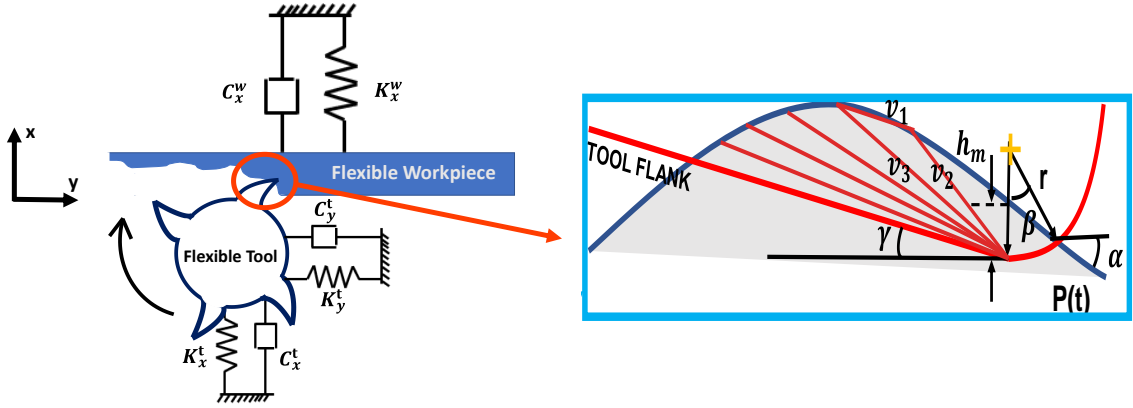


Figure 4.2. Process damping in milling for flexible tool-workpiece system.

The equation of motion in two orthogonal directions for an end milling system can be presented as in the Eq. (4.2), where $k, c^{pd}, c^{st}, m, F, \omega_n, x$ stand for modal stiffness, process and structural damping constants, modal mass, dynamic milling force, modal frequency and vibration amplitude respectively.

$$\begin{aligned}
 m_x \frac{d^2 x}{dt^2} + (c_x^{pd} + c_x^{st}) \frac{dx}{dt} + k_x x(t) &= F_x \\
 m_y \frac{d^2 y}{dt^2} + (c_y^{pd} + c_y^{st}) \frac{dy}{dt} + k_y y(t) &= F_y
 \end{aligned}
 \tag{4.2}$$

The penetration force, which occurs at low cutting speeds due to dynamic penetration of cutting edge and wavy surface creates additional damping by absorbing energy in dynamic chip thickness direction, which needs to be known to determine the average process damping coefficients. Penetration constant (K_D), which depends on tool-workpiece material pair since this constant is directly related to elastic property of the material is identified as 30,000 N/mm³ for Ti6Al4V workpiece and carbide tool from conservation of energy in the cutting system [6].

Process damping forces ($F_{r,j}^{pd}$ and $F_{t,j}^{pd}$) in radial and tangential directions, which are calculated using penetration volume $V(t)$ can be expressed in milling system as follows:

$$\begin{aligned} F_{r,j}^{pd}(t) &= K_D V_j(t) \\ F_{t,j}^{pd}(t) &= \mu K_D V_j(t) = \mu F_{r,j}^{pd}(t) \end{aligned} \quad (4.3)$$

In Eq. (4.3) μ is friction constant, which arises due to flank-part contact is generally taken as 0.3 [83]. Process damping attenuates vibrations, since they generate damping force in the inverse direction of dynamic milling forces, and thus they should be extracted from local milling forces as given below:

$$\begin{aligned} F_{t,j}(t) &= K_{tc} ah(\phi_j) - F_{r,j}^{pd}(t) \\ F_{r,j}(t) &= K_{rc} ah(\phi_j) - \mu F_{r,j}^{pd}(t) \end{aligned} \quad (4.4)$$

In Eq. (4.4), K_{tc} and K_{rc} are tangential and radial milling force coefficients, which are identified as 1750 N/mm² and 456 N/mm² respectively for Ti6Al4V workpiece and carbide tool with the rake and helix angles of 7° and 38°, and the used feed rate is 0.05 mm/rev/tooth in each simulation.

Derived local milling forces with process damping force acting on cutting edge ($F_{t,j}$ and $F_{r,j}$) should be converted global planar forces (F_x and F_y) as follows:

$$\begin{aligned} F_x &= \sum_{j=1}^N -F_{t,j} \cos(\phi_j) - F_{r,j} \sin(\phi_j) \\ F_y &= \sum_{j=1}^N F_{t,j} \sin(\phi_j) - F_{r,j} \cos(\phi_j) \end{aligned} \quad (4.5)$$

Stability analysis of milling was derived by taking average terms of periodic directional dynamic milling force factors that enables to find stable limits analytically [19]:

$$a_{LIM} = -\frac{2\pi\Lambda_R}{NK_{tc}}(1 + \kappa^2)$$

where,

(4.6)

$$\Lambda = -\frac{1}{2a_0} \left(a_1 \pm \sqrt{a_1^2 - 4a_0} \right) \text{ and } \kappa = \frac{\Lambda_I}{\Lambda_R}$$

In Eq. (4.6), Λ_R stands for the real part of the eigenvalue (Λ), which is a function of direct FRFs and directional dynamic milling force factors.

In milling, interaction between cutting tool and workpiece is determined by the parameters such as radial immersion, depth of cut and helix angle. The process damping constants can be written as the multiplication of specific process damping coefficients and the interaction length over a cutter rotation. The energy dissipation due to cutter-workpiece penetration, planar process damping forces is related to process damping coefficients presented in reference [61].

In this study, the same procedure is used for stability limit under process damping effect calculation. Stability limits at low cutting speeds are found in frequency domain by the following iterative procedure proposed by [6] provided as follows:

Step 1. Sweep chatter frequency ω_c around dominant modal frequencies, set vibration amplitude $A = A'$ and stability limit $a = a_{ABS}^{HS}$ and find specific process damping coefficients \widetilde{c}_x^{pd} and \widetilde{c}_y^{pd}

Step 2. Find interaction length of cutting flute l_i to calculate c_x^{pd} and c_y^{pd}

Step 3. Update FRF of dominant modes using new c_x^{pd} and c_y^{pd}

Step 4. Recalculate stability limit using Eq. (4.6) with updated c_x^{pd} and c_y^{pd}

Step 5. If $|a_{LIM} - a| > \epsilon$, set $a = a_{LIM}$ and run *Step 2* again until $|a_{LIM} - a| < \epsilon$

In the following sections, stability analysis at low cutting speed is carried out using the previously explained analytical process damping method. It is known that modal frequencies of the system and cutting edge geometry have significant effect on stability limit under process damping effect [63]. As tool with higher hone radius and lower clearance angle is used, higher amount of cutting edge penetration arises that increases penetration volume, and thus stability limit under process damping effect. In addition to

cutting edge geometry, higher modal frequency of the system results shorter wavelength (i.e. vibration waves with higher slope) that provides more stabilizing effect. For instance, second twisting mode of the plate provides higher stable depths at relatively higher speeds in some cases, where the structure is dynamically rigid enough. In the following part of the thesis, influence of modal frequency and cutting edge geometry on stability limit under process damping effect in milling of thin-walled part is investigated through simulations.

4.2.1. Influence of The Cutting Edge Geometry and Modal Frequency

It is demonstrated that the cutting tool with honed edge results higher amount of penetration of the cutting edge into vibration waves left on the cutting surface in literature [57,73,79,84]. On the other hand, if the edge geometry is sharp, process damping can only be achieved with reducing cutting speed and clearance angle drastically to increase slope of the vibration wave and the flank contact. It is also known that higher frequency reduces wavelength, and thus increases slope of the wave undulations resulting high process damping constants.

The cutting edge with higher hone radius and lower clearance angle result the increment in penetration volume, and thus improved process damping. Higher modal frequency leads to shorter wavelength, hence the slope of vibration amplitude left on the surface increases that also results higher process damping effect. The effect of edge geometry and modal parameters such as modal frequency was investigated and discussed in reference [63] in depth. However, here the workpiece flexibility provides additional outcomes in terms of the relation between multi-modal frequencies and stability limit with process damping. While the cutting edge parameters (i.e., hone radius and clearance angle) depend on the tool, which is fixed for a case, modal frequency differs as material removed from the workpiece. On the other hand, as cutter location (CL) varies contributions of dominant modes of the thin-walled workpiece in stability changes. For instance, as the CL reaches to middle of the thin-walled part, second twisting mode has infinite stability since first bending mode is dominant in that CL. The effect of IPW dynamics is discussed further sections of the study.

Effect of cutting edge geometry (i.e. hone radius and clearance angle) and multi-modal frequencies of the workpiece on stability limit under process damping effect is showed through simulations for a thin-walled Ti6Al4V plate with the dimensions of 40x65x3 (in mm) in Figure 4.3.

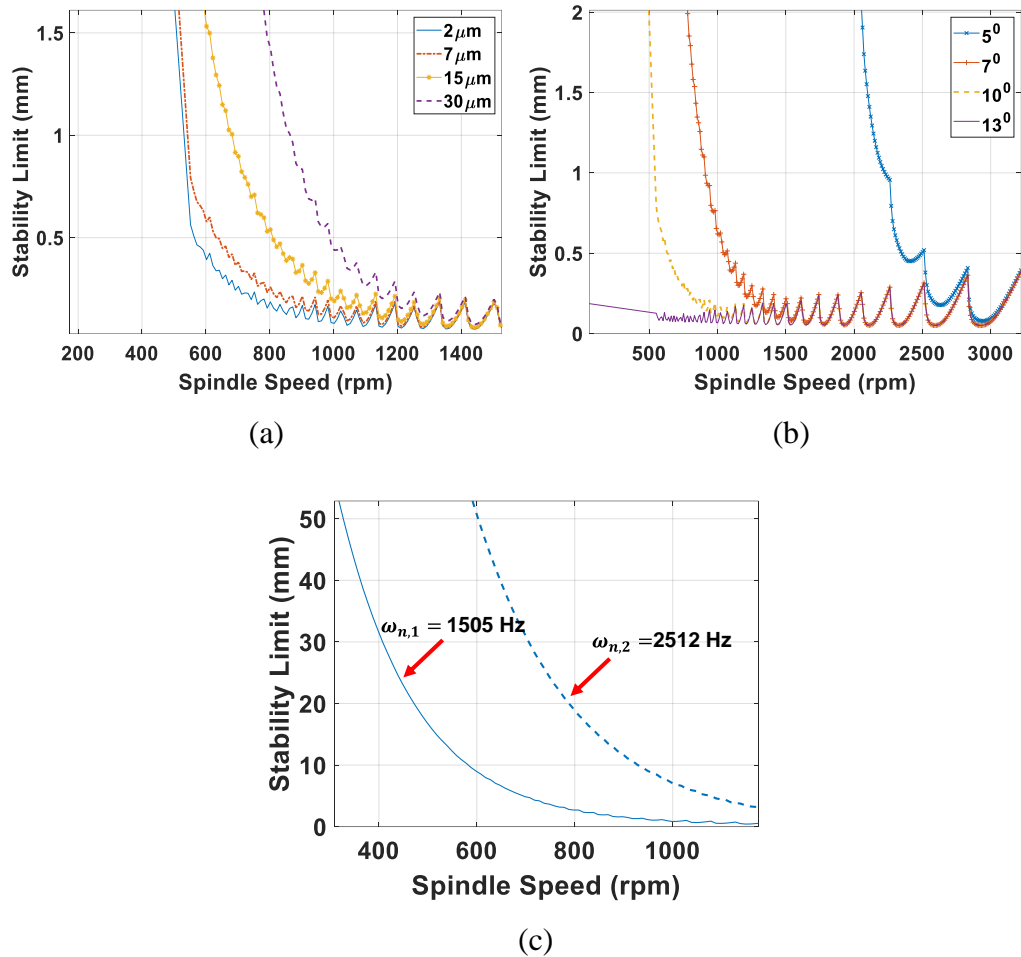


Figure 4.3. Effect of cutting edge geometry (a) hone radius (b) clearance angle (c) modal frequency on process stability at low cutting speeds.

As depicted in Figure 4.3, selection of hone radius and clearance angle is significant for improved low-speed stability. The main reasons are the higher amount of penetration volume arises as discussed in previously. In addition, low and high frequency modes of thin-walled structure generate different stability limits. Stability limits shift higher speeds, where the high frequency twisting mode can be suppressed, and thus higher stable limits can be achieved, whereas the first bending mode cannot be suppressed using that speed-axial depth pairs.

Hone radii of the cutting tools are measured using 3D confocal microscope (μsurf

NanoFocus) device at different locations of cutting edge and average hone radius of cutting edge is found and used in simulations as given in Figure 4.4.

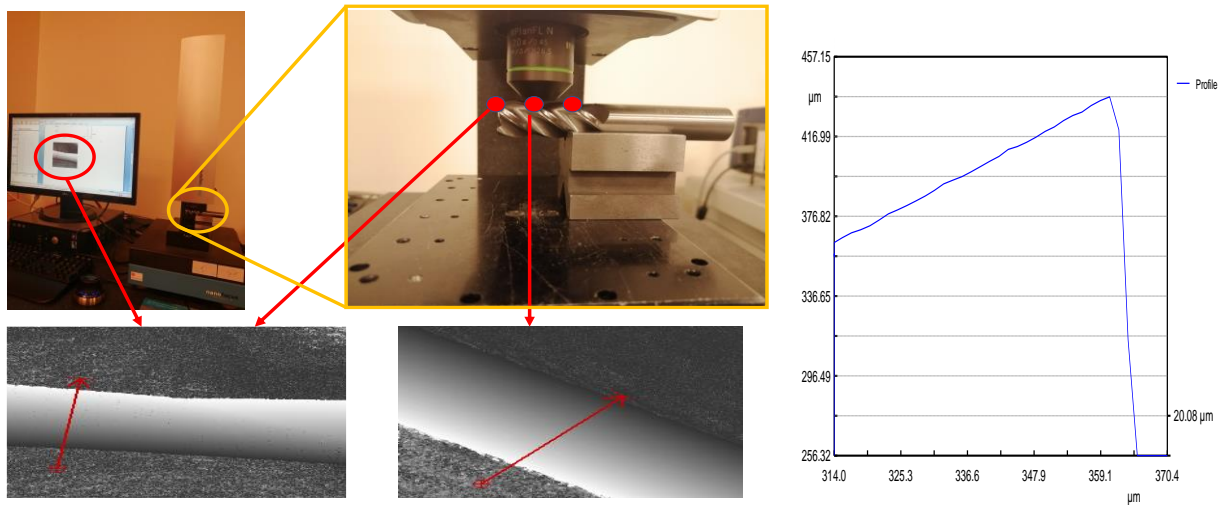


Figure 4.4. Measurement of cutting edge radius.

In finishing of thin-walled parts, deeper chatter-free axial depths can be achieved with proper selection of semi-finish stock thickness with the effect of process damping. Increasing stock thickness results higher dynamic rigidity of the structure. On the other hand, required radial depth of cut increases that reduces stability limit. Therefore, there is a trade-off between stock thickness and stability limits. In following section, optimal selection of stock thickness in finish milling of thin-walled parts is performed to reach higher cutting depths at low cutting speeds.

4.2.2. Selection of Stock Thickness

As stock thickness of the thin-walled workpiece increases, FRF amplitude reduces, at the same time natural frequency increases that leads to increased stability limit and shift lobes to higher speeds. In addition, using thicker stock shape means to use higher radial depth of cut that reduces stability limits. Therefore, the optimal selection of stock thickness, which offers higher stable depths should be carried out to decide the highest possible stock thickness for reduced semi-finishing time and chatter-free finishing operation for improved productivity.

In this part of the thesis, low-speed stability analysis is performed with the effect of

process damping in milling of thin-walled part to carry out optimal selection of stock thickness left on the finishing part. Titanium-alloy (Ti6Al4V) used as workpiece material with the final part dimensions of 40x65x3 (in mm). In simulations, modal parameters of the thin-walled workpiece are extracted using FEA for uncut case at first. After, the maximum allowable vibration amplitude of the thin-walled workpiece is assumed as 15 μ m. The stability analysis is conducted to find optimal stock thicknesses for this case. In the stability analysis, the effective modes (i.e. 1st bending and 2nd twisting) of thin-walled workpiece are considered as seen in Figure 4.5. The stability limits at low cutting speeds and the effect of stock thickness are depicted in Figure 4.9.

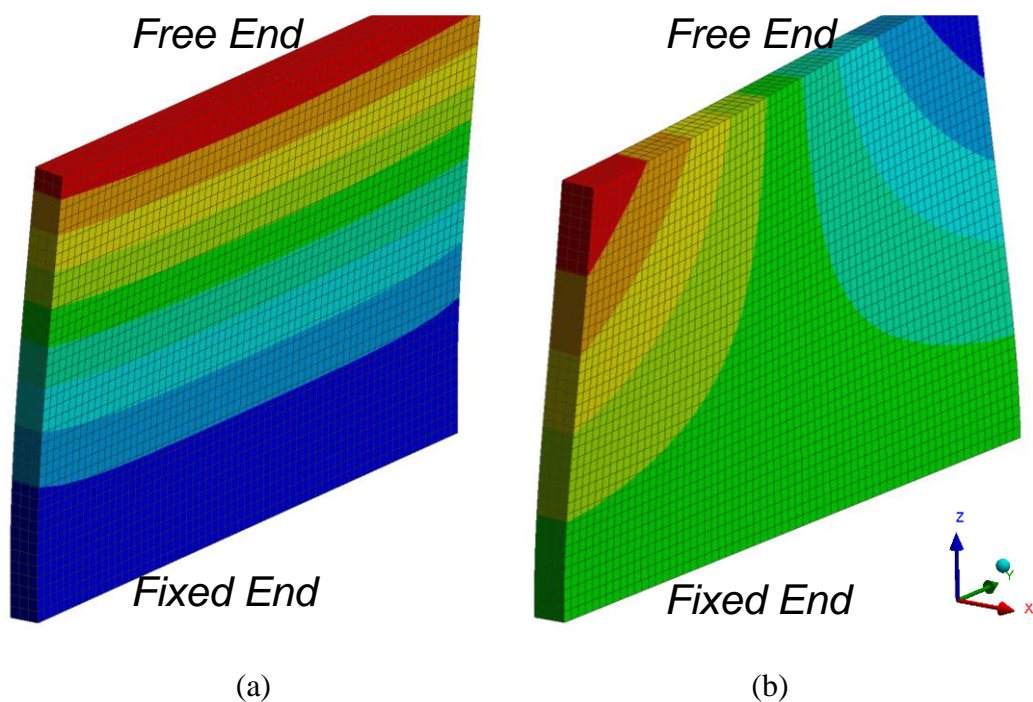


Figure 4.5. Dominant (a) bending (b) twisting (torsional) modes of thin-walled workpiece with boundary conditions

Frequency response function (FRF) of the finished thin-walled workpiece and 16 mm diameter carbide end mill are measured using modal testing with impact hammer, in addition, the workpiece dynamics is simulated in FEM.

The measured modal parameters of the cutting tool clamped with 150Nm torque and 50 mm overhand length in two orthogonal x and y -directions are provided in Table 8.

Table 8. Modal Parameters of the Milling Tool

D-16 Carbide End Mill	Natural Freq. (Hz)	Modal Stiffness (N/m)	Damping Ratio (%)	Modal Mass (kg)	Magnitude FRF Peak (m)
<i>x-direction</i>	4066	2.4×10^7	1,96	0.037	1.21×10^{-6}
<i>y-direction</i>	4068	2.6×10^7	1,86	0.040	1.15×10^{-6}

The measured FRF of the tool and the simulated FRF of the workpiece at the most flexible points (tool tip and workpiece tip-edge) are given in Figure 4.6.

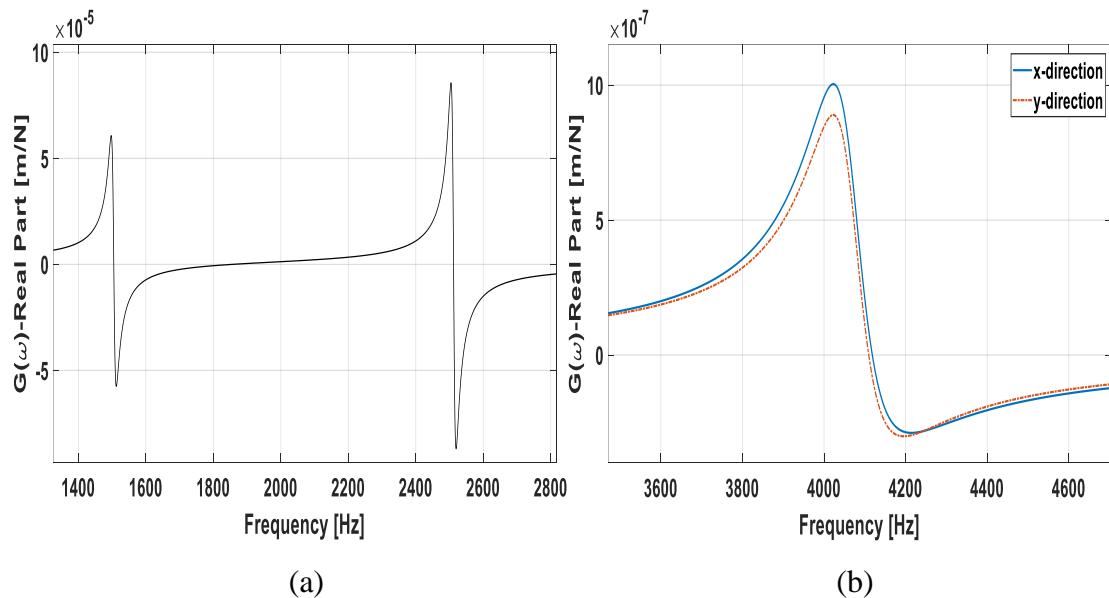


Figure 4.6. (a) Workpiece and (b) measured tool FRFs

As shown in Figure 4.7 as vibration amplitude and natural frequency of thin-walled workpiece increase (i.e. low ‘first’ modal frequency and high ‘second’ modal frequency), the effect of stock thickness on stability limits becomes non-linear due to non-linear relationship between process damping force and vibration amplitude, which is a function of frequency as given in Eq. (4.1). In addition, increasing semi-finish stock thickness (i.e. higher radial depth) leads to reduction in absolute stability limit, on the contrary stability limit may increase due to higher modal stiffness of the workpiece with higher stock thickness.

In this case, as finish milling is considered, the lower and upper limits of candidate stock

thickness values are taken as 0.1 mm and 1.5 mm respectively. The main reason is to demonstrate the selection of optimal stock thickness from high range of values. These stock thickness values are in the range between 3% and 50% of final workpiece thickness and these cases are given in Table 9 to show effect of stock thickness on modal parameters of the workpiece.

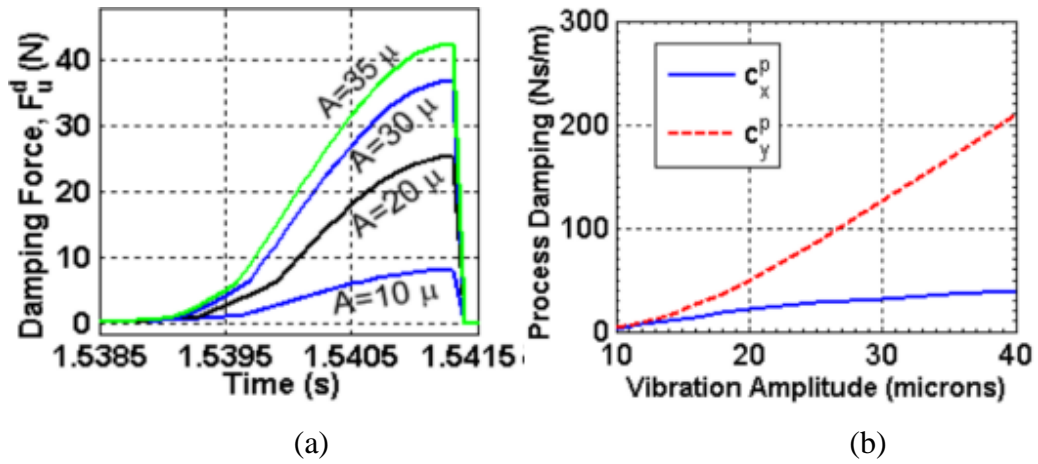


Figure 4.7. Process damping (a)force and (b)constant variation with vibration amplitude

[3]

Modal analyses are performed for different stock shapes using FEM. Variation in natural frequency and mode shape is given in Table 9 for various stock thickness values, as the natural frequencies and normalized mode shapes of finished part are found as 1505 Hz, 2512 Hz, 10.28 and 16.06 respectively.

Table 9. Change of natural frequency and normalized mode shape with stock thickness

Stock Thickness (mm)	1st & 2nd Nat. Freq.	1st & 2nd Mode Shape	Change% in Nat. Freq.	Change% in Mode Shapes
0.1	1553-2607	10.12-15.80	3	2
0.2	1582-2655	9.95-15.56	5	3
0.3	1633-2733	9.80-15.31	8	5
0.4	1681-2812	9.65-15.09	12	6
0.5	1731-2891	9.51-14.87	15	8
0.6	1775-2963	9.37-14.66	18	10
0.7	1823-3038	9.24-14.46	21	11
0.8	1868-3112	9.12-14.26	24	13
0.9	1905-3170	8.99-14.08	26	14
1	1952-3245	8.77-13.90	30	17
1.1	2000-3320	8.76-13.72	33	17
1.2	2047-3396	8.66-13.56	36	19
1.3	2094-3470	8.55-13.40	39	20
1.4	2139-3541	8.45-13.24	42	21
1.5	2178-3601	8.36-13.13	45	23

After performing modal analysis, frequency response functions (FRFs) of the workpiece are calculated from Eq. (4.7) for each stock thickness.

$$\phi(\omega) = \sum_{k=1}^m \frac{\{u_k\}^2}{-\omega_j^2 + \sqrt{-1}\omega_j 2\zeta_k \omega_{n,k} + \omega_{n,k}^2} \quad (4.7)$$

$$G(\omega) = Re\{\phi(\omega)\} + \sqrt{-1} Im\{\phi(\omega)\}$$

In Eq. (4.7), $\{u_k\}$, ζ_k , $\omega_{n,k}$ stand for mode shape, damping ratio and natural modal frequency respectively. "m = 2" for this case since the first two dominant modes of the thin-walled workpiece are considered in the analysis. $G(\omega)$ stand for FRF, which is calculated from real and imaginary parts.

FRFs of thin-walled workpiece with various stock thicknesses are simulated and provided in Figure 4.8 (b). In addition, increasing stock thickness increases modal frequencies that

is shown in Figure 4.8 (a).

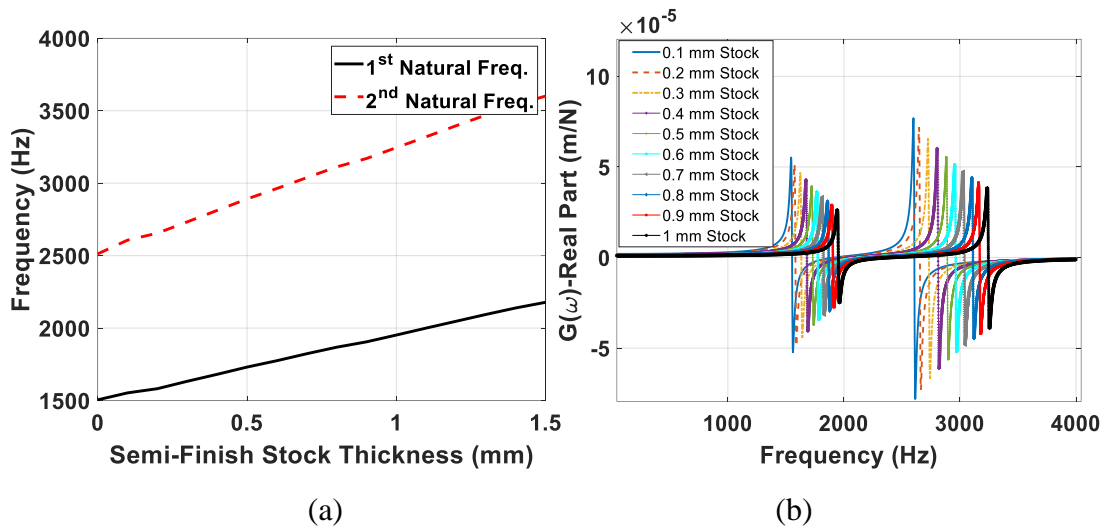


Figure 4.8. Variation in (a) natural frequencies and (b) FRFs with the change of stock thickness

As seen from Figure 4.8, as stock thickness increases the workpiece becomes more rigid and the modal frequencies shift higher frequency values. After extraction of structural dynamics of thin-walled part with different stock thicknesses, stability analysis is performed to select optimal stock thickness value. Stability analysis for various stock thickness is provided in Figure 4.9.

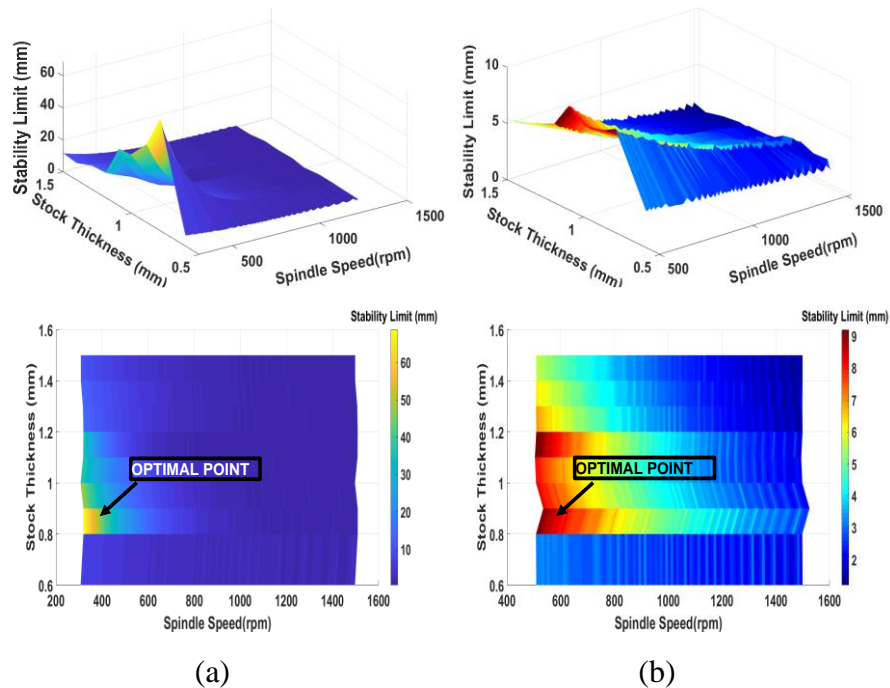


Figure 4.9. Optimal stock thickness selection as the system vibrates with 15 μ m amplitude (a)1st mode (b)2nd mode.

As a result, considering both cutting speed and depth of cut, the highest possible stable depth of cuts can be achieved with using 0.8 mm and 0.9 mm stock thicknesses as the system is allowed to vibrate maximum 15 μ m vibration amplitude.

According to the demonstrated stability simulations with assuming marginal stable vibration amplitude, which is under the effect of process damping as 15 μ m amplitude in Figure 4.9, higher stable limit, which equal to workpiece height is not possible. However, as discussed in the section 4.2.1 it is known that increased hone provides higher amount of penetration, and thus higher stable limits. On the other hand, the surface quality requirement may be another limitation in finish milling. In this regard, low-speed stability is simulated for the cutting tool with 35 μ m hone radius and assuming vibration amplitude as 5 μ m to show the effect of hone radius for different stock thicknesses.

Flank milling of thin-walled parts is possible (i.e. higher stability limits), that can be obtained without trading-off surface quality of the workpiece using a proper cutting edge geometry.

It is clear that as given in Figure 4.10, 5 μ m vibration amplitude can be achieved by performing flank finishing using the tool with 35 μ m hone radius. On the other hand, process damping effect is lost with using the cutting tool, which has 7 μ m hone radius as the system is allowed to vibrate with maximum 5 μ m amplitude.

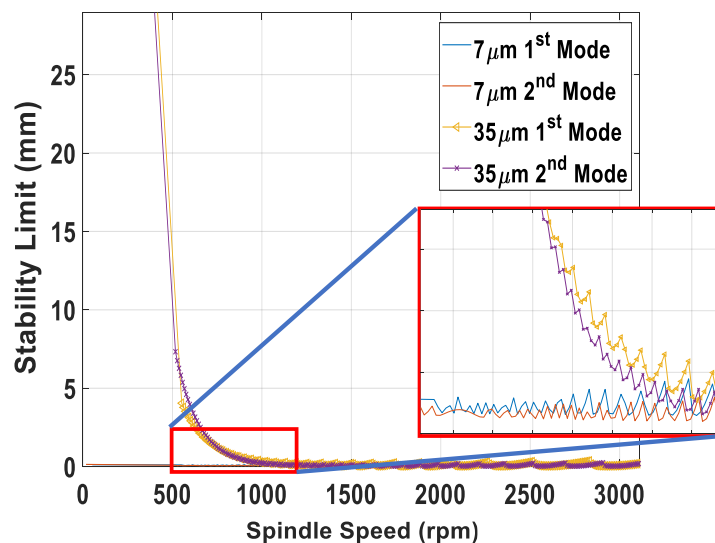


Figure 4.10. Low-speed stability limit comparison of 7 μ m and 35 μ m hone radii in flank

milling of thin-walled part at $5\mu\text{m}$ vibration amplitude considering multi-mode.

The effect of semi-finish stock thickness on stability limit with process damping is given in Figure 4.11 for honed tool ($35\mu\text{m}$) and the system vibrates at $5\mu\text{m}$ amplitude. Stability analysis results demonstrates that after a certain cutting speed, process damping effect lost and drastic decrement is observed in stability limit. Moreover, optimal stock thickness, which does not depend on hone radius and vibration amplitude values are obtained as 0.8 mm and 0.9 mm again.

It can be seen from Figure 4.11, even the vibration amplitude of the cutting system reduces, higher cutting depths can be achieved as hone radius is $35\mu\text{m}$.

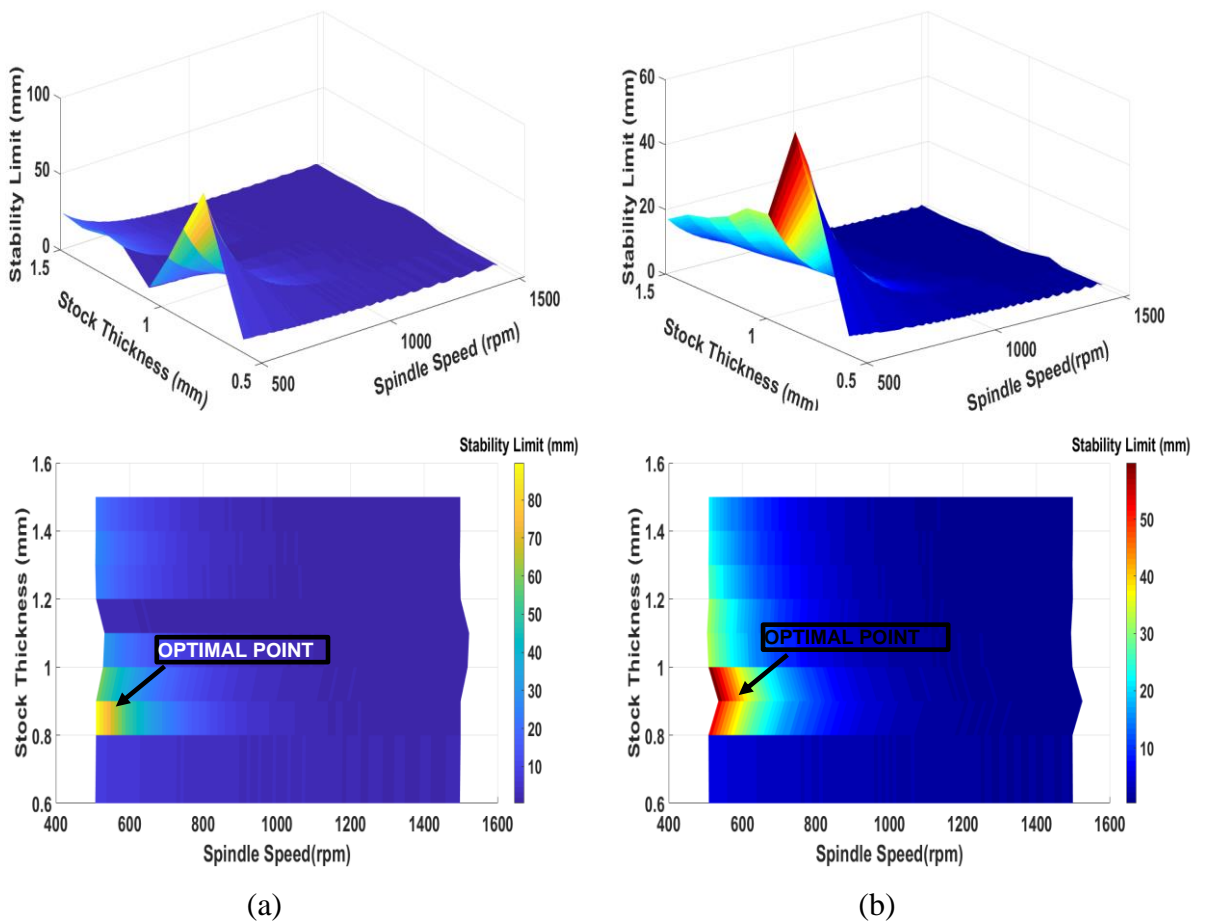


Figure 4.11. Optimal stock thickness selection as the system vibrates with $5\mu\text{m}$ amplitude (a)1st mode (b)2nd mode.

As depicted in Figure 4.11, end mill with honed edge may provide to cut deeper due to its higher penetration volume at low cutting speed as discussed in section 4.2.1.

Moreover, it is possible that thin-walled part milling with lower vibration amplitude using end mill with honed edge that enable to use optimally selected semi-finish stock thicknesses to finish the workpiece with one pass as demonstrated in Figure 4.11.

The case, where the stock thickness is equal to 0.9mm (i.e. 3.9mm workpiece thickness) and the thin-walled part is relatively rigid in comparison to other stock thicknesses, stability analysis at low cutting speed performed. Since the workpiece modes are the most flexible elements of the dynamic milling system, the stability limit, which comes from the most flexible mode of the cutting tool provides the highest depth that does not a limitation in terms of chatter as given in Figure 4.12.

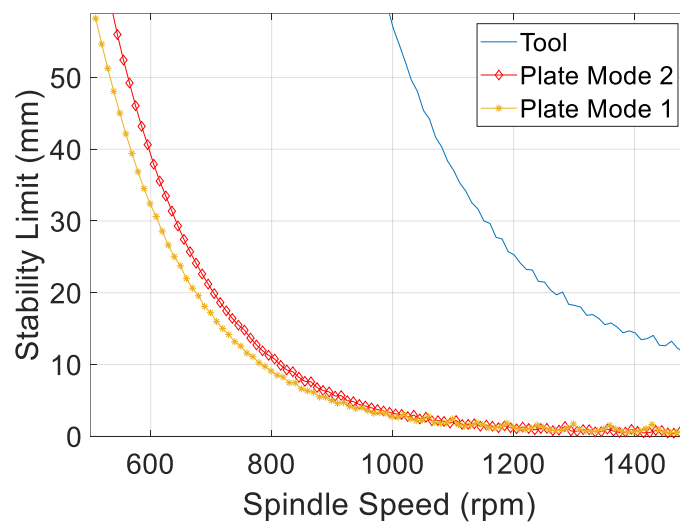


Figure 4.12. Stability limit including tool dynamics for 5 μ m vibration amplitude and 3.9mm stock thickness

4.3. Stability Analysis Considering Varying-Dynamics of IPW at Low Cutting

Speeds

According to the stability analysis performed in previous section, optimal stock thicknesses of the thin-walled workpiece are determined as 0.8 mm and 0.9 mm depicted in Figure 4.9 and Figure 4.11 without considering varying-dynamics of IPW for each case.

After selection of optimal stock thickness according to the low-speed stability limits, as material removed in each cutting steps, change of workpiece dynamics and CL in flank milling operation is considered in stability analysis with process damping effect. IPW dynamics is analyzed for optimal stock thickness at first. Then, the stability analysis is performed considering the effect of process damping in each cutting stages. The IPW is modelled using ANSYS APDL software and the flowchart of the macrocode, which extracts the modal parameters of varying-dynamics of IPW for milling considering CL is provided in Figure 4.13.

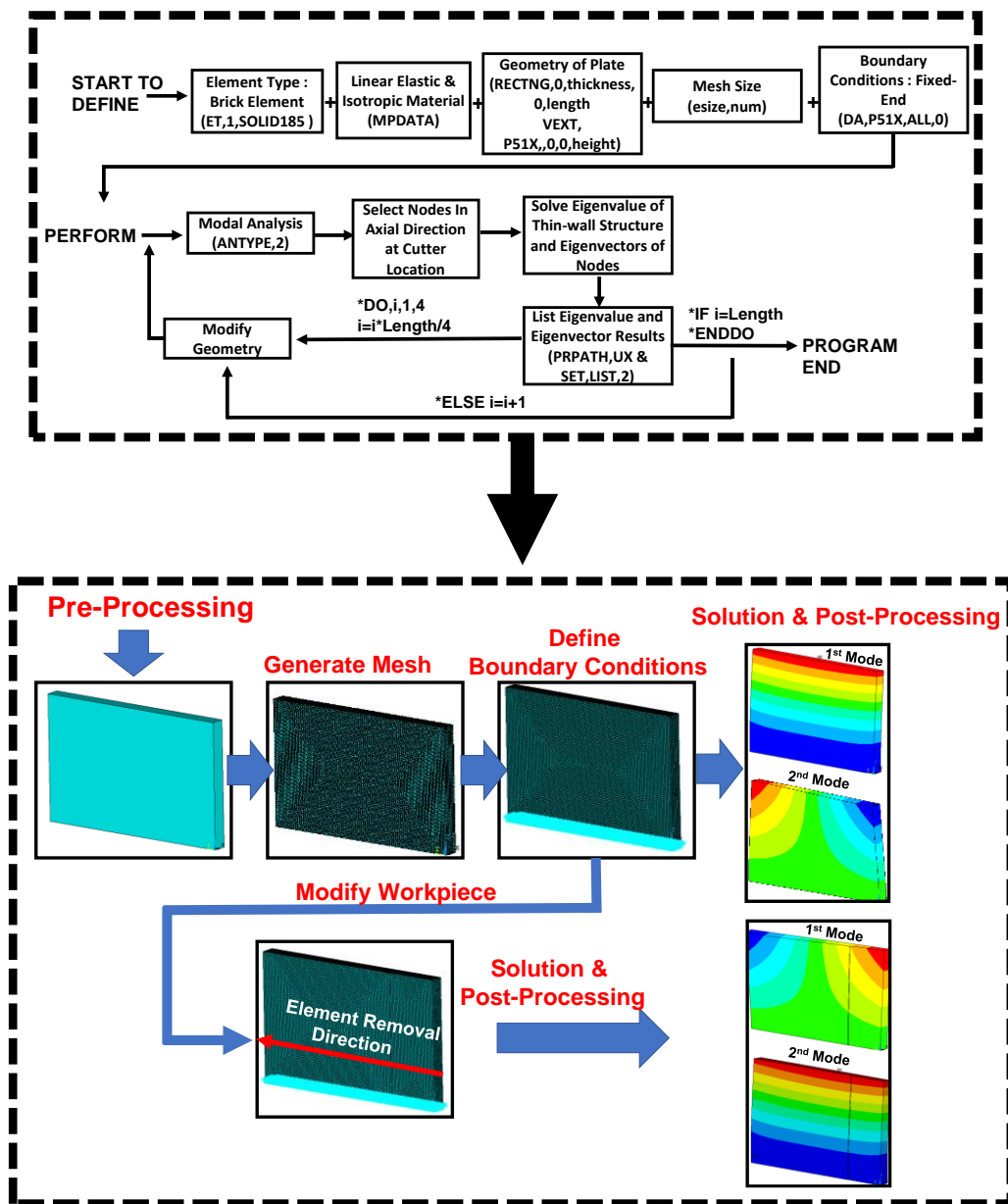


Figure 4.13. Flowchart of the FE macro code

In Figure 4.13, a general FEA procedure is followed to perform pre-processing and mesh generation at first. After, an amount of volume removed from initial form of the 3D geometry iteratively and obtained modal parameters in each iteration.

A representative illustration of flank element removal modeling in FEA is provided in Figure 4.14. Basically, the workpiece divided into five sections in feed direction, then in each element removal stage, modal parameters, which are natural frequencies and normalized mode shapes of the IPW are extracted considering cutter location (CL) in this case from FEA at first, then they used in calculation of frequency response function (FRF) in Eq. (4.7).

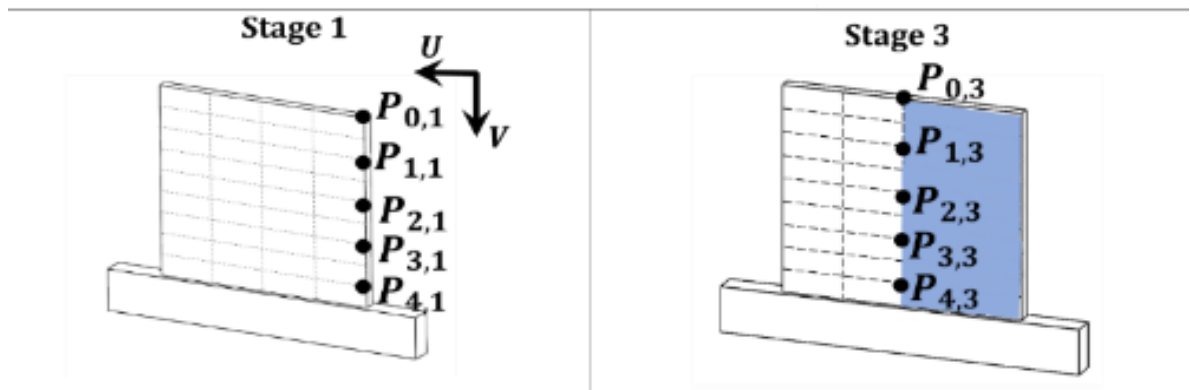


Figure 4.14. Material removal stages in flank milling of thin-walled part.

FRFs are found considering the CL and material removal effect in each cutting stages by considering the dynamic response of the most flexible points (i.e. free-end) of the workpiece ($P_{0,1}$, $P_{0,2}$, $P_{0,3}$, $P_{0,4}$, $P_{0,5}$) as provided in Figure 4.15 (a). CL determines only the local dynamic response of the IPW and element removal has effect on both modal frequencies and mode shapes of the part. The structural damping ratio values for first two dominant modes are identified as 0.5% and 0.3% respectively from impact hammer test. Stability analysis is performed with the effect of process damping for the thin-walled part with 0.8mm stock thickness, and the maximum allowable vibration amplitude is kept as $20\mu\text{m}$ in these simulations that is shown in Figure 4.15 (b) and (c).

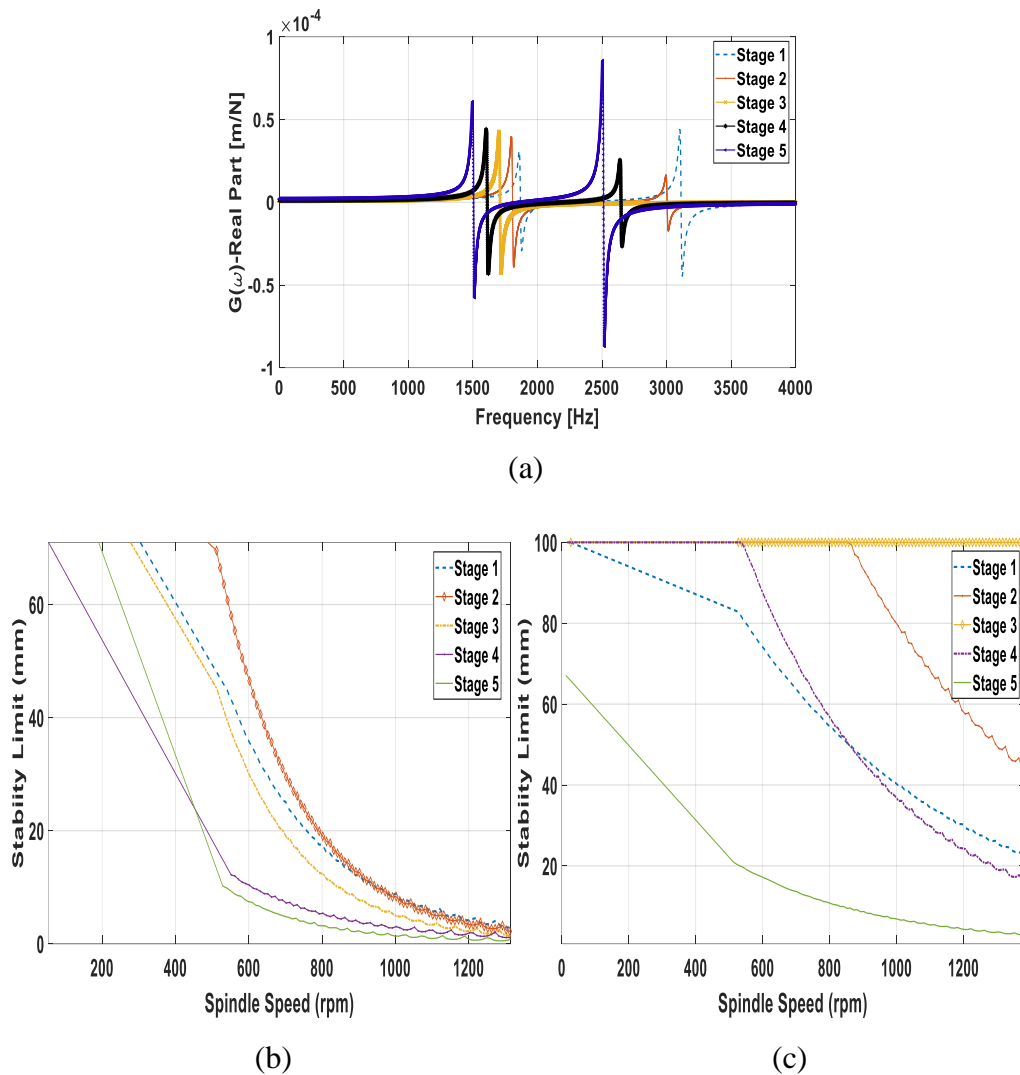


Figure 4.15. Varying (a) FRF and stability limits at different cutting stages (b) 1st Mode (c) 2nd Mode for 20 μ m vibration amplitude and 0.8mm stock thickness.

As depicted in Figure 4.15, material removal reduces modal frequency from cutting Stage 1 to Stage 5, since the 21% of semi-finished volume removed in finishing. In addition, the thin-walled workpiece becomes more flexible that also provides reduced stability limit. On the other hand, as CL changes, local response of thin-walled workpiece varies as each mode is considered.

The case, where the semi-finish part geometry is kept as 3mm, varying-dynamic of IPW simulated for different radial depth of cuts. When the workpiece becomes more flexible, FRF peak increases seriously that results drastic decrement in stability limit even the existing of process damping. Here, varying-dynamics of IPW simulated for various radial depth of cuts as given in Figure 4.16.

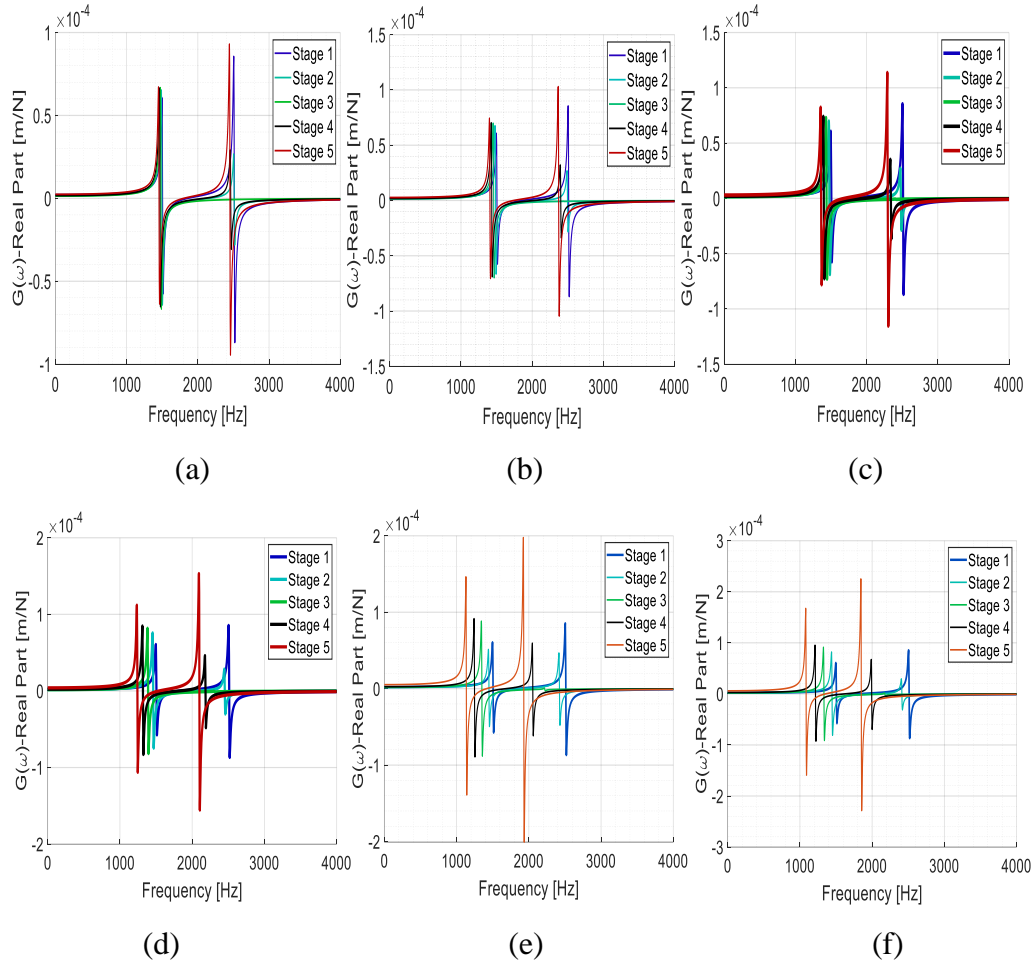


Figure 4.16. Varying-IPW dynamics FRFs for different finished part thickness (a) 2.9mm (b) 2.8mm (c) 2.7mm (d) 2.4mm (e) 2.2mm (f) 2.1mm

As discussed previously, variation in natural frequency of the system leads to shift stability pockets to high or low cutting speeds. However, at low cutting speeds, it is known that the stability pockets are narrow. Stability limit under process damping effect analysis updates absolute limit as mentioned in section 4.2. Therefore, it is expected that the quite changes in natural frequency (i.e. shifting of lobes) does not influence stability limit with process damping effect since there is no lobes at low cutting speeds.

According to the workpiece dynamics simulation results (see Figure 4.16), as the semi-finished (initial) and finished (final) form of the workpiece are considered, variations in natural frequencies and FRF amplitudes do not change in final part with the thicknesses of 2.9 mm, 2.8mm and 2.7mm presented as material removed for each case. In this regard, as low radial immersion is used, dynamic flexibility of the thin-walled IPW does not change drastically and the stability analysis can be performed considering initial form of

the workpiece. As the variation in natural frequencies of the initial form and the finished form of the thin-walled workpiece are considered, natural frequencies and modal displacements vary higher than 30% and 20% respectively, where 0.8 mm and 0.9 mm stock thicknesses are removed from the semi-finished workpiece. It is expected that dynamic flexibility (FRF) of IPW increases from the beginning of cutting to end of the cutting since FRF is proportional to square of modal displacements as expressed in Eq. (4.7) . Hence, the stability analysis is performed considering varying-dynamics of IPW with 0.9 mm radial immersion to demonstrate the effect of change in flexibility and modal frequency considering multi-mode as the system vibrates at maximum $25\mu\text{m}$ amplitude. Stability analysis with process damping effect performed considering IPW and the results are given in Figure 4.17.

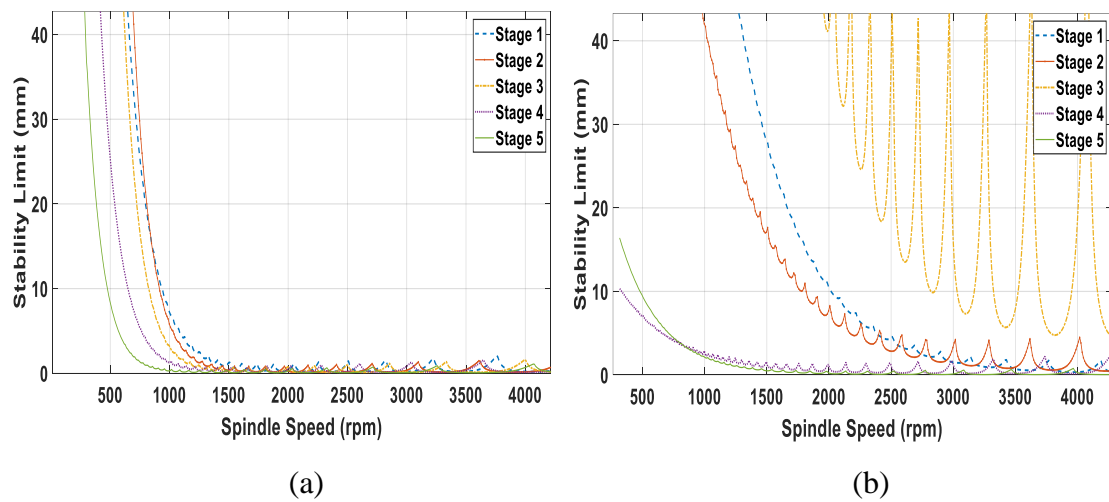


Figure 4.17. Varying stability limits at different cutting stages (a)1st Mode (b)2nd Mode for $25\mu\text{m}$ vibration amplitude and 0.9 mm radial depth of cut.

According to the stability results considering IPW provided in Figure 4.17, as material removed, stability limits shift low cutting speeds and the stability limit decreases due to increasing FRF amplitude of the workpiece. On the other hand, chatter suppression cannot be achieved with full axial depth for the second twisting mode, at the last cutting two stages (Stage 4 and Stage 5) due to varying dynamics of IPW. However, flank milling can be performed with the chatter suppression as the first bending mode is considered.

4.4. Experimental Verification

The dynamic response of the workpiece is verified using impact hammer test as seen in Figure 4.18 and the verified FRFs are demonstrated in Figure 4.19. Here, the thin-walled workpiece is clamped with 120Nm torque, and the measurement is performed at the tip-edge ($P_{0,1}$) and the tip-middle ($P_{0,3}$) of the workpiece by attaching accelerometer at these locations. As a result, direct transfer functions (i.e. FRFs) are measured. Although, the excitation at the point of tip-middle provides only FRF of the first bending mode, the excitation at the point of tip-edge enables to obtain both first bending and second twisting modes of the thin-walled workpiece.

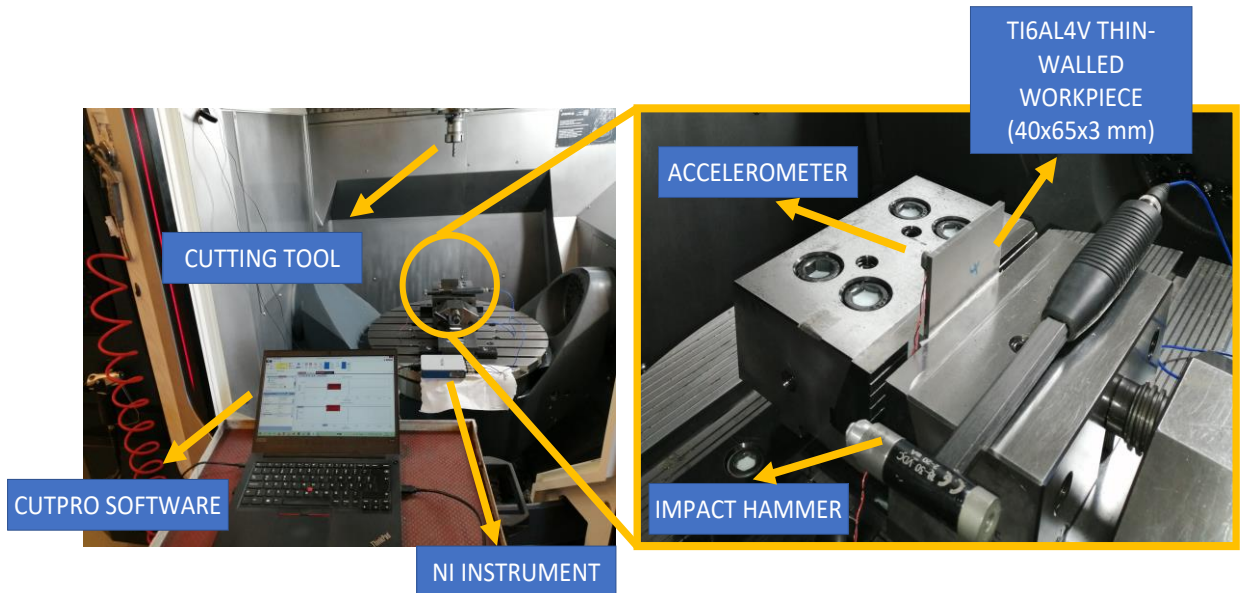


Figure 4.18. Experiment setup for workpiece dynamics verification

In this case, the structural damping ratio, that is used in stability analysis are obtained from impact hammer tests at different plate locations considering the finished form of the workpiece, where the thickness is 3 mm. In Figure 4.19, experimental verification of numerically calculated FRF results at two points on the flexible workpiece are presented. The locations of corresponding measurement points are presented in Figure 4.14.

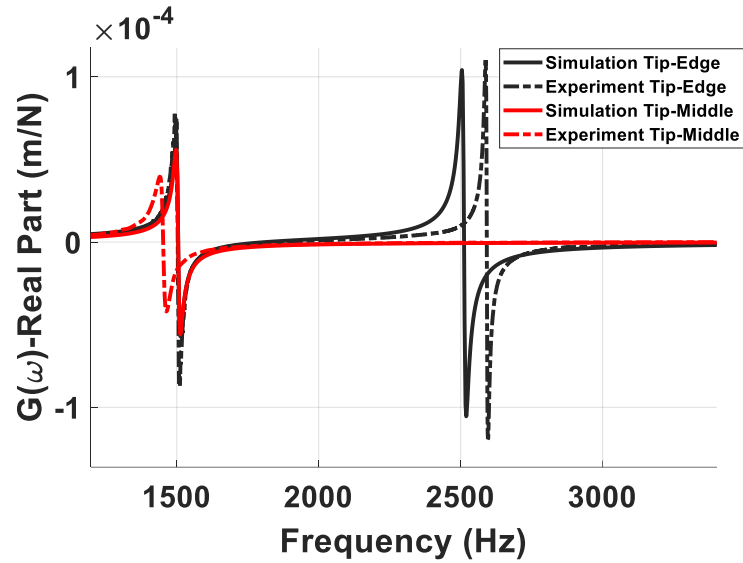


Figure 4.19. IPW dynamics simulation verification

The maximum difference between predicted and experimentally identified natural frequencies is less than 4%. Thus, FRF calculations is in a good agreement with impact hammer test results.

In this part, various milling tests are carried out to verify simulation results. These test conditions are given in Table 10 for different cases. In each test, feed rate is kept as 0.05 mm/(rev-tooth), and down milling is used as milling mode.

Table 10. Simulation Cases for Verification with Tests

Case No	Semi-Finished Part Thickness (mm)	Finished Part Thickness (mm)	Milling Strategy	Vibration Amplitude (μm)
Case 1	3	2.9	Flank	15
Case 2	3	2.7	Point	15
Case 3	3.8	3	Point	15
Case 4	3.6	3	Point	15
Case 5	3.8	3	Flank	20
Case 6	3	2.1	Flank	25

For the cases 1, 5 and 6; stability limits are selected as 40 mm, which is equal to height of the thin-walled workpiece to achieve flank milling operation as depicted in Figure 4.20

(a), (e) and (f).

Stable, marginally stable and unstable conditions are investigated for these cases through simulations and tests. In other cases, point milling strategy is used and simulation results with test points are provided in Figure 4.20.

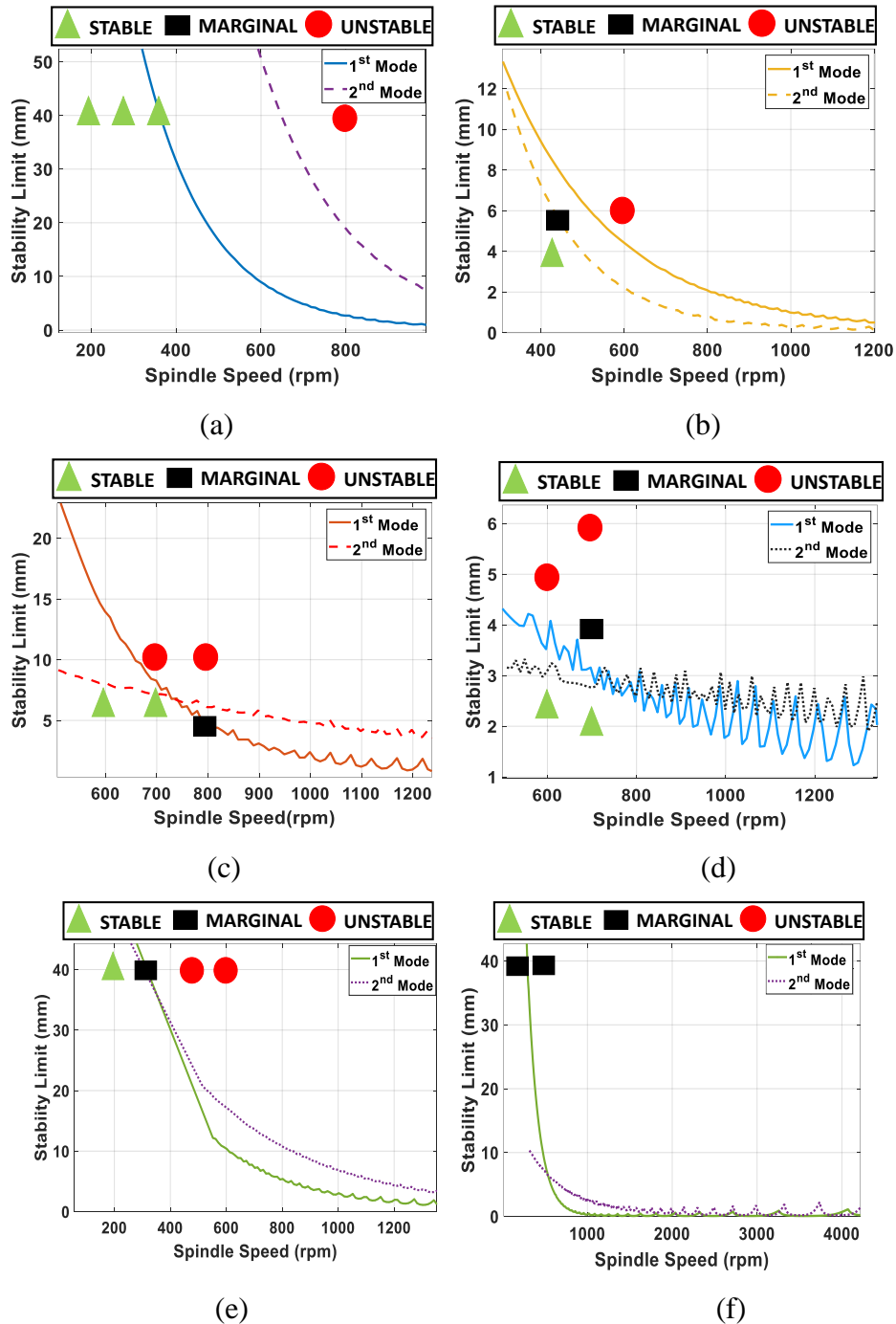


Figure 4.20. Experiment points (a) Case 1 (b) Case 2 (c) Case 3 (d) Case 4 (e) Case 5 (f) Case 6

As cases 3 and 4 are considered, it is obvious that case 3, where the optimal stock thickness (0.8 mm) is used provides higher stability limit in comparison to case 4, where the stock thickness is 0.6 mm. In cases 1 and 3, thin-wall milling system behaves local stable, where the only second mode of the workpiece is suppressed. However, self-excitation of the first mode left error along the feed direction since the bending mode is dominant in each cutting stage. In cases 5 and 6, as higher amount of stock is removed during finish milling, IPW dynamics is simulated and the minimum in-process stability limits are demonstrated. It can be seen from Figure 4.20, consideration of varying-IPW dynamics provides better stability prediction results. Some of the verification results are given with sound and surface measurements.

Sound measurements and finished surface textures of Case 1 is given in Figure 4.21.

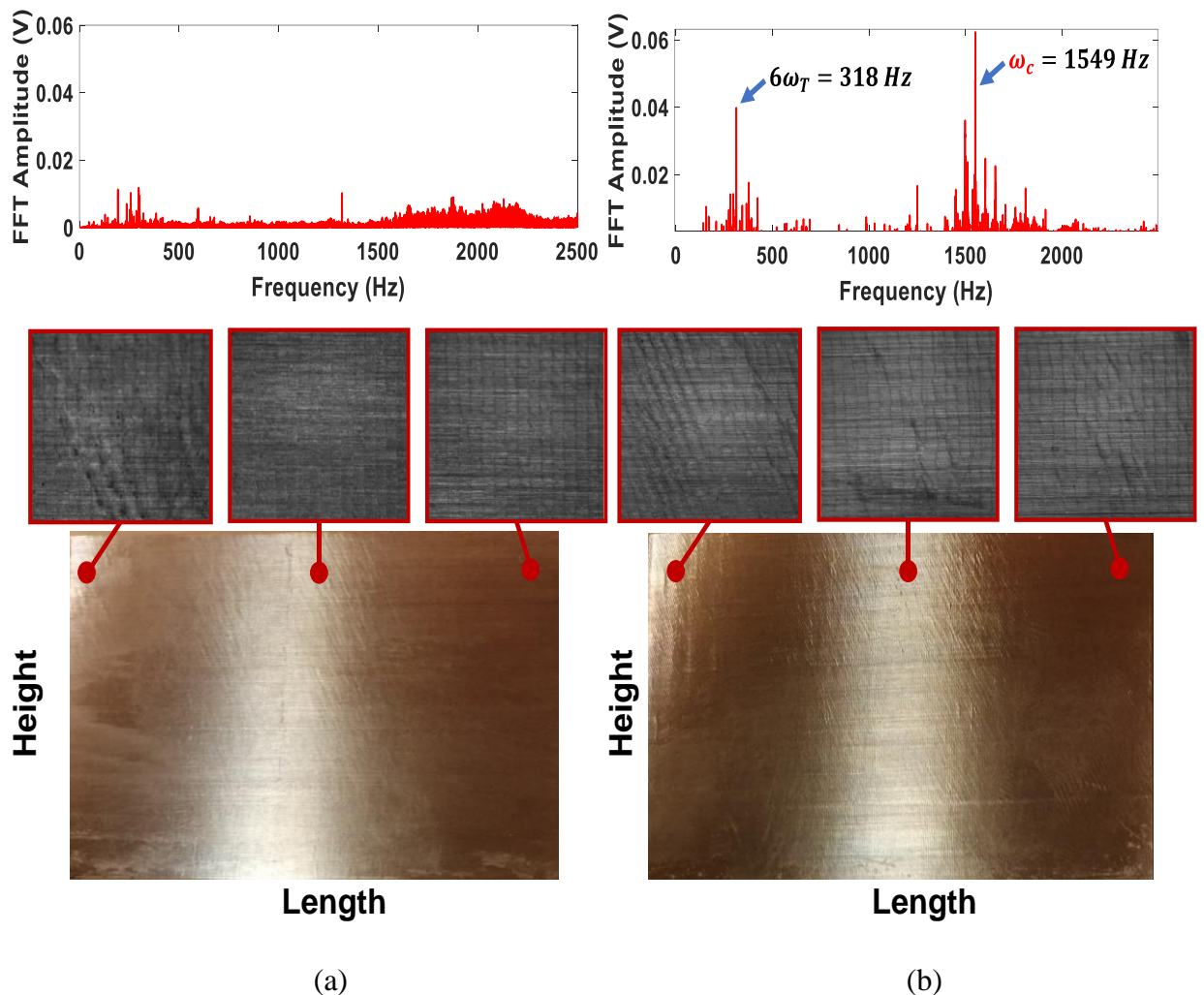


Figure 4.21. Sound and surface measurements of Case 1, $a=40$ mm (a) $n=365$ rpm (b) $n=800$ rpm.

It can be seen from Figure 4.21, flank milling is achieved without chatter for case 1, and both sound and surface measurement results verify proposed approach. As cutting speed increases from 365 rpm to 800 rpm, the dynamic contact is lost between tool-wavy surface, and thus the system becomes unstable, where chatter frequency is measured as 1549 Hz.

Surface finish and sound measurements of case 3 is demonstrated in Figure 4.22.

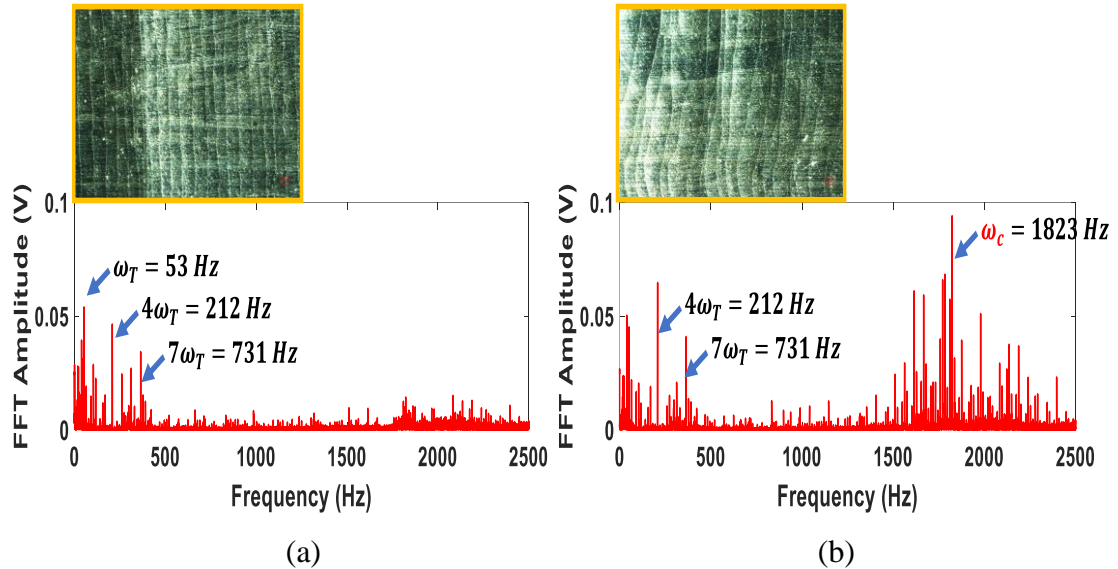


Figure 4.22. Sound and surface measurements of Case 3, $n=800$ rpm (a) $a=5$ mm (b) $a=10$ mm.

According to the Figure 4.22, system behaves marginally stable, where the axial cutting depth is 5 mm. On the other hand, as the depth increases from 5 mm to 10 mm process damping effect lost and the process returns unstable. Some of the tooth passing frequency, its harmonics and chatter frequency are demonstrated on FFT plots.

Surface finish and sound measurements of case 3 is demonstrated in Figure 4.23. As maximum $25 \mu\text{m}$ vibration amplitude is assumed, system behaves marginally stable at both spindle speeds of 300 rpm and 500 rpm. Vibration marks are more prominent at the edges of the thin-walled workpiece since the second mode is more flexible and both vibration modes are excited at that location.

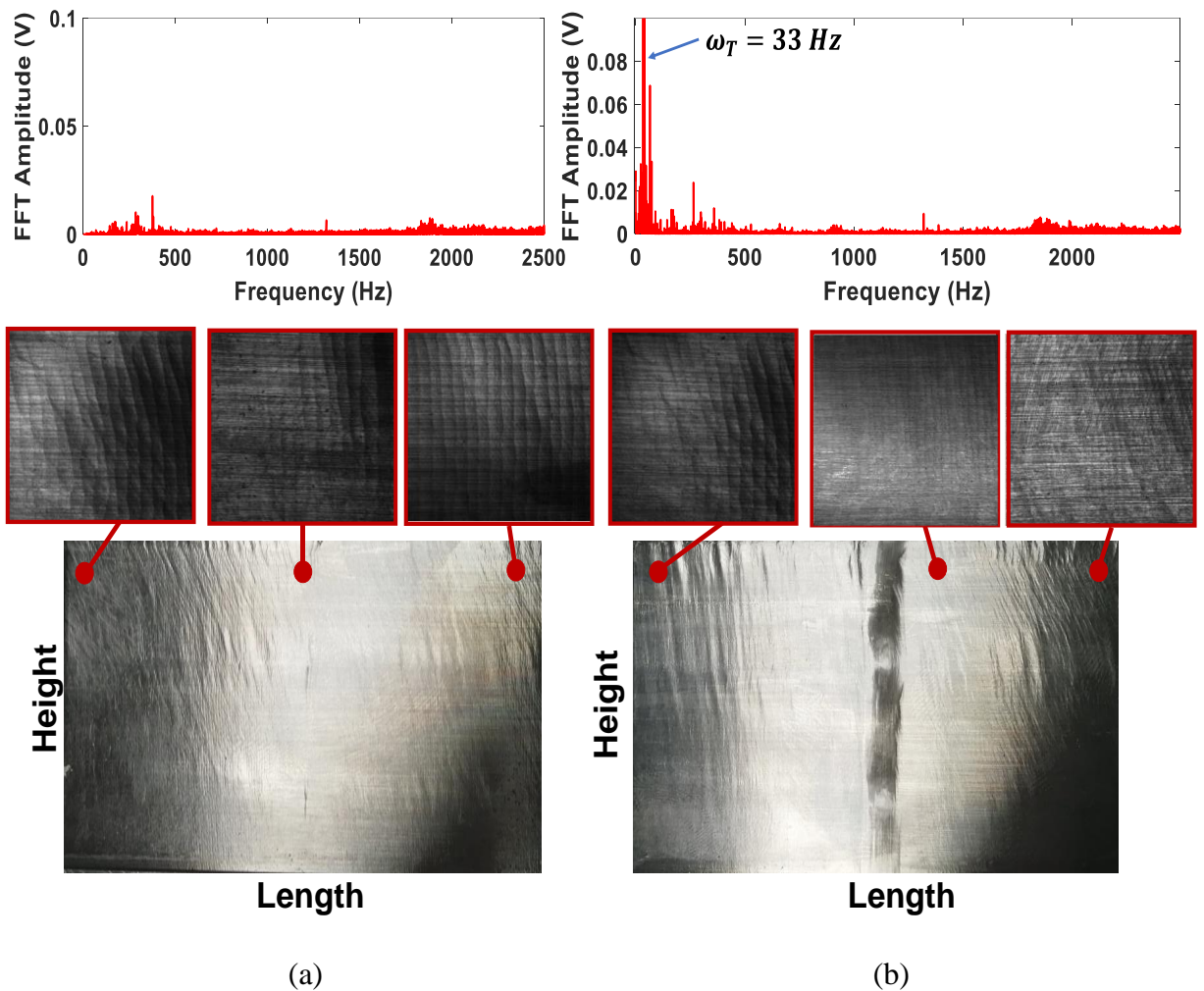


Figure 4.23. Sound and surface measurements of Case 6, $a=40$ mm (a) $n=300$ rpm (b) $n=500$ rpm.

As seen from Figure 4.21, Figure 4.22 and Figure 4.23, vibration marks left on the finished surface, which are generated due to vibrations (forced or self-excited) along in flexible direction of the thin-walled workpiece are measured at middle-tip points of the finished workpieces, where the first bending mode is dominant using 3D confocal microscope (μ surf NanoFocus) to demonstrate effect of vibration amplitudes on part surface during process damping effect in marginal stable, stable and chatter conditions. These surface texture measurements are given in Table 11 and they are in a good agreement with simulation results.

Table 11. Surface finish results with stability condition

	CASE 1		CASE 3		CASE 4		CASE 6	
Depth (mm) / Spindle Speed (rpm)	40/365	40/800	5/800	10/800	2.5/600	6/700	40/300	40/500
Surface Amplitude (μm)	13	19	14	26	14	18	23	27
Stability Condition	Stable	Unstable	Marginal	Unstable	Stable	Unstable	Marginal	Marginal

4.5. Conclusions

In this part of the thesis, influence of stock thickness left on the semi-finished part on stability of low-speed milling of flexible parts is investigated through simulations and experimental studies. Furthermore, effect of IPW dynamics simulated to demonstrate dynamic interaction induced process damping effect may lost as material removed from the thin-walled workpiece. In addition, as vibration amplitude assumed before deciding stable limits at first, forced vibration and its effect on finished surface evaluated, and used for simulation verification. The process damping model developed by [1,2] used in prediction of thin-wall milling at low cutting speeds. These analysis and tests are performed to arrive the following outcomes:

- Increasing stock thickness of the thin-walled workpiece increases dynamic stiffness and modal frequency, which increase stability limit and shift higher speeds, at the same time higher requirement of radial depth for finishing reduces stability limits. Therefore, the optimal selection of stock thickness, which offers higher stable depths is carried out to demonstrate stock thickness nonlinearly affects stability limits that should be selected according to various simulation results.
- If higher amount of material is removed from the semi-finished thin-walled workpiece in finishing stage, varying-dynamics of IPW should be considered,

since the variation in modal parameters of the thin-walled workpiece such as modal frequency and stiffness, and they may drastically decrease stability limit at low-speeds. In addition, it is demonstrated that the change in CL and flexibility of the thin-walled workpiece results local stable regions, where the only one of the dominant structural modes are suppressed.

- Even though increasing radial depth of cut decreases stability limit, as the minimum and maximum stock thickness cases, which are 0.6 mm and 1.5 mm are compared, higher radial depth of cut increases interaction length in addition to the dynamic stiffness, and thus process damping.
- Low-speed stability performance of cutting tools with different edge geometry demonstrated through simulations that the optimally selected stocks with proper cutting edge may provide to finish thin-walled part with one or a few passes that reduce machining time drastically.
- The vibration marks are measured at middle-tip of the plate to demonstrate surface location error. Evaluation of surface finish for chatter and marginally stable conditions is needed in thin-wall machining to demonstrate improvement on surface finish, and these results are used for simulation verification.

In this study, an end mill with higher stiffness in comparison to workpiece is used and it does not limit stability. However, it is expected that using flexible end mill contributes stability limit under process damping effect and the tool modes have some influences. In addition, modal stiffness varies from free-end to fixed-end, that results to obtain higher stability limit in some cases. Furthermore, static deflections bring limitation to the selection of process parameters in finishing of thin-walled parts, since that should be considered especially in selection of stock thickness. In this regard, these are further investigations of this study.

5. SUMMARY OF THESIS

5.1. Important Outcomes

In this thesis, multi-axial element model is presented for multi-mode thin-wall milling system and validated by milling tests as the first time in literature. Higher stable depths can be achieved using this stability model. In this respect, various machining strategies are proposed to show that productivity can be increased using multi-element model.

Special end mills such as variable pitch and crest-cut are firstly applied in milling of thin-walled parts. Due to their special geometries, they provide enhanced stability limits even at low cutting speeds. For this purpose, thin-walled part dynamics is modeled using FE algorithm and a practical approach is proposed to reduce solving time of stability limit. In this approach, workpiece dynamics extracted at first, then it used in stability analysis. Intermediate normalized mode shape values are found by interpolating upper and lower responses of each mesh element. As a result, crest-cut tools demonstrate excellent performance in milling of thin-walled parts in comparison to the variable pitch and standard end mills. In addition, variable pitch tools may prevent chatter in one of the workpiece modes, whereas they lose their suppression effect as the material removed (i.e. modal frequency changes). On the other hand, crest-cut tools enable to obtain extended stable region with higher stability limits in a higher spindle speed range.

Process damping effect generally observed at low cutting speeds provides significant enhancement in stability. Therefore, finish milling of thin-walled parts can be improved using process damping effect. In this regard, process parameter, cutting edge geometry and semi-finish stock thickness selection approach is proposed to achieve higher chatter-free axial depths in milling of thin-walled parts at low cutting speeds with the effect of process damping. A detailed stability analysis is performed considering varying-dynamics of IPW. Hone radius and clearance angle have an important influence on process damping that directly effects penetration volume. Stable finish milling of thin-walled parts can be carried out with one pass with proper selection of semi-finish stock thickness and cutting edge geometry. Vibrations at marginally stable condition also lefts surface finish location errors. In this respect, these errors are identified with surface

measurements. Surface finish quality can be improved even at high cutting depths using the proposed approach that is also important for reducing polishing time.

5.2. Futureworks

Proposed approach, which includes axial elements of workpiece in Chapter 3 can be generalized by combining stability limit under process damping effect at low cutting speeds. Furthermore, multi-element model can be solved for crest-cut and variable pitch tools since they provide higher stable depths even at low cutting speeds, thus the multi-element model can be also effective at low cutting speeds with special end mills.

As high cutting depths are used, this may lead to significant static deflections that have influence on actual local radial depth from free-end to fixed-end. This variation in radial depth of cut can be predicted and included stability analysis for more accurate predictions. In addition, static deflection induced dimensional errors can be predicted and compensated with feed rate scheduling in addition to stability analysis.

Process damping model can be generalized for special end mills such as serrated, crest-cut and variable pitch and mills. Their performance at low cutting speed is still under further investigation.

REFERENCES

- [1] J. Munoa, X. Beudaert, Z. Dombovari, Y. Altintas, E. Budak, C. Brecher, G. Stepan, Chatter suppression techniques in metal cutting, *CIRP Ann.* 65 (2016) 785–808. <https://doi.org/10.1016/J.CIRP.2016.06.004>.
- [2] D. Xuebin, W.A.N. Min, Y. Yun, Prediction and suppression of chatter in milling of structures with low-rigidity: A review, *J. Adv. Manuf. Sci. Technol.* 1 (2021) 2021010–2021011.
- [3] A. Calleja, M.A. Alonso, A. Fernández, I. Taberero, I. Ayesta, A. Lamikiz, L.N. López de Lacalle, Flank milling model for tool path programming of turbine blisks and compressors, *Int. J. Prod. Res.* 53 (2015) 3354–3369.
- [4] F. Tehranizadeh, K.R. Berenji, E. Budak, Dynamics and chatter stability of crest-cut end mills, *Int. J. Mach. Tools Manuf.* 171 (2021) 103813.
- [5] E. Budak, Y. Altintaş, Analytical Prediction of Chatter Stability in Milling—Part I: General Formulation, *J. Dyn. Syst. Meas. Control.* 120 (1998) 22–30. <https://doi.org/10.1115/1.2801317>.
- [6] L.T. Tunc, E. Budak, Identification and modeling of process damping in milling, *J. Manuf. Sci. Eng. Trans. ASME.* 135 (2013). <https://doi.org/10.1115/1.4023708/375042>.
- [7] F.W. Taylor, On the Art of Cutting Metals--75 Years Later: A Tribute to FW Taylor, in: ASME, 1982.
- [8] J. Tlustý, Analysis of the state of research in cutting dynamics, (1978). <https://pascal-francis.inist.fr/vibad/index.php?action=getRecordDetail&idt=PASCAL7900160889> (accessed May 24, 2022).
- [9] S. Tobias, W.F.-T. engineer, undefined 1958, Theory of regenerative machine tool chatter, *Vibration.Fr.* (n.d.). <http://www.vibration.fr/images/stories/Documents/1erePresentationLobesTobias.pdf> (accessed May 31, 2022).
- [10] J.T.-P.I.R. in P. Engineering, undefined Pittsburgh, undefined 1963, The stability of the machine tool against self-excited vibration in machining, *Ci.Nii.Ac.Jp.* (n.d.). <https://ci.nii.ac.jp/naid/10003574189/> (accessed June 5, 2022).
- [11] S.A. Tobias, *Machine-tool vibration*, Blackie, 1965.

- [12] F. (Franz) Koenigsberger, J. Tlustý, Machine tool structures, (1970).
- [13] H.E. Merritt, Theory of Self-Excited Machine-Tool Chatter: Contribution to Machine-Tool Chatter Research—1, *J. Eng. Ind.* 87 (1965) 447–454. <https://doi.org/10.1115/1.3670861>.
- [14] S. Smith, J.T.-C. *annals*, 1993, Efficient simulation programs for chatter in milling, Elsevier. (n.d.). <https://www.sciencedirect.com/science/article/pii/S000785060762486X> (accessed June 8, 2022).
- [15] J. Tlustý, F. Ismail, Basic Non-Linearity in Machining Chatter, *CIRP Ann.* 30 (1981) 299–304. [https://doi.org/10.1016/S0007-8506\(07\)60946-9](https://doi.org/10.1016/S0007-8506(07)60946-9).
- [16] R. Sridhar, R. Hohn, G. Long, A stability algorithm for the general milling process: contribution to machine tool chatter research—7, (1968). <https://asmedigitalcollection.asme.org/manufacturingscience/article-abstract/90/2/330/426306> (accessed June 8, 2022).
- [17] I. Minis, R. Yanushevsky, A. Tembo, R. Hocken, Analysis of Linear and Nonlinear Chatter in Milling, *CIRP Ann. - Manuf. Technol.* 39 (1990) 459–462. [https://doi.org/10.1016/S0007-8506\(07\)61096-8](https://doi.org/10.1016/S0007-8506(07)61096-8).
- [18] A. Lee, C.L.-I.J. of M.T. and, 1991, Analysis of chatter vibration in the end milling process, Elsevier. (n.d.). <https://www.sciencedirect.com/science/article/pii/0890695591900307> (accessed June 8, 2022).
- [19] Y. Altıntaş, E. Budak, Analytical Prediction of Stability Lobes in Milling, *CIRP Ann.* 44 (1995) 357–362. [https://doi.org/10.1016/S0007-8506\(07\)62342-7](https://doi.org/10.1016/S0007-8506(07)62342-7).
- [20] E. Budak, Y. Altıntaş, Analytical Prediction of Chatter Stability in Milling—Part II: Application of the General Formulation to Common Milling Systems, *J. Dyn. Syst. Meas. Control.* 120 (1998) 31–36. <https://doi.org/10.1115/1.2801318>.
- [21] S. Merdol, Y.A.-J.M.S. *Eng.*, 2004, Multi frequency solution of chatter stability for low immersion milling, *Asmedigitalcollection.Asme.Org.* (n.d.). <https://asmedigitalcollection.asme.org/manufacturingscience/article-abstract/126/3/459/476865> (accessed June 8, 2022).
- [22] T. Insperger, G. Stépán, Semi-discretization method for delayed systems, *Int. J. Numer. Methods Eng.* 55 (2002) 503–518. <https://doi.org/10.1002/NME.505>.
- [23] E. Budak, L.T. Tunç, S. Alan, H.N. Özgüven, Prediction of workpiece dynamics

- and its effects on chatter stability in milling, *CIRP Ann.* 61 (2012) 339–342. <https://doi.org/10.1016/J.CIRP.2012.03.144>.
- [24] D. Montgomery, Y. Altintas, Mechanism of Cutting Force and Surface Generation in Dynamic Milling, *J. Eng. Ind.* 113 (1991) 160–168. <https://doi.org/10.1115/1.2899673>.
- [25] U. Bravo, O. Altuzarra, L.N.L. De Lacalle, J.A. Sánchez, F.J. Campa, Stability limits of milling considering the flexibility of the workpiece and the machine, *Int. J. Mach. Tools Manuf.* 45 (2005) 1669–1680.
- [26] V. Thévenot, L. Arnaud, G. Dessein, G. Cazenave–Larroche, Influence of material removal on the dynamic behavior of thin-walled structures in peripheral milling, *Mach. Sci. Technol.* 10 (2006) 275–287.
- [27] D. Biermann, P. Kersting, T. Surmann, A general approach to simulating workpiece vibrations during five-axis milling of turbine blades, *CIRP Ann.* 59 (2010) 125–128.
- [28] E. Budak, Improving Productivity and Part Quality in Milling of Titanium Based Impellers by Chatter Suppression and Force Control, *CIRP Ann.* 49 (2000) 31–36. [https://doi.org/10.1016/S0007-8506\(07\)62890-X](https://doi.org/10.1016/S0007-8506(07)62890-X).
- [29] S. Alan, E. Budak, H.N. Özgüven, Analytical Prediction of Part Dynamics for Machining Stability Analysis, *Int. J. Autom. Technol.* 4 (2010) 259–267. <https://doi.org/10.20965/IJAT.2010.P0259>.
- [30] O. Tuysuz, Y. Altintas, Frequency domain updating of thin-walled workpiece dynamics using reduced order substructuring method in machining, *J. Manuf. Sci. Eng.* 139 (2017).
- [31] S. Smith, R. Wilhelm, B. Dutterer, H. Cherukuri, G. Goel, Sacrificial structure preforms for thin part machining, *CIRP Ann.* 61 (2012) 379–382. <https://doi.org/10.1016/J.CIRP.2012.03.142>.
- [32] Y. Koike, A. Matsubara, S. Nishiwaki, ... K.I.-I.J. of, 2012, Cutting path design to minimize workpiece displacement at cutting point: Milling of thin-walled parts, Fujipress.Jp. (n.d.). <https://www.fujipress.jp/ijat/au/ijate000600050638/> (accessed June 8, 2022).
- [33] L. Tunc, M.Z.-C. Annals, 2019, Stability optimal selection of stock shape and tool axis in finishing of thin-wall parts, Elsevier. (n.d.). <https://www.sciencedirect.com/science/article/pii/S0007850619301258> (accessed

May 24, 2022).

- [34] J. Slavicek, The effect of irregular tooth pitch on stability of milling, in: Proc. 6th MTDR Conf., 1965: pp. 15–22.
- [35] E. Budak, An Analytical Design Method for Milling Cutters With Nonconstant Pitch to Increase Stability, Part I: Theory, *J. Manuf. Sci. Eng.* 125 (2003) 29–34. <https://doi.org/10.1115/1.1536655>.
- [36] N. Suzuki, R. Ishiguro, T. Kojima, Design of irregular pitch end mills to attain robust suppression of regenerative chatter, *CIRP Ann.* 65 (2016) 129–132.
- [37] A. Comak, E. Budak, Modeling dynamics and stability of variable pitch and helix milling tools for development of a design method to maximize chatter stability, *Precis. Eng.* 47 (2017) 459–468. <https://doi.org/http://dx.doi.org/10.1016/j.precisioneng.2016.09.021>.
- [38] S. Turner, D. Merdol, Y. Altintas, K. Ridgway, Modelling of the stability of variable helix end mills, *Int. J. Mach. Tools Manuf.* 47 (2007) 1410–1416. <https://doi.org/10.1016/j.ijmachtools.2006.08.028>.
- [39] N.D. Sims, Fast chatter stability prediction for variable helix milling tools, *Proc. Inst. Mech. Eng. Part C J. Mech. Eng. Sci.* 230 (2016) 133–144.
- [40] Z. Dombovari, Y. Altintas, G. Stepan, Stability of serrated milling cutters, *Methods.* 5 (2009) 12–18.
- [41] F. Tehranizadeh, R. Koca, E. Budak, Investigating effects of serration geometry on milling forces and chatter stability for their optimal selection, *Int. J. Mach. Tools Manuf.* (2019) 103425.
- [42] P. Bari, Z.M. Kilic, M. Law, P. Wahi, Rapid stability analysis of serrated end mills using graphical-frequency domain methods, *Int. J. Mach. Tools Manuf.* 171 (2021) 103805. <https://doi.org/10.1016/j.ijmachtools.2021.103805>.
- [43] Z. Dombovari, G. Stepan, The Effect of Helix Angle Variation on Milling Stability, *J. Manuf. Sci. Eng.* 134 (2012) 51015–51016. <https://doi.org/10.1115/1.4007466>.
- [44] M. Sanz, A. Iglesias, J. Munoa, Z. Dombovari, The effect of geometry on harmonically varied helix milling tools, *J. Manuf. Sci. Eng. Trans. ASME.* 142 (2020). <https://doi.org/10.1115/1.4046901>.
- [45] M.K. Das, S.A. Tobias, The relation between the static and the dynamic cutting of metals, *Int. J. Mach. Tool Des. Res.* 7 (1967) 63–89. <https://doi.org/10.1016/0020->

7357(67)90026-1.

- [46] T.R. Sisson, R.L. Kegg, An Explanation of Low-Speed Chatter Effects, *J. Eng. Ind.* 91 (1969) 951–958. <https://doi.org/10.1115/1.3591778>.
- [47] H.J.J. Kals, On the Calculation of Stability Charts on the Basis of the Damping and Stiffness of the Cutting Process, *Ann. CIRP.* 19 (1971) 297–303.
- [48] S.C. Lin, R.E. Devor, S.G. Kapoor, J.W. Sutherland, A new approach to estimating the cutting process damping under working conditions, *Trans. North Am. Manuf. Res. Inst. SME* 1990. (1990) 154–160.
- [49] J. Tlustý, F. Ismail, Special Aspects of Chatter in Milling, *J. Vib. Acoust. Stress. Reliab. Des.* 105 (1983) 24–32. <https://doi.org/10.1115/1.3269061>.
- [50] D.W. Wu, Application of a comprehensive dynamic cutting force model to orthogonal wave-generating processes, *Int. J. Mech. Sci.* 30 (1988) 581–600.
- [51] M.A. Elbestawi, F. Ismail, R. Du, B.C. Ullagaddi, Modelling Machining Dynamics Including Damping in the Tool-Workpiece Interface, *J. Eng. Ind.* 116 (1994) 435–439. <https://doi.org/10.1115/1.2902125>.
- [52] Y.S. Chiou, E.S. Chung, S.Y. Liang, Analysis of tool wear effect on chatter stability in turning, *Int. J. Mech. Sci.* 37 (1995) 391–404. [https://doi.org/10.1016/0020-7403\(94\)00070-Z](https://doi.org/10.1016/0020-7403(94)00070-Z).
- [53] B.E. Clancy, Y.C. Shin, A comprehensive chatter prediction model for face turning operation including tool wear effect, *Int. J. Mach. Tools Manuf.* 42 (2002) 1035–1044. [https://doi.org/10.1016/S0890-6955\(02\)00036-6](https://doi.org/10.1016/S0890-6955(02)00036-6).
- [54] C.Y. Huang, J.J.J. Wang, Mechanistic Modeling of Process Damping in Peripheral Milling, *J. Manuf. Sci. Eng.* 129 (2007) 12–20. <https://doi.org/10.1115/1.2335857>.
- [55] Y. Altintas, M. Eynian, H.O.-C. annals,2008, Identification of dynamic cutting force coefficients and chatter stability with process damping, Elsevier. (n.d.). <https://www.sciencedirect.com/science/article/pii/S0007850608000395> (accessed May 18, 2022).
- [56] M. Eynian, Y. Altintas, Chatter stability of general turning operations with process damping, *J. Manuf. Sci. Eng. Trans. ASME.* 131 (2009) 0410051–04100510. <https://doi.org/10.1115/1.3159047/419358>.
- [57] E. Budak, L.T. Tunc, A new method for identification and modeling of process damping in machining, *J. Manuf. Sci. Eng. Trans. ASME.* 131 (2009) 0510191–05101910. <https://doi.org/10.1115/1.4000170/444810>.

- [58] K. Ahmadi, F. Ismail, Experimental investigation of process damping nonlinearity in machining chatter, *Int. J. Mach. Tools Manuf.* 50 (2010) 1006–1014. <https://doi.org/10.1016/J.IJMACHTOOLS.2010.07.002>.
- [59] D. Bachrathy, D. Bachrathy, G. Stépán, Time-periodic velocity-dependent process damping in milling processes Dry friction View project Evaluation of mechanical contact View project Time-periodic velocity-dependent process damping in milling processes, (2010). <https://www.researchgate.net/publication/265794510> (accessed May 19, 2022).
- [60] T.G. Molnár, · Tamás Insperger, · Dániel Bachrathy, · Gábor Stépán, D. Bachrathy, G. Stépán, S.B. Hu, Extension of process damping to milling with low radial immersion, *Int. J. Adv. Manuf. Technol.* 2016 899. 89 (2016) 2545–2556. <https://doi.org/10.1007/S00170-016-9780-0>.
- [61] E. Budak, L.T. Tunc, Identification and modeling of process damping in turning and milling using a new approach, *CIRP Ann.* 59 (2010) 403–408. <https://doi.org/10.1016/J.CIRP.2010.03.078>.
- [62] K. Ahmadi, F. Ismail, Analytical stability lobes including nonlinear process damping effect on machining chatter, *Int. J. Mach. Tools Manuf.* 51 (2011) 296–308. <https://doi.org/10.1016/J.IJMACHTOOLS.2010.12.008>.
- [63] L.T. Tunc, E. Budak, Effect of cutting conditions and tool geometry on process damping in machining, *Int. J. Mach. Tools Manuf.* 57 (2012) 10–19. <https://doi.org/10.1016/J.IJMACHTOOLS.2012.01.009>.
- [64] X. Jin, Y. Altintas, Chatter stability model of micro-milling with process damping, *J. Manuf. Sci. Eng. Trans. ASME.* 135 (2013). <https://doi.org/10.1115/1.4024038/377005>.
- [65] C.T. Tyler, T.L. Schmitz, Analytical process damping stability prediction, *J. Manuf. Process.* 15 (2013) 69–76. <https://doi.org/10.1016/J.JMAPRO.2012.11.006>.
- [66] K. Ahmadi, Y. Altintas, Identification of machining process damping using output-only modal analysis, *J. Manuf. Sci. Eng. Trans. ASME.* 136 (2014). <https://doi.org/10.1115/1.4027676/376985>.
- [67] M. Wan, J. Feng, Y.C. Ma, W.H. Zhang, Identification of milling process damping using operational modal analysis, *Int. J. Mach. Tools Manuf.* 122 (2017) 120–131. <https://doi.org/10.1016/J.IJMACHTOOLS.2017.06.006>.

- [68] M. Wan, J. Feng, W. Zhang, Mechanistic Modeling of Milling Process Damping Including Velocity and Ploughing Effects, *Procedia CIRP*. 56 (2016) 124–127. <https://doi.org/10.1016/J.PROCIR.2016.10.036>.
- [69] M. Yaser, T.L. Taner, B. Erhan, Investigation of Process Damping Effect for Multi-mode Milling Systems, *Procedia CIRP*. 58 (2017) 198–203. <https://doi.org/10.1016/J.PROCIR.2017.03.209>.
- [70] L.T. Tunc, Y. Mohammadi, E. Budak, Destabilizing effect of low frequency modes on process damped stability of multi-mode milling systems, *Mech. Syst. Signal Process*. 111 (2018) 423–441. <https://doi.org/10.1016/J.YMSSP.2018.03.051>.
- [71] Z. Li, S. Jiang, Y. Sun, Chatter stability and surface location error predictions in milling with mode coupling and process damping:, *Https://Doi.Org/10.1177/0954405417708225*. 233 (2017) 686–698. <https://doi.org/10.1177/0954405417708225>.
- [72] Z. Li, Y. Sun, D. Guo, Chatter prediction utilizing stability lobes with process damping in finish milling of titanium alloy thin-walled workpiece, *Int. J. Adv. Manuf. Technol.* 2016 899. 89 (2016) 2663–2674. <https://doi.org/10.1007/S00170-016-9834-3>.
- [73] O. Tuysuz, Y. Altintas, Analytical modeling of process damping in machining, *J. Manuf. Sci. Eng. Trans. ASME*. 141 (2019). <https://doi.org/10.1115/1.4043310/727642>.
- [74] X. Tang, F. Peng, R. Yan, Z. Zhu, Z. Li, S. Xin, Nonlinear process damping identification using finite amplitude stability and the influence analysis on five-axis milling stability, *Int. J. Mech. Sci.* 190 (2021) 106008. <https://doi.org/10.1016/J.IJMECSCI.2020.106008>.
- [75] F. Tehranizadeh, K.R. Berenji, S. Yıldız, E. Budak, Chatter stability of thin-walled part machining using special end mills, *CIRP Ann.* (2022). <https://doi.org/10.1016/J.CIRP.2022.04.057>.
- [76] J. Feng, M. Wan, T.Q. Gao, W.H. Zhang, Mechanism of process damping in milling of thin-walled workpiece, *Int. J. Mach. Tools Manuf.* 134 (2018) 1–19. <https://doi.org/10.1016/J.IJMACHTOOLS.2018.06.001>.
- [77] D. Wang, M. Löser, S. Ihlenfeldt, X. Wang, Z. Liu, Milling stability analysis with considering process damping and mode shapes of in-process thin-walled workpiece, *Int. J. Mech. Sci.* 159 (2019) 382–397.

<https://doi.org/10.1016/J.IJMECSCI.2019.06.005>.

- [78] J. Feng, M. Wan, Z.Y. Dong, W.H. Zhang, A unified process damping model considering the varying stiffness of the milling system, *Int. J. Mach. Tools Manuf.* 147 (2019) 103470. <https://doi.org/10.1016/J.IJMACHTOOLS.2019.103470>.
- [79] M. Li, W. Zhao, L. Li, N. He, M. Jamil, Study the effect of anti-vibration edge length on process stability of milling thin-walled Ti-6Al-4V alloy, *Int. J. Adv. Manuf. Technol.* 113 (2021) 2563–2574. <https://doi.org/10.1007/S00170-021-06781-5/FIGURES/12>.
- [80] , Y Altintas, , AA Ber, Manufacturing Automation: Metal Cutting Mechanics, Machine Tool Vibrations, and CNC Design, *Appl. Mech. Rev.* 54 (2001) B84–B84. <https://doi.org/10.1115/1.1399383>.
- [81] E. Budak, L. Kops, Improving productivity and part quality in milling of titanium based impellers by chatter suppression and force control, *CIRP Ann.* 49 (2000) 31–36.
- [82] T. Insperger, G. Stépán, Updated semi-discretization method for periodic delay-differential equations with discrete delay, *Int. J. Numer. Methods Eng.* 61 (2004) 117–141. <https://doi.org/10.1002/NME.1061>.
- [83] D.W. Wu, A New Approach of Formulating the Transfer Function for Dynamic Cutting Processes, *J. Eng. Ind.* 111 (1989) 37–47. <https://doi.org/10.1115/1.3188730>.
- [84] M. Elbestawi, F. Ismail, R. Du, B. Ullagaddi, Modelling machining dynamics including damping in the tool-workpiece interface, (1994). <https://asmedigitalcollection.asme.org/manufacturingscience/article-abstract/116/4/435/393068> (accessed May 18, 2022).